

**SYNTHESIS AND CHARACTERIZATION OF CHALCONE
DERIVATIVES AND THEIR ANTIOXIDANT ACTIVITY**

By

CHANG LING YING

A project report submitted to the Department of Chemical Science

Faculty of Science

Universiti Tunku Abdul Rahman

in partial fulfilment of the requirement for the degree of

Bachelor of Science (Hons) Chemistry

May 2022

ABSTRACT

SYNTHESIS AND CHARACTERIZATION OF CHALCONE DERIVATIVES AND THEIR ANTIOXIDANT ACTIVITY

Chang Ling Ying

Chalcones (1,3-diphenyl-2-propen-1-ones) have been reported to possess a broad spectrum of biological activities that are associated to their unique core structure consisting of two aromatic rings attached by an α,β -unsaturated carbonyl system. Several evidence have demonstrated that the chalcone derived Mannich bases showed enhanced biological activities than their parent chalcone compounds. In this study, a series of chalcones and their Mannich base derivatives has been synthesized and assessed for their antioxidant activity. The synthesis of chalcones was performed by Claisen-Schmidt condensation of 4'-hydroxyacetophenone and benzaldehyde derivatives. The synthesis of Mannich bases was carried out through Mannich reaction between the synthesized chalcones, formaldehyde and secondary amines including dimethylamine, pyrrolidine and piperidine. The synthesized compounds were characterized using FTIR, LC-MS and NMR spectroscopy. The synthesized chalcone derivatives are 3-(4-chlorophenyl)-1-(4-hydroxyphenyl)-prop-2-en-1-one (**CA**) and 1-(4-hydroxyphenyl)-3-phenyl-prop-2-en-1-one (**CA2**). The synthesized Mannich bases using **CA** as parent compound are 3-(4-chlorophenyl)-1-{3-

[(dimethylamino)methyl]-4-hydroxyphenyl}-prop-2-en-1-one (**DA**), 3-(4-chlorophenyl)-1-{4-hydroxy-3-[(pyrrolidin-1-yl)methyl]phenyl}prop-2-en-1-one (**PY**) and 3-(4-chlorophenyl)-1-{4-hydroxy-3-[(piperidin-1-yl)methyl]phenyl}-prop-2-en-1-one (**PI**). The Mannich bases derived from **CA2** include 1-{3-[(dimethylamino)methyl]-4-hydroxyphenyl}3-phenylprop-2-en-1-one (**DA2**), 1-{4-hydroxy-3-[(pyrrolidin-1-yl)methyl]phenyl}-3-phenylprop-2-en-1-one (**PY2**) and 1-{4-hydroxy-3-[(piperidin-1-yl)methyl]phenyl}-3-phenylprop-2-en-1-one (**PI2**). Antioxidant activity evaluation was performed on the synthesized compounds using DPPH antioxidant assay. The results indicated that chalcone derived Mannich bases exhibited better antioxidant activity than their corresponding chalcone parent compounds. The Mannich bases **PY** and **PY2** showed IC₅₀ values at 550 and 700 ppm, respectively, whereas their parent compounds **CA** and **CA2** showed IC₅₀ values at above 1000 ppm.

ABSTRAK

SINTESIS DAN PENCIRIAN TERBITAN KALKON DENGAN AKTIVITI ANTIOKSIDANYA

Chang Ling Ying

Kalkon (1,3-difenil-2-propen-1-on) telah dilaporkan memiliki pelbagai aktiviti biologi yang dikaitkan dengan struktur teras uniknya yang terdiri daripada dua cincin aromatik yang dihubungkan dengan sebatian karbonil $\alpha\beta$ tak tepu. Beberapa bukti telah menunjukkan bahawa bes Mannich yang diperolehi daripada kalkon menunjukkan aktiviti biologi yang kuat daripada sebatian kalkon induknya. Dalam kajian ini, sintesis untuk satu siri kalkon dan terbitan bes Mannich dan penilaian ke atas aktiviti antioksidanya telah dilakukan. Sintesis senyawa kalkon telah dilakukan melalui kondensasi Claisen-Schmidt dengan 4'-hidroksiasetofenon dan terbitan benzaldehid. Sintesis bes Mannich telah dilakukan melalui reaksi Mannich dengan senyawa kalkon, formaldehid dan amina sekunder termasuk dimetilamina, pirolidina dan piperidina. Senyawa kalkon dan bes Mannich disintesis telah dicirikan menggunakan spektroskopi FTIR, LC-MS dan NMR. Kalkon yang disintesis termasuk 3-(4-klorofenil)-1-(4-hidroksifenil)-prop-2-en-1-one (**CA**) dan 1-(4-hidroksifenil)-3-fenil-prop-2-en-1-one (**CA2**). Terbitan bes Mannich menggunakan **CA** sebagai sebatian induk adalah 3-(4-klorofenil)-1-{3-[(dimetilamino)metil]-4-hidroksifenil}-

prop-2-en-1-one (**DA**), 3-(4-klorofenil)-1-{4-hidroksi-3-[(pyrolidin-1-il)metil]fenil}prop-2-en-1-one (**PY**) dan 3-(4-klorofenil)-1-{4-hidroksi-3-[(piperidin-1-il)metil]fenil}-prop-2-en-1-one (**PI**). Manakala bes Mannich yang disintesis daripada **CA2** termasuk 1-{3-[(dimetilamino)metil]-4-hidroksifenil}3-fenilprop-2-en-1-one (**DA2**), 1-{4-hidroksi-3-[(pyrolidin-1-il)metil]fenil}-3-fenilprop-2-en-1-one (**PY2**) and 1-{4-hidroksi-3-[(piperidin-1-il)metil]fenil}-3-fenilprop-2-en-1-one (**PI2**). Penilaian aktiviti antioksidasi telah dilakukan dengan menggunakan ujian antioksidasi DPPH. Senyawa bes Mannich menunjuk aktiviti antioksidasi yang lebih baik daripada senyawa kalkon induk sepadan. Bes Mannich **PY** dan **PY2** menunjukkan nilai IC_{50} pada 550 dan 700 ppm, manakala nilai IC_{50} bagi senyawa kalkon **CA** dan **CA2** melebihi 1000 ppm.

ACKNOWLEDGEMENTS

First and foremost, I would like to express my special thanks to my supervisor, Ms. Chang Chew Cheen. Her guidance and advice carried me throughout all stages of my project.

Heartfelt gratitude also goes to the lab officers of Department of Chemical Science for their assistance throughout this project.

I am extending my sincere gratitude and appreciation to my friends and family for their continuous support, either morally, financially or physically. The completion of this project could not have been possible without them.

Last but not least, I would like to thank my university, Universiti Tunku Abdul Rahman (UTAR), for giving me this golden opportunity and providing a well-equipped working space to carry out this project.

DECLARATION

I hereby declare that this final year project is based on my original work except for quotations and citations which have been duly acknowledged. I also declare that it has not been previously or concurrently submitted for any other degree at UTAR or other institutions

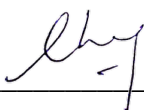
ying

Chang Ling Ying

APPROVAL SHEET

This final year project report entitled “**SYNTHESIS AND CHARACTERIZATION OF CHALCONE DERIVATIVES AND THEIR ANTIOXIDANT ACTIVITY**” was prepared by CHANG LING YING and submitted as partial fulfilment of the requirements for the degree of Bachelor of Science (Hons) Chemistry at Universiti Tunku Abdul Rahman.

Approved by:



Ms. Chang Chew Cheen

Date: 30 May 2022

Supervisor

Department of Chemical Science

Faculty of Science

Universiti Tunku Abdul Rahman

FACULTY OF SCIENCE
UNIVERSITI TUNKU ABDUL RAHMAN

Date: 30 May 2022

PERMISSION SHEET

It is here by certified that **CHANG LING YING** (ID No.: **19ADB01683**) has completed this final year project report entitled “SYNTHESIS AND CHARACTERIZATION OF CHALCONE DERIVATIVES AND THEIR ANTIOXIDANT ACTIVITY” under the supervision of Ms. Chang Chew Cheen from the Department of Chemical Science, Faculty of Science.

I hereby give permission to the University to upload the softcopy of my final year project report in pdf format into the UTAR Institutional Repository, which may be made accessible to the UTAR community and public.

Yours truly,



(CHANG LING YING)

TABLE OF CONTENTS

	Page
ABSTRACT	ii
ABSTRAK	iv
ACKNOWLEDGEMENTS	vi
DECLARATION	vii
APPROVAL SHEET	viii
PERMISSION SHEET	ix
TABLE OF CONTENTS	x
LIST OF TABLES	xii
LIST OF FIGURES	xiv
LIST OF ABBREVIATIONS	xvii
CHAPTER	
1 INTRODUCTION	1
1.1 Chalcone	1
1.2 Claisen-Schmidt Condensation	2
1.3 Mannich Base	3
1.4 Antioxidant Activity of Phenolic Compounds	5
1.5 DPPH Radical Scavenging Capacity Assay	6
1.6 Hypothesis	8
1.7 Objectives	8
2 LITERATURE REVIEW	9
2.1 Synthesis of Chalcone Derivatives	9
2.2 Synthesis of Chalcone Derived Mannich Bases	11
2.3 Antioxidant Activity of the Chalcone and Mannich Base Derivatives	14
3 MATERIALS AND METHODOLOGY	20
3.1 Materials	20

3.2	Instrumentation	22
3.3	Methodology	23
3.3.1	Synthesis of Chalcones	23
3.3.2	Synthesis of Chalcone Mannich Base Derivatives	24
3.3.3	Thin Layer Chromatography (TLC) Analysis	25
3.3.4	Characterization of Chalcone Derivatives	26
3.3.5	DPPH Radical Scavenging Capacity Assay	27
4	RESULTS AND DISCUSSION	29
4.1	Molecular Structure of Compounds	29
4.2	Physical Properties of Compounds	30
4.3	Fourier Transform Infrared (FTIR) Spectroscopy	33
4.4	Liquid Chromatography-Mass Spectroscopy (LC-MS)	41
4.5	Nuclear Magnetic Resonance (NMR) Spectroscopy	46
4.5.1	Structural Elucidation of 4-Chloro-4'-hydroxychalcone	46
4.5.2	Structural Elucidation of 4-Chloro-4'-hydroxy-3'-dimethylaminomethylchalcone	58
4.5.3	Structural Elucidation of 4-Chloro-4'-hydroxy-3'-pyrrolidinomethylchalcone	69
4.5.4	Structural Elucidation of 4-Chloro-4'-hydroxy-3'-piperidinomethylchalcone	78
4.6	DPPH Radical Scavenging Capacity Assay	82
5	CONCLUSION	87
5.1	Conclusion	87
5.2	Further Studies	88
	REFERENCES	89
	APPENDICES	92

LIST OF TABLES

Table		Page
2.1	Compound's name and substituents on chalcones 1-8	11
2.2	Substituents on the chalcone derivatives 3a-5	14
2.3	Antioxidant activity of the chalcone derivatives 3a-5	15
2.4	Antioxidant activity evaluation of chalcones C1-C7	17
2.5	Antioxidant activity evaluation of Mannich base derivatives 7an, 8a-b, 9a-b and 10a-b	19
3.1	Chemicals used in the synthesis of chalcones	20
3.2	Chemicals used in the synthesis of chalcone Mannich base derivatives	21
3.3	Material and chemicals used in TLC analysis	21
3.4	Chemicals used in characterization of the chalcones derivatives	21
3.5	Chemicals used in DPPH antioxidant assay test	22
3.6	Instruments used in this study	22
3.7	Starting materials used to synthesize the chalcones	23
3.8	Starting materials used to synthesize the Mannich base derivatives	24
4.1	Molecular structure of compounds CA , CA2 , DA , DA2 , PY , PY2 , PI and PI2	29
4.2	Physical properties of the compounds CA , CA2 , DA , DA2 , PY , PY2 , PI and PI2	31
4.3	FTIR spectral data of compound CA and CA2	33
4.4	FTIR spectral data of compound DA , DA2 , PY , PY2 , PI and PI2	37
4.5	LC-MS spectral data of the synthesized compounds	41
4.6	¹ H, ¹³ C and DEPT NMR spectral data of CA	49
4.7	¹ H – ¹³ C correlations in CA	50
4.8	¹ H, ¹³ C and DEPT NMR spectral data of DA	60
4.9	¹ H – ¹³ C correlations in DA	61
4.10	¹ H, ¹³ C and DEPT NMR spectral data of PY	71

4.11	$^1\text{H} - ^{13}\text{C}$ correlations in PY	72
4.12	^1H and ^{13}C NMR spectral data of PI	79
4.13	% DPPH radical scavenging of compounds CA , CA2 , DA and DA2 at different concentrations	82
4.14	% DPPH radical scavenging of compounds PY , PY2 , PI and PI2 at different concentrations.	82
4.15	IC_{50} values of the synthesized chalcones and their Mannich base derivatives	83
4.16	% DPPH radical scavenging of ascorbic acid at different concentrations	84

LIST OF FIGURES

Figure	Page	
1.1	General structure of chalcone	1
1.2	Claisen-Schmidt condensation	2
1.3	Mechanism scheme for the synthesis of chalcone	3
1.4	Mannich reaction	4
1.5	Mechanism scheme of the Mannich reaction	4
1.6	The DPPH reaction	7
2.1	Reaction schemes of the chalcones synthesized	9
2.2	Reagents and conditions of synthesis: (i) 40 % NaOH, ethanol, stir overnight at room temperature; (ii) secondary amine (R = morpholine, piperidine, diethylamine), formaldehyde, ethanol, stir overnight	11
2.3	Structure of the Mannich bases synthesized	12
2.4	Structure of the 4'-hydroxychalcones (1A, 2A) and Mannich base derivatives (1B, 2B) synthesized	12
2.5	Synthetic scheme of Mannich bases 3 and 4 from the 4'-hydroxychalcones 1 and 2. Reagents and conditions for synthesis: (i) 4-ClC ₆ H ₄ CHO/NaOH/MeOH, 24 hours (reflux); (ii) 3-OCH ₃ C ₆ H ₄ CHO/NaOH/MeOH, 24 hours (reflux); (iii) CH ₂ =N ⁺ (CH ₃)Cl ⁻ /ACN, 78 hours (reflux), HCl(g)/diethyl ether; (iv) C ₄ H ₅ NO/formalin/HCl/EtOH, 96 hours (reflux), HCl(g)/diethyl ether	13
2.6	Substituents on the chalcones C1-C7 and their percentage yields	16
2.7	Reagents and conditions of synthesis: (i) <i>m</i> -hydroxybenzaldehyde, 50 % KOH, EtOH, r.t., 4-24 hours; (ii) paraformaldehyde, secondary amine (HNRR'), EtOH, reflux for 24-48 hours; (iii) AlCl ₃ , CH ₂ Cl ₂ , r.t., 6 hours	18
4.1	FTIR spectrum of CA (KBr)	34
4.2	FTIR spectrum of CA2 (KBr)	35

4.3	FTIR spectrum of DA (KBr)	38
4.4	FTIR spectrum of PY (KBr)	39
4.5	FTIR spectrum of PI (KBr)	40
4.6	LC-MS spectrum and spectrum identification of CA	42
4.7	LC-MS spectrum and spectrum identification of DA	43
4.8	LC-MS spectrum and spectrum identification of PY	44
4.9	LC-MS spectrum and spectrum identification of PI	45
4.10	Expanded (downfield region) ¹ H NMR spectrum of 4-chloro-4'-hydroxychalcone (400 MHz, DMSO-d ₆)	51
4.11	¹ H NMR spectrum of 4-chloro-4'-hydroxychalcone (CA) (400 MHz, DMSO-d ₆)	52
4.12	Expanded (downfield region) ¹³ C NMR spectrum of 4-chloro-4'-hydroxychalcone (CA) (100 MHz, DMSO-d ₆)	53
4.13	¹³ C NMR spectrum of 4-chloro-4'-hydroxychalcone (CA) (100 MHz, DMSO-d ₆)	54
4.14	DEPT NMR spectrum of 4-chloro-4'-hydroxychalcone (CA)	55
4.15	Expanded (downfield region) HMQC spectrum of 4-chloro-4'-hydroxychalcone (CA)	56
4.16	Expanded (downfield region) HMBC spectrum of 4-chloro-4'-hydroxychalcone (CA)	57
4.17	Expanded (downfield region) ¹ H NMR spectrum of 4-chloro-4'-hydroxy-3'-dimethylaminomethylchalcone (DA) (400 MHz, CDCl ₃)	62
4.18	¹ H NMR spectrum of 4-chloro-4'-hydroxy-3'-dimethylaminomethylchalcone (DA) (400 MHz, CDCl ₃)	63
4.19	Expanded (downfield region) ¹³ C NMR spectrum of 4-chloro-4'-hydroxy-3'-dimethylaminomethylchalcone (DA) (100 MHz, CDCl ₃)	64
4.20	¹³ C NMR spectrum of 4-chloro-4'-hydroxy-3'-dimethylaminomethylchalcone (DA) (100 MHz, CDCl ₃).	65

4.21	DEPT NMR spectrum of 4-chloro-4'-hydroxy-3'-dimethylaminomethylchalcone (DA)	66
4.22	HMQC NMR spectrum of 4-chloro-4'-hydroxy-3'-dimethylaminomethylchalcone (DA)	67
4.23	HMBC NMR spectrum of 4-chloro-4'-hydroxy-3'-dimethylaminomethylchalcone (DA)	68
4.24	¹ H NMR spectrum of 4-chloro-4'-hydroxy-3'-pyrrolidinomethylchalcone (PY) (400 MHz, CDCl ₃)	73
4.25	¹³ C NMR spectrum of 4-chloro-4'-hydroxy-3'-pyrrolidinomethylchalcone (PY) (100 MHz, CDCl ₃)	74
4.26	DEPT NMR spectrum of 4-chloro-4'-hydroxy-3'-pyrrolidinomethylchalcone (PY)	75
4.27	HMQC NMR spectrum of 4-chloro-4'-hydroxy-3'-pyrrolidinomethylchalcone (PY)	76
4.28	HMBC NMR spectrum of 4-chloro-4'-hydroxy-3'-pyrrolidinomethylchalcone (PY)	77
4.29	¹ H NMR spectrum of 4-chloro-4'-hydroxy-3'-piperdinomethylchalcone (PI) (400 MHz, CDCl ₃)	80
4.30	¹³ C NMR spectrum of 4-chloro-4'-hydroxy-3'-piperdinomethylchalcone (PI) (100 MHz, CDCl ₃)	81
4.31	Graph of % DPPH radical scavenging against concentration of the chalcone and Mannich base derivatives	83
4.32	Graph of % DPPH radical scavenging against concentration of ascorbic acid	85

LIST OF ABBREVIATIONS

<i>m/z</i>	Mass-to-charge ratio
<i>J</i>	Coupling constant
AlCl ₃	Aluminium chloride
AR	Analytical reagent
BF ₃ -Et ₂ O	Boron trifluoride etherate
CDCl ₃	Deuterated chloroform
CH ₂ Cl ₂	Dichloromethane
DEPT	Distortionless Enhancement by Polarization Transfer
DMSO-d ₆	Deuterated dimethyl sulfoxide
DPPH	2,2-diphenyl-1-picrylhydrazyl
EtOH	Ethanol
FTIR	Fourier transform infrared spectroscopy
HCl	Hydrochloric acid
HMBC	Heteronuclear Multiple Bond Correlation
HMQC	Heteronuclear Single Quantum Coherence
HPLC	High-performance liquid chromatography
IC ₅₀	Half maxima inhibitory concentration
KOH	Potassium hydroxide
LC-MS	Liquid chromatography-mass spectrometry
Min	Minutes
NaOH	Sodium hydroxide
NaH	Sodium Hydride
NMR	Nuclear Magnetic Resonance
OH	Hydroxyl
r.t.	Room temperature
ROS	Reactive oxygen species
TLC	Thin-layer chromatography
UV	Ultraviolet
w/v	Weight by volume

CHAPTER 1

INTRODUCTION

1.1 Chalcone

Chalcone, also known as 1,3-diphenyl-2-propene-1-one, is a polyphenolic compound that belongs to the group of flavonoid. It can be obtained both naturally and synthetically. The general molecular formula of a chalcone is $C_{15}H_{12}O$ and its core structure contains two aromatic rings that are linked through a three-carbon- α,β -unsaturated carbonyl system. The ring directly connected to the ketone is commonly labelled as ring A, while the other is referred as ring B. Figure 1.1 shows the general structure and numbering scheme of a chalcone.

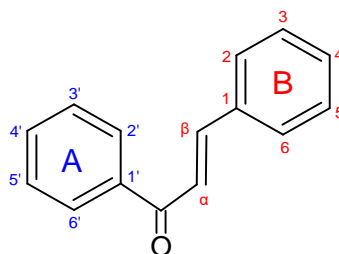


Figure 1.1: General structure of chalcone.

It has been reported that chalcones exhibit a wide variety of biological activity, including antibacterial, antiviral, anti-inflammatory, antioxidant, antiulcer, anticancer, antimalarial, insecticidal, amoebicidal and cytotoxic anti-HIV activities (Koçyiğit, Gezezen and Taslimi, 2020).

1.2 Claisen-Schmidt Condensation

The Claisen-Schmidt condensation is a classical method used to synthesize chalcones and their derivatives. It involves the condensation of an aromatic aldehyde with an aromatic ketone in a suitable polar solvent at about 50 – 100 °C for several hours in the presence of an acid or a base catalyst. The schematic representation of general Claisen-Schmidt condensation is shown in Figure 1.2.

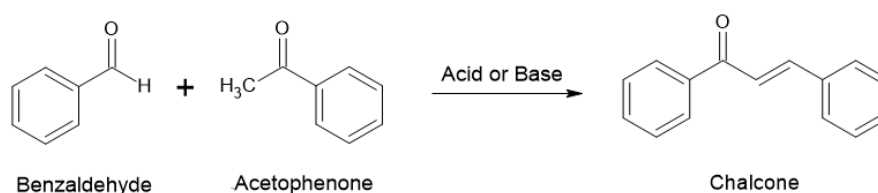


Figure 1.2: Claisen-Schmidt condensation.

Under base catalysis, the formation of chalcone occurs from an aldol product via dehydration of the enolate mechanism. As for acid catalysis, the product is formed via the enol mechanism. The common base reagents used include NaOH, KOH and NaH, while Bronsted acids and Lewis acids such as HCl and BF₃-Et₂O have been employed in the acid-catalysed Claisen-Schmidt condensation. Generally, base catalysis is more widely used in the synthesis of chalcones comparing to acid catalysis (Rammohan, et al., 2020).

The Claisen-Schmidt condensation reaction under base catalysis begins with the removal of alpha proton of the acetophenone by a strong base, giving a resonance-stabilized enolate ion. Subsequently, the enolate ion

initiates a nucleophilic attack on the carbonyl carbon belonging to the benzaldehyde, leading to the formation of an alkoxide ion with excess electron charge on the oxygen atom. Next, the alkoxide ion takes proton from the solvent molecule to form the aldol compound, a β -hydroxyketone, thereby regenerating the base catalyst at the same time. Finally, dehydration of the aldol compound takes place spontaneously, giving a conjugated α, β unsaturated ketone, which is also known as the chalcone (Susanti and Setyowati, 2019). The general mechanism scheme for the chalcone synthesis is shown in Figure 1.3.

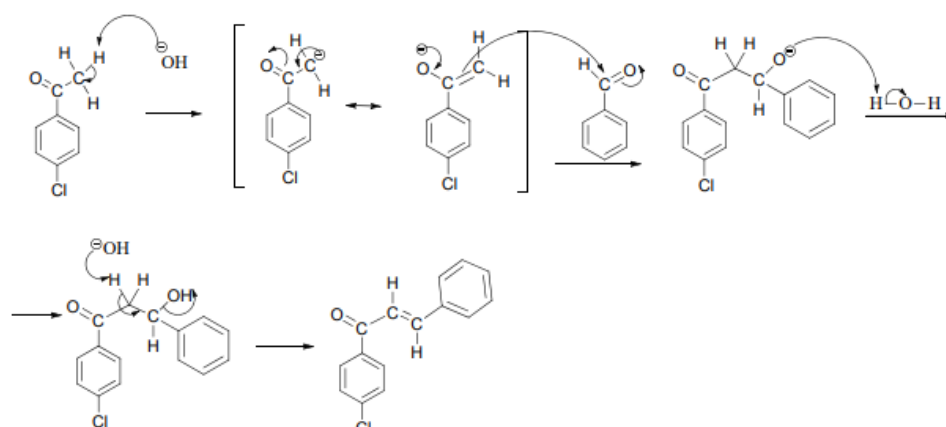


Figure 1.3: Mechanism scheme for the synthesis of chalcone
(The Royal Society of Chemistry, 2017).

1.3 Mannich Base

Mannich bases are compounds consisting of beta-amino ketone that are synthesized through the Mannich reaction. The Mannich reaction occurs via a nucleophilic addition reaction which involves a compound consisting active hydrogen(s) being condensed with a primary or secondary amine and

a nonenolizable aldehyde, typically formaldehyde. The general reaction scheme of Mannich reaction is represented in Figure 1.4.

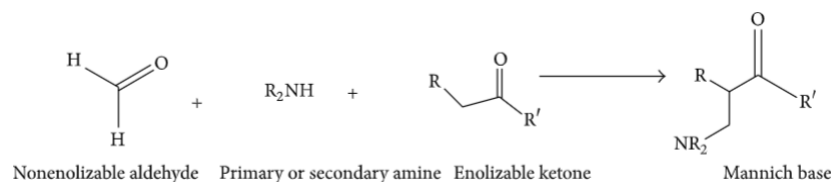


Figure 1.4: Mannich reaction (Bala, et al., 2014).

The Mannich reaction is initiated by the formation of an iminium ion through the nucleophilic addition of the amine to the formaldehyde, which also results in the loss of a water molecule. The enolizable ketone is then converted into enol form, and the enol subsequently attacks the iminium ion at the positively charged carbon adjacent to the nitrogen atom. This yields a β -aminocarbonyl compound, which is the Mannich product (Vutturi, 2011). The schematic diagram of the mechanism of Mannich reaction is shown in Figure 1.5.

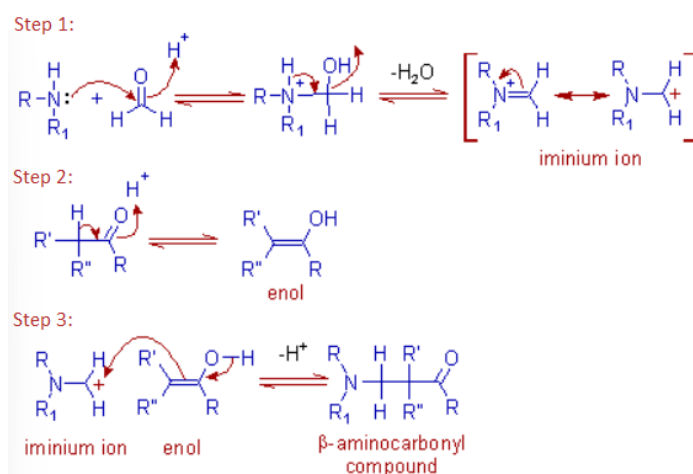


Figure 1.5: Mechanism scheme of the Mannich reaction (Vutturi, 2011).

The chalcone derived Mannich bases also exhibit many useful medicinal properties, such as antimicrobial, antiviral, anti-inflammatory, antioxidant, anticancer, antimalarial, anti-HIV, anti-Alzheimer, anthelmintic, analgesic and so forth (Marinescu, et al., 2020).

1.4 Antioxidant Activity of Phenolic Compounds

Reactive oxygen species (ROS) are constantly being generated in our bodies during normal cell aerobic respiration. Besides, they are also being produced by neutrophils which are involved in the host defence system of our bodies. The neutrophils achieve this role by generating ROS, which act as potent antimicrobial oxidant to destroy the pathogenic microorganisms. However, this oxidative stress produced by the free radicals from ROS can damage biomolecules such as cellular proteins, membrane lipids and nucleic acids. This process is associated to the pathological process of aging and also several diseases such as cancer, arteriosclerosis, certain tumours, cardiovascular disease and Alzheimer's disease (Leopoldini, et al., 2004; Sökmen and Khan, 2017; Xue, et al., 2013).

Therefore, antioxidants play a crucial role in neutralising and inactivating these ROS free radicals, thereby protecting the biomolecules from undergoing oxidative damage. Phenolic compounds are potent antioxidants that react with a variety of free radicals. The antioxidant activity of phenolic compounds is contributed by their strong chain-breaking actions and ability to scavenge free radicals by the transfer of a hydrogen atom from their phenolic hydroxyl group (Xue, et al., 2013). Their antioxidant capacity, on

the other hand, is affected by multiple factors, including their molecular structures, particularly the number and position of the hydroxyl group present in the structure, and the nature of substituents on the aromatic rings (Minatel, et al., 2017).

Chalcones, which consist of two phenyl rings in their general structure, are polyphenols when attached to hydroxyl group(s). Hence, they are expected to show antioxidant activity. Besides, the antioxidant properties of chalcones are hypothesized to be also contributed by the conjugated α , β unsaturated bond and the delocalized π electrons over the aromatic rings. It has been reported that chalcones with hydroxyl groups substituted at *ortho* or *para* positions show especially high antioxidant activity compared to that of *meta* position due to enhanced stability of the semiquinone radicals they form. Additionally, halogenated chalcones have also been known as stronger antioxidants than their corresponding non-halogenated chalcones, with bromine and fluorine derivatives showing higher antioxidant potential over that of chlorine (Prabhakar, Iqbal and Balasubramanian, 2019).

1.5 DPPH Radical Scavenging Capacity Assay

DPPH radical scavenging capacity assay is one of the most common spectrophotometric methods used to determine the antioxidant activity of a compound. It works by measuring the extent of colour decay of the DPPH reagent when interacted with an antioxidant. DPPH is an unstable free radical consisting of an odd electron, and it absorbs at the maximum wavelength of 517 nm. When reacted with an antioxidant or a reducing

agent, the antioxidant or reducing agent may supply an extra electron or hydrogen to the DPPH free radical. As a result, it bleaches the black-purple DPPH to a colourless or yellow solution, as shown in Figure 1.6.



Figure 1.6: The DPPH reaction (Behrendorff, et al., 2013).

The radical scavenging capacity of a compound can be evaluated by determining the IC₅₀ (half maxima inhibitory concentration) value of the compound, which is the concentration of the sample required to inhibit 50 % of the DPPH free radical. Lower IC₅₀ value indicates lower concentration is needed to reduce the DPPH radical by 50 %, and hence, higher antioxidant ability of a compound. The IC₅₀ value of a sample can be obtained by reacting the DPPH reagent with the sample at different concentrations, then measuring the absorbance after a fixed period of time. The percentage of DPPH radical scavenging can be calculated using the equation below:

$$\% \text{ DPPH radical scavenging} = \frac{\text{Blank absorbance} - \text{Sample absorbance}}{\text{Blank absorbance}} \times 100 \%$$

1.6 Hypothesis

Chalcone and its derivatives possess a broad spectrum of useful pharmacological activity. Particularly, they can act as antioxidants which help in the treatment of various diseases such as cancer, heart diseases and neurodegenerative diseases such as Alzheimer's disease and Parkinson's disease. This project studies the antioxidant activity of different chalcones and their derivatives and how the antioxidant activity is affected by the substituents on the chalcones.

1.7 Objectives

The objectives of this project are:

1. To synthesize chalcone derivatives through Claisen-Schmidt condensation.
2. To synthesize chalcone Mannich base derivatives through Mannich reaction.
3. To characterize the synthesized chalcones and Mannich base derivatives using FTIR, LC-MS and NMR analysis.
4. To study the antioxidant activity of the synthesized chalcones and Mannich base derivatives using DPPH antioxidant assay.

CHAPTER 2

LITERATURE REVIEW

2.1 Synthesis of Chalcone Derivatives

Attarde, et al. (2014) have studied the synthesis of chalcone derivatives through Claisen-Schmidt condensation. They have synthesized four different chalcones by reacting acetophenone with benzaldehyde consisting of different substituted groups, including 4-nitro, 4-hydroxy, 4-chloro and furfural. The synthesis was performed under base catalysis with 30 % NaOH as the catalyst and ethanol as the solvent. The reaction mixture was stirred in iced cold water bath until solidification had started, and the reaction mixture was then kept under cold condition overnight for the solidification process to take place.

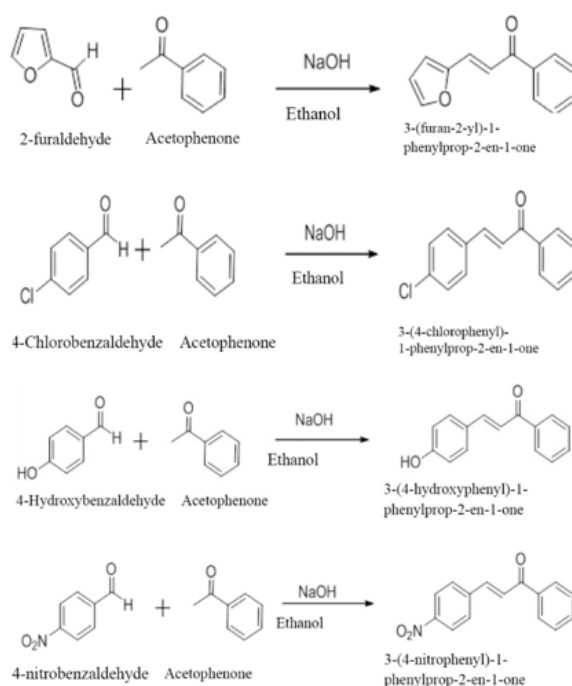


Figure 2.1: Reaction schemes of the chalcones synthesized (Attarde, et al., 2014).

Similar study was performed by Amole, Bello and Oyewale (2019). They have synthesized three 2-hydroxychalcone derivatives, namely 3-(4'-methoxyphenyl)-1-(2-hydroxyphenyl)prop-2-en-1-one, 3-(4'-methoxyphenyl)-1-(2-hydroxyphenyl)prop-2-en-1-one and 3-(2'-chlorophenyl)-1-(2-hydroxyphenyl)prop-2-en-1-one, through the base-catalyzed Claisen-Schmidt condensation of 2-hydroxyacetophenone with 4'-methyl-, 4'-methoxyl- and 2'-chloro- benzaldehyde, respectively. 50 % NaOH was used as the base catalyst and absolute ethanol was used as the solvent in this study. The reaction mixture was refluxed under constant stirring for five hours. The yields of the products ranged from 66 to 81 %.

Furthermore, the synthesis of 2'-hydroxychalcone derivatives was performed by Kristanti, et al. (2020). Eight chalcones, as listed in Table 2.1, were synthesized through the Claisen-Schmidt condensation of 2'-hydroxyacetophenone and various benzaldehyde derivatives in ethanol using 40 % NaOH as catalyst. The reaction mixture was stirred at below 10 °C for one hour before it was allowed to stir overnight for the reaction to take place. The products formed were recrystallized using ethanol, giving yields between 40 and 90 %.

Table 2.1: Compound's name and substituents on chalcones 1-8.

Compounds	R	Compound's Name
1	2-OMe	2-methoxy-2'-hydroxychalcone
2	3-OMe	3-methoxy-2'-hydroxychalcone
3	4-OMe	4-methoxy-2'-hydroxychalcone
4	2,4-diOMe	2,4-dimethoxy-2'-hydroxychalcone
5	2,5-diOMe	2,5-dimethoxy-2'-hydroxychalcone
6	4-(N,N-diCH ₃)	4-N,N-dimethyl-2'-hydroxychalcone
7	4-F	4-fluoro-2'-hydroxychalcone
8	4-Cl	4-chloro-2'-hydroxychalcone

2.2 Synthesis of Chalcone Derived Mannich Bases

In the study by Syahri, et al. (2020), a 4'-chlorochalcone derivative was first synthesized from 4-chloroacetophenone and vanillin. Subsequently, four Mannich base derivatives were synthesized by reacting the chalcone derivative with formaldehyde and multiple secondary amines, including morpholine, piperidine and diethylamine through the Mannich reaction. Ethanol was used as the solvent, and the reaction was refluxed for 24 hours. The yields of the products ranged from 70 to 80 %.

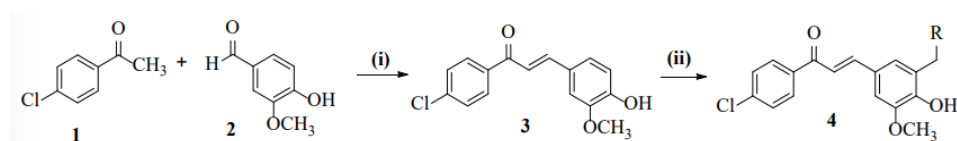


Figure 2.2: Reagents and conditions of synthesis: (i) 40 % NaOH, ethanol, stir overnight at room temperature; (ii) secondary amine (R = morpholine, piperidine, diethylamine), formaldehyde, ethanol, stir overnight (Syahri, et al., 2020).

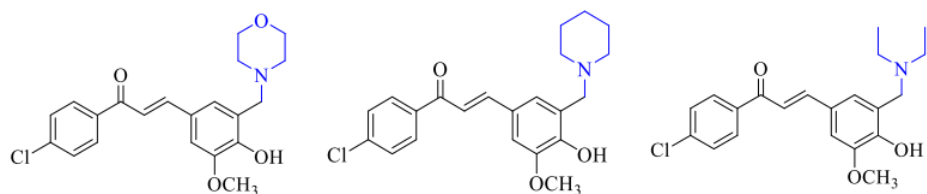


Figure 2.3: Structure of the Mannich bases synthesized (Syahri, et al., 2020).

On the other hand, Rozmer, et al. (2020) have performed the study on the synthesis of Mannich base derivatives from 4'-hydroxychalcone. The Mannich derivatives **1B** and **2B** were synthesized from 4'-hydroxychalcone **1A** and **2A** through Mannich reaction. The synthesis was carried out by first refluxing the secondary amine with excess formaldehyde in ethanol for two hours. Then, the chalcone derivative was added into the reaction medium, followed by a few drops of 37 % HCl, and the reaction mixture was stirred for 96 hours. The yield of the Mannich base **1B** obtained was 39 %.

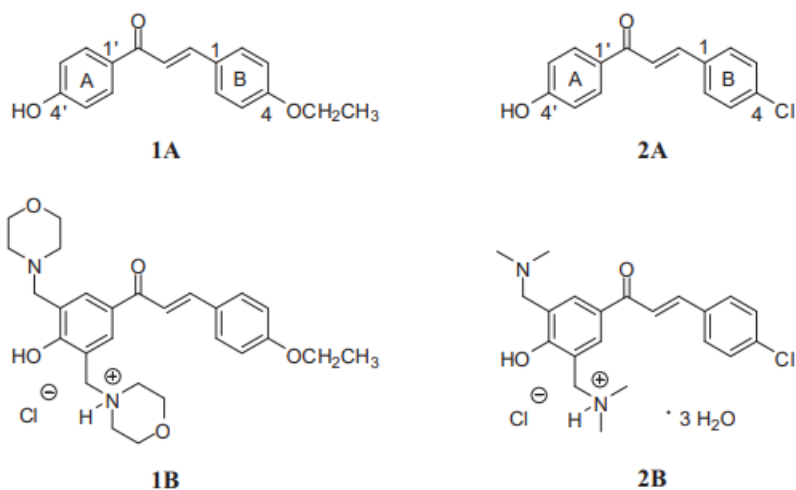


Figure 2.4: Structure of the 4'-hydroxychalcones (**1A**, **2A**) and Mannich base derivatives (**1B**, **2B**) synthesized (Rozmer, et al., 2020).

The synthesis of Mannich base derivatives from 4'-hydroxychalcone was also performed by Bernardes, et al. (2017). In this study, the Mannich chalcone **3** was synthesized from the 4'-hydroxychalcone **1** using the Mannich reagent *N,N*-dimethylmethyleiminium chloride. The hydroxychalcone was first dissolved in acetonitrile, followed by the addition of Mannich reagent. The reaction mixture was then heated under reflux for 78 hours. Upon completion of the reaction, a hydrogen chloride solution in diethyl ether was added to obtain the corresponding hydrochloride salt. The yield obtained was 78 %. While the Mannich base **4** was synthesized from 4'-hydroxychalcone **2** using the same method as in the study by Rozmer, et al. (2020).

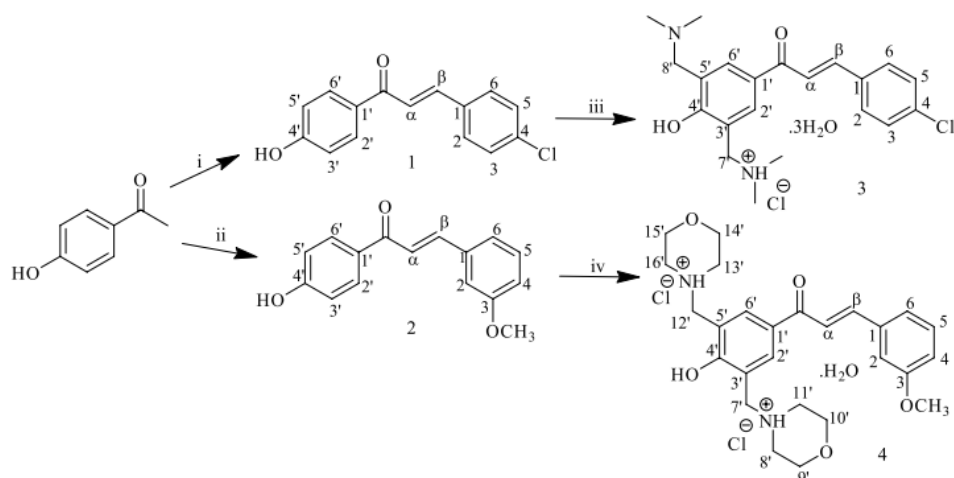


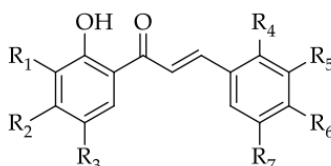
Figure 2.5: Synthetic scheme of Mannich bases **3** and **4** from the 4'-hydroxychalcones **1** and **2**. Reagents and conditions for synthesis:

- (i) 4-ClC₆H₄CHO/NaOH/MeOH, 24 hours (reflux);
 - (ii) 3-OCH₃C₆H₄CHO/NaOH/MeOH, 24 hours (reflux);
 - (iii) CH₂=N⁺(CH₃)Cl⁻/ACN, 78 hours (reflux), HCl(g)/diethyl ether;
 - (iv) C₄H₅NO/formalin/HCl/EtOH, 96 hours (reflux), HCl(g)/diethyl ether
- (Bernades, et al., 2017).

2.3 Antioxidant Activity of the Chalcone and Mannich Base Derivatives

In the study conducted by Kostopoulou, et al. (2021), the antioxidant activity of a series of 2'-hydroxychalcone derivatives, as listed in Table 2.2, was studied. The compounds were treated with 100 μ M of ethanolic DPPH solution and allowed to stand for 20 or 60 min before the absorbance was read at 517 nm. The percentage of DPPH radical scavenging of the chalcones is shown in Table 2.3.

Table 2.2: Substituents on the chalcone derivatives **3a-5**.



Compound	R ₁	R ₂	R ₃	R ₄	R ₅	R ₆	R ₇
3a	H	OMOM	H	H	OMOM	OMOM	H
3b	H	H	H	OCH ₃	H	OCH ₃	OCH ₃
3c	H	OMOM	H	OCH ₃	H	OCH ₃	OCH ₃
3d	H	H	Cl	H	OCH ₃	OCH ₃	H
3e	H	H	Cl	OCH ₃	OCH ₃	H	H
3f	H	H	Br	H	OCH ₃	OCH ₃	H
3g	Br	H	Br	H	OCH ₃	OCH ₃	H
3h	H	H	Br	H	OMOM	OMOM	H
3i	Br	H	Br	H	OMOM	OMOM	H
3j	H	H	H	H	H	COOH	H
3k	H	H	Cl	H	H	COOH	H
3l	H	H	H	H	H	H	H
4a	H	OH	H	H	OH	OH	H
4b	H	H	Br	H	OH	OH	H
5	H	H	H	H	H	COOCH ₃	H

Table 2.3: Antioxidant activity of the chalcone derivatives **3a-5**.

Compound	Interaction with the Free Radical DPPH (%)	
	20 min	60 min
3a	18.9	21.6
3b	No	No
3c	No	2.3
3d	No	No
3e	No	No
3f	No	No
3g	No	No
3h	5.3	6.0
3i	No	No
3j	No	No
3k	No	No
3l	No	No
4a	95.7	95.3
4b	82.4	82.0
5	No	No

The results revealed that chalcone derivatives consisting of -OCH₃ and -OMOM substituents at ring B possess totally no (**3f**, **3g**, **3i**) or insignificant (**3a**, **3h**) antioxidant activity. Their hydroxylated analogues **4a** and **4b**, however, showed remarkable antioxidant activity with DPPH scavenging ability of up to 95.7 % and 82.4 %, respectively. All the studied compounds possessed phenolic hydroxyl (OH) group which could contribute to the antioxidant activity of the compounds. However, as the phenolic OH group was substituted at position 2' of ring A, it would form strong hydrogen bonding with the adjacent carbonyl oxygen. This consequently interrupted

the interaction between OH group and DPPH free radical. On the other hand, the antioxidant activity of the chalcones **4a** and **4b** was greatly enhanced by other OH groups and the Br group in **4b** substituted at different positions of the compounds.

The antioxidant activity of various substituted chalcones has also been studied by Rashdan, et al. (2018). The chalcone derivatives as shown in Figure 2.6 were prepared through Claisen-Schmidt condensation.

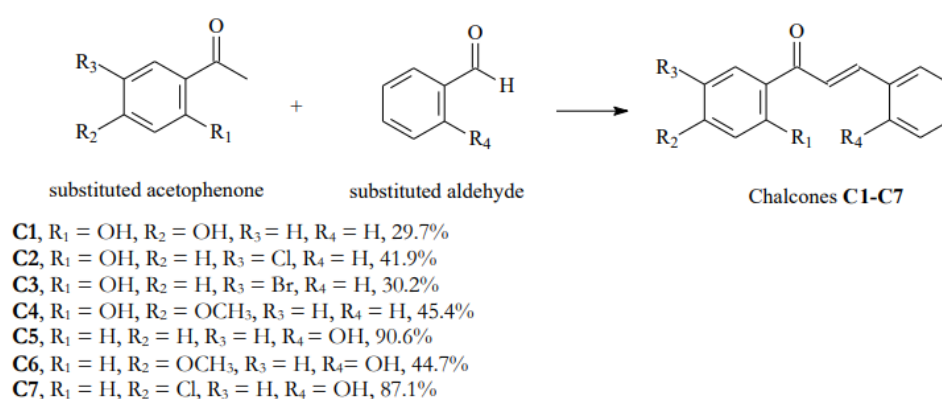
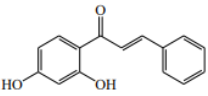
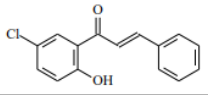
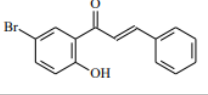
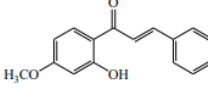
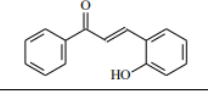
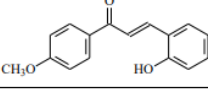
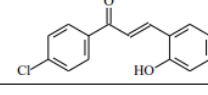


Figure 2.6: Substituents on the chalcones **C1-C7** and their percentage yields (Rashdan, et al., 2018).

The synthesized chalcones were then prepared at concentrations ranging from 25 to 200 µg/mL and treated with 2 mL of 45 mg/L methanolic DPPH solution. The mixture was allowed to stand for 30 min before the absorbance of the mixture was read at 517 nm. The percentage of DPPH scavenging at different concentrations and IC₅₀ values of the compounds are listed in Table 2.4.

Table 2.4: Antioxidant activity evaluation of chalcones **C1-C7**.

Chalcone	Chalcone structure	% antioxidant activity (mean \pm S*)				IC ₅₀ μ g/mL	IC ₅₀ mM
		25 μ g/mL	50 μ g/mL	100 μ g/mL	200 μ g/mL		
C1		36.56 \pm 1.4	40.73 \pm 1.2	50.67 \pm 2.3	60.24 \pm 1.1	87.5	364
C2		40.66 \pm 1.0	41.32 \pm 2.0	43.85 \pm 1.0	51.17 \pm 0.6	187.1	723
C3		36.53 \pm 2.5	44.02 \pm 0.8	46.69 \pm 0.2	58.68 \pm 1.2	124.0	409
C4		37.65 \pm 1.2	42.22 \pm 0.9	43.58 \pm 0.6	56.97 \pm 0.8	140.4	552
C5		21.99 \pm 2.2	31.44 \pm 1.1	32.37 \pm 1.3	50.95 \pm 0.3	198.0	883
C6		29.02 \pm 2.2	31.75 \pm 2.3	34.08 \pm 1.2	48.65 \pm 1.3	221.0	868
C7		29.42 \pm 1.0	34.05 \pm 1.7	36.22 \pm 1.6	53.87 \pm 2.3	179.3	693

Zhang, et al. (2019) have performed a study on the antioxidant activity of several Mannich bases synthesized from 3'-hydroxychalcone derivatives, as shown in Figure 2.7, using the oxygen radical absorbance capacity assay which uses fluorescein (ORAC-FL). Trolox, a water-soluble vitamin E analogue, was used as the standard and the antioxidant capacity of the compounds was expressed in Trolox equivalent, as listed in Table 2.5.

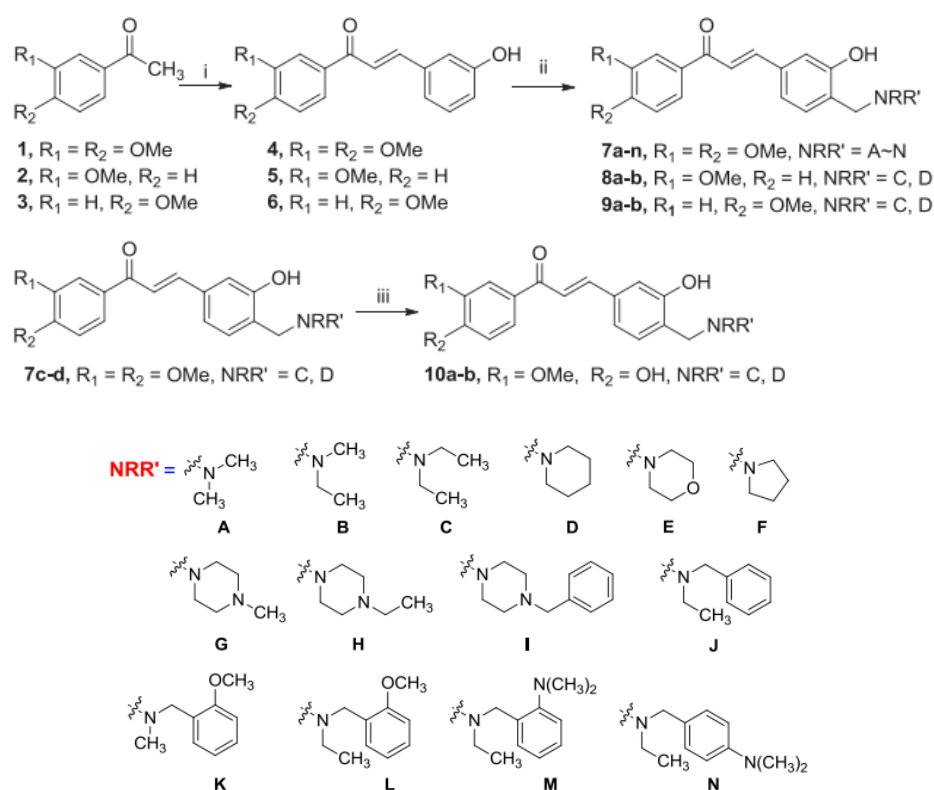


Figure 2.7: Reagents and conditions of synthesis: (i) *m*-hydroxybenzaldehyde, 50 % KOH, EtOH, r.t., 4-24 hours; (ii) paraformaldehyde, secondary amine (HNRR'), EtOH, reflux for 24-48 hours; (iii) AlCl₃, CH₂Cl₂, r.t., 6 hours (Zhang, et al., 2019).

Table 2.5: Antioxidant activity evaluation of Mannich base derivatives **7a-n**, **8a-b**, **9a-b** and **10a-b**.

Compound	ORAC	Compound	ORAC
7a	1.99	7k	1.49
7b	2.21	7l	1.56
7c	1.93	7m	1.69
7d	1.34	7n	1.86
7e	1.76	8a	1.51
7f	1.89	8b	1.17
7g	1.81	9a	1.28
7h	1.76	9b	1.19
7i	0.99	10a	0.96
7j	1.31	10b	1.13

Based on the results, all the Mannich base derivatives showed moderate to good antioxidant activity with ORAC-FL values ranging from 0.96 to 2.21 Trolox equivalent. Zhang, et al. (2019) concluded that the antioxidant capacity of the Mannich bases may be influenced by the number of methoxy group within the compound. Besides, compounds substituted with aliphatic amine also showed better antioxidant activity than those substituted with benzylamine.

CHAPTER 3

MATERIALS AND METHODOLOGY

3.1 Materials

Tables 3.1 and 3.2 show the chemicals used in the synthesis of chalcones and their derivatives. Table 3.3 shows the material and chemicals used in the TLC analysis, while Table 3.4 shows the chemicals used during characterization of the synthesized products. Table 3.5 shows the chemicals used in the DPPH antioxidant assay test.

Table 3.1: Chemicals used in the synthesis of chalcones.

Chemicals	Molecular Formula	Manufacturer
4-chlorobenzaldehyde (AR grade)	C ₇ H ₅ ClO	Acros Organics
Benzaldehyde (AR grade)	C ₇ H ₆ O	Acros Organics
4'-hydroxyacetophenone (AR grade)	C ₈ H ₈ O ₂	Merck
Absolute ethanol	C ₂ H ₆ O	HmbG Chemicals
Sodium hydroxide	NaOH	R&M Chemicals
Hydrochloric acid	HCl	Fischer Scientific

Table 3.2: Chemicals used in the synthesis of chalcone Mannich base derivatives.

Chemicals	Molecular Formula	Manufacturer
Formaldehyde	CH ₂ O	Merck
Acetonitrile	C ₂ H ₃ N	RCI Labscan
Piperidine	C ₅ H ₁₁ N	Acros Organics
Pyrrolidine	C ₅ H ₁₁ N	Merck
Dimethylamine	C ₂ H ₇ N	Merck
Absolute ethanol	C ₂ H ₆ O	HmbG Chemicals
Acetone	C ₃ H ₆ O	Bendosen

Table 3.3: Material and chemicals used in TLC analysis.

Chemicals	Molecular Formula	Manufacturer
Acetone (Industrial grade)	C ₃ H ₆ O	LabServ
Hexane (Industrial grade)	C ₆ H ₁₄	R&M Chemicals
Chloroform (Industrial grade)	CHCl ₃	System
TLC silica gel 60 F254	-	Merck

Table 3.4: Chemicals used in characterization of the chalcones derivatives.

Chemicals	Molecular Formula	Manufacturer
Deuterated dimethyl sulfoxide	DMSO ₄ -D ₆	Merck
Deuterated chloroform	CDCl ₄	Acros Organics
Methanol (HPLC grade)	CH ₃ OH	Fisher Scientific
KBr salt	KBr	Fisher Scientific

Table 3.5: Chemicals used in DPPH antioxidant assay test.

Chemicals	Molecular Formula	Manufacturer
Methanol (AR grade)	CH ₃ OH	Merck
Ascorbic acid	C ₆ H ₈ O ₆	Fisher Scientific
DPPH powder	C ₁₈ H ₁₂ N ₅ O ₆	Aldrich

3.2 Instrumentation

Table 3.6 shows the instruments used in the synthesis and characterization of the chalcone and Mannich base derivatives, and the instruments used in the DPPH antioxidant assay test.

Table 3.6: Instruments used in this study.

Instrument	Manufacturer
Melting Point Apparatus	Stuart, SMP 10
FTIR Spectrometer	Perkin Elmer Spectrum RX1
NMR Spectrometer	JOEL ECX-400
LCMS	Agilent Technologies G6520B
Sonicator	Cole-Parmer EW-08895-07
Rotary Evaporator	Heidolph WB eco Laborota 4000 efficient
Microplate reader	BMG Labtech

3.3 Methodology

3.3.1 Synthesis of Chalcones

Table 3.7: Starting materials used to synthesize the chalcones.

Product Code	Product Name	Starting Materials
CA	4-chloro-4'-hydroxychalcone	4'-hydroxyacetophenone + 4-chlorobenzaldehyde
CA2	4'-hydroxychalcone	4'-hydroxyacetophenone + benzaldehyde

To synthesize **CA**, equimolar portions of 4'-hydroxyacetophenone (20 mmol) and 4-chlorobenzaldehyde (20 mmol) were first dissolved in 6 mL of ethanol. Subsequently, 10 mL of 10 % w/v NaOH solution was added dropwise into the mixture solution. The reaction mixture was stirred at room temperature for 24 hours, until the end of reaction was indicated by TLC. After completion of reaction, 50 mL of cold distilled water was added into the mixture solution, followed by dropwise addition of 10 % w/v HCl with constant stirring. The precipitate formed was then filtered using vacuum filtration and washed with cold distilled water.

Recrystallization was performed on the resulting solid using absolute ethanol. The product was dissolved in hot absolute ethanol and subsequently allowed to cool at room temperature for recrystallization process to take place. The recovered product was later filtered through hot filtration. TLC was performed to ensure the product was pure. The

procedure was repeated with benzaldehyde substituting the 4-chlorobenzaldehyde to obtain **CA2**.

3.3.2 Synthesis of Chalcone Mannich Base Derivatives

Table 3.8: Starting materials used to synthesize the Mannich base derivatives.

Product Code	Product Name	Starting Materials
DA	4-chloro-4'-hydroxy-3'-dimethylaminomethylchalcone	CA + formaldehyde + dimethylamine
DA2	4'-hydroxy-3'-dimethylaminomethylchalcone	CA2 + formaldehyde + dimethylamine
PY	4-chloro-4'-hydroxy-3'-pyrrolidinomethylchalcone	CA + formaldehyde + pyrrolidine
PY2	4'-hydroxy-3'-pyrrolidinomethylchalcone	CA2 + formaldehyde + pyrrolidine
PI	4-chloro-4'-hydroxy-3'-piperidinomethylchalcone	CA + formaldehyde + piperidine
PI2	4'-hydroxy-3'-piperidinomethylchalcone	CA2 + formaldehyde + piperidine

To synthesize the Mannich base derivative of the corresponding chalcone, 0.5 mmol of chalcone was first dissolved in 10 mL of acetonitrile in a 50 mL round-bottom flask. Next, 0.15 mmol of formaldehyde was added and the reaction mixture was stirred at room temperature for 15 min. Subsequently, 0.15 mmol of secondary amine was added and the reaction mixture was further stirred for another 30 min under room temperature. The

reaction mixture was then refluxed for 48 hours at 70 °C. The progression of the reaction was monitored using TLC.

Once the completion of reaction had been indicated by TLC, the reaction was stopped, and the mixture was subjected to rotary evaporation to remove all the solvent. A small amount of acetone was added to dissolve the resulting product left in the round-bottom flask. The mixture solution was then poured into a sample vial and allowed to dry under air. The mass of the Mannich base derivative formed was measured and recorded after it was completely dry, and the percentage yield was calculated.

3.3.3 Thin Layer Chromatography (TLC) Analysis

To prepare the sample, the product was dissolved in small amount of chloroform. A solvent system consisting of hexane and acetone at ratio of 6:3 was prepared. The sample was spotted on the TLC plate and the plate was then introduced into the solvent system. Once the solvent had reached the solvent front, the plate was removed from the solvent system. The resulted spot was observed under UV light and marked. When the spot of the starting material is not shown on the plate, it indicates that the reaction has completed.

3.3.4 Characterization of Chalcone Derivatives

3.3.4.1 Nuclear Magnetic Resonance (NMR) Spectroscopy

To prepare the sample for NMR analysis, 15 mg of the solid product was dissolved in small amount of appropriate solvent in a sample vial. The solution was then transferred to an NMR tube to a height of approximately 4 cm. Deuterated dimethyl sulfoxide (DMSO- d_6) was used as the solvent to dissolve CA and CA2, while deuterated chloroform ($CDCl_3$) was used as the solvent for the Mannich base derivatives. The 1H NMR, ^{13}C NMR, HMQC and HMBC spectra of the compound were obtained.

3.3.4.2 Liquid Chromatography Mass Spectroscopy (LCMS)

The sample for LCMS analysis was prepared by dissolving 1 mg of the solid product in 1 mL of HPLC grade methanol to make up a concentration of 1000 ppm. The sample solution was then diluted to 50 ppm and transferred to a sample vial before sending it for analysis.

3.3.4.3 Fourier Transform Infrared (FTIR) Spectroscopy

The potassium bromide (KBr) pellet was prepared by first mixing a little amount of solid product with KBr salt in a ratio of approximately 1:10. The mixture was grinded into fine powder form using pestle and mortar and transferred to the pellet die and pressed into pellet form with the manual hydraulic press. The resulting pellet was then inserted into the sample holder and scanned within the range of $4000 - 400\text{ cm}^{-1}$.

3.3.5 DPPH Radical Scavenging Capacity Assay

Each sample was prepared at a concentration of 1000 ppm in a 10 mL volumetric flask using methanol as diluent. Ascorbic acid was used as the positive control, and it was prepared at a concentration of 25 ppm in a 10 mL volumetric flask using methanol as diluent as well. Next, 0.1 mM of DPPH reagent was prepared by dissolving 3.8 mg of DPPH in 100 mL of methanol in a covered volumetric flask. The solution was sonicated to ensure all DPPH powder dissolved well. The prepared DPPH reagent was kept in a dark, cool place before use.

By using a micropipette, 100 μ L of methanol was added into all well in a 96-well plate except for the first row. Subsequently, 200 μ L of sample (in duplicate), positive control and blank (methanol) were introduced into the first row of the plate. Serial dilutions were performed by transferring 100 μ L of the solution from the first row to the second row, then the second row to the third row and so on. The 100 μ L solution that was taken out from the last row was discarded. With this, a series of concentrations (1000, 500, 250, 125, 62.5, 31.25, 15.625 and 7.8125 ppm) of each sample compound and another series of concentrations (25, 12.5, 6.25, 3.125, 1.5625, 0.78125, 0.39062 and 0.19531 ppm) were prepared. Then, 50 μ L of DPPH reagent was added into each well, and the plate was covered with aluminium foil and kept in a darkened room for 30 min.

After 30 min, the plate was scanned with a microplate reader at an absorbance of 517 nm. The absorbance readings for each sample, positive control and blank were recorded, and the percentage of DPPH radical scavenging was calculated based on the readings. A graph of concentration of sample versus percentage of DPPH radical scavenging was plotted to determine the IC₅₀ value of each sample and control.

CHAPTER 4

RESULTS AND DISCUSSION

4.1 Molecular Structure of Compounds

A total of eight compounds were synthesized, including two chalcone intermediates and their Mannich base derivatives. Table 4.1 shows the molecular structures of the synthesized compounds.

Table 4.1: Molecular structure of compounds **CA**, **CA2**, **DA**, **DA2**, **PY**, **PY2**, **PI** and **PI2**.

Product Code	Compound's Name	Molecular Structure
CA	4-chloro-4'-hydroxychalcone	
CA2	4'-hydroxychalcone	
DA	4-chloro-4'-hydroxy-3'-dimethylaminomethylchalcone	
DA2	4'-hydroxy-3'-dimethylaminomethylchalcone	

Table 4.1 (continued): Molecular structure of compounds **CA**, **CA2**, **DA**, **DA2**, **PY**, **PY2**, **PI** and **PI2**.

Product code	Compound's name	Molecular structure
PY	4-chloro-4'-hydroxy-3'-pyrrolidinomethylchalcone	
PY2	4'-hydroxy-3'-pyrrolidinomethylchalcone	
PI	4-chloro-4'-hydroxy-3'-piperidinomethylchalcone	
PI2	4'-hydroxy-3'-piperidinomethylchalcone	

4.2 Physical Properties of Compounds

The physical appearance, percentage yield, melting point and R_f values of the synthesized compounds are listed in Table 4.2. The yields of the chalcones **CA** and **CA2** obtained were 46.5 % and 37.3 %, respectively. While the yields for the Mannich bases ranged from 10.3 % to 75.9 %. Generally, higher yields were obtained for the halogenated chalcone and Mannich base derivatives than their corresponding non-halogenated

compounds, with the halogenated Mannich bases showing approximately twofold of the yield of their corresponding non-halogenated derivatives.

Table 4.2: Physical properties of the compounds **CA**, **CA2**, **DA**, **DA2**, **PY**, **PY2**, **PI** and **PI2**.



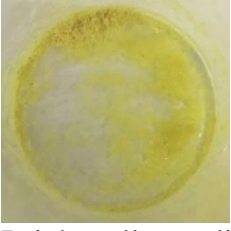
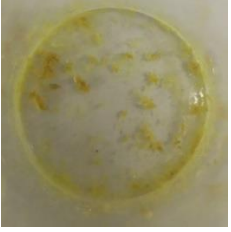




Compound	Physical Appearance	Percentage Yield, Melting Point and R_f values
CA	 <p>Pale yellow crystalline solid.</p>	% yield: 46.5 % Melting point: 190 °C Literature melting point: 188-190 °C (Sreedhar, et al., 2010) R _f value: 0.38 Solvent system: hexane: acetone at ratio of 6:3
CA2	 <p>Pale yellow crystalline solid.</p>	% yield: 37.3 % Melting point: 179 °C Literature melting point: 174-178 °C (Merck, 2022) R _f value: 0.39 Solvent system: hexane: acetone at ratio of 6:3
DA	 <p>Bright yellow solid.</p>	% yield: 64.4 % Melting point: 118 °C R _f value: 0.22 Solvent system: hexane: acetone at ratio of 6:3
DA2	 <p>Bright yellow solid.</p>	% yield: 33.2 % Melting point: 122 °C R _f value: 0.24 Solvent system: hexane: acetone at ratio of 6:3

Table 4.2 (continued): Physical properties of the compounds **CA**, **CA2**, **DA**, **DA2**, **PY**, **PY2**, **PI** and **PI2**.

Compound	Physical Appearance	Percentage Yield and Melting Point
PY	 Dark yellow solid.	% yield: 24.3 % Melting point: 105-107 °C R _f value: 0.19 Solvent system: hexane: acetone at ratio of 6:3
PY2	 Dark yellow solid.	% yield: 10.3 % Melting point: 113-115 °C R _f value: 0.21 Solvent system: hexane: acetone at ratio of 6:3
PI	 Orange-yellow solid.	% yield: 75.9 % Melting point: 120-122 °C R _f value: 0.48 Solvent system: hexane: acetone at ratio of 6:3
PI2	 Orange-yellow solid.	% yield: 32.2 % Melting point: 123-125 °C R _f value: 0.53 Solvent system: hexane: acetone at ratio of 6:3

4.3 Fourier Transform Infrared (FTIR) Spectroscopy

The absorption bands presented in the FTIR spectra of the chalcones **CA** and **CA2** are similar as they possess identical functional groups and structural backbones. The characteristic absorption bands that were observed in both spectra are tabulated in Table 4.3, and their spectra are shown in Figure 4.1 and 4.2. Some of the characteristic peaks include the broad O-H stretch observed at 3435 cm^{-1} in both spectra. Besides, the aromatic C-H and alkene =C-H stretch were seen overlapping between the wavenumbers of 3067 and 3123 cm^{-1} . Additionally, the sharp intense peak at 1643 and 1645 cm^{-1} in the spectrum of **CA** and **CA2**, respectively, was indicative of the C=O stretching of the carbonyl group. While the α , β unsaturated stretch was positioned at 1601 and 1605 cm^{-1} , the aromatic C=C stretch at 1591 and 1590 cm^{-1} , and the C-O stretch at 1036 and 1043 cm^{-1} in the spectrum of **CA** and **CA2**, respectively. Furthermore, the C-Cl stretch was observed at 815 cm^{-1} in the spectrum of **CA** but not **CA2**. The values were in agreement with the spectral data as reported by Anwar, et al. (2018).

Table 4.3: FTIR spectral data of compound **CA** and **CA2**.

Compound	IR Absorption Bands, ν (cm^{-1})						
	O-H stretch	Aromatic C-H and alkene =C-H stretch (overlapping)	C=O stretch	α , β unsaturated stretch	Aromatic C=C stretch	C-O stretch	C-Cl stretch
CA	3435	3093, 3067	1643	1601	1592	1036	815
CA2	3435	3123, 3067	1645	1605	1591	1043	-

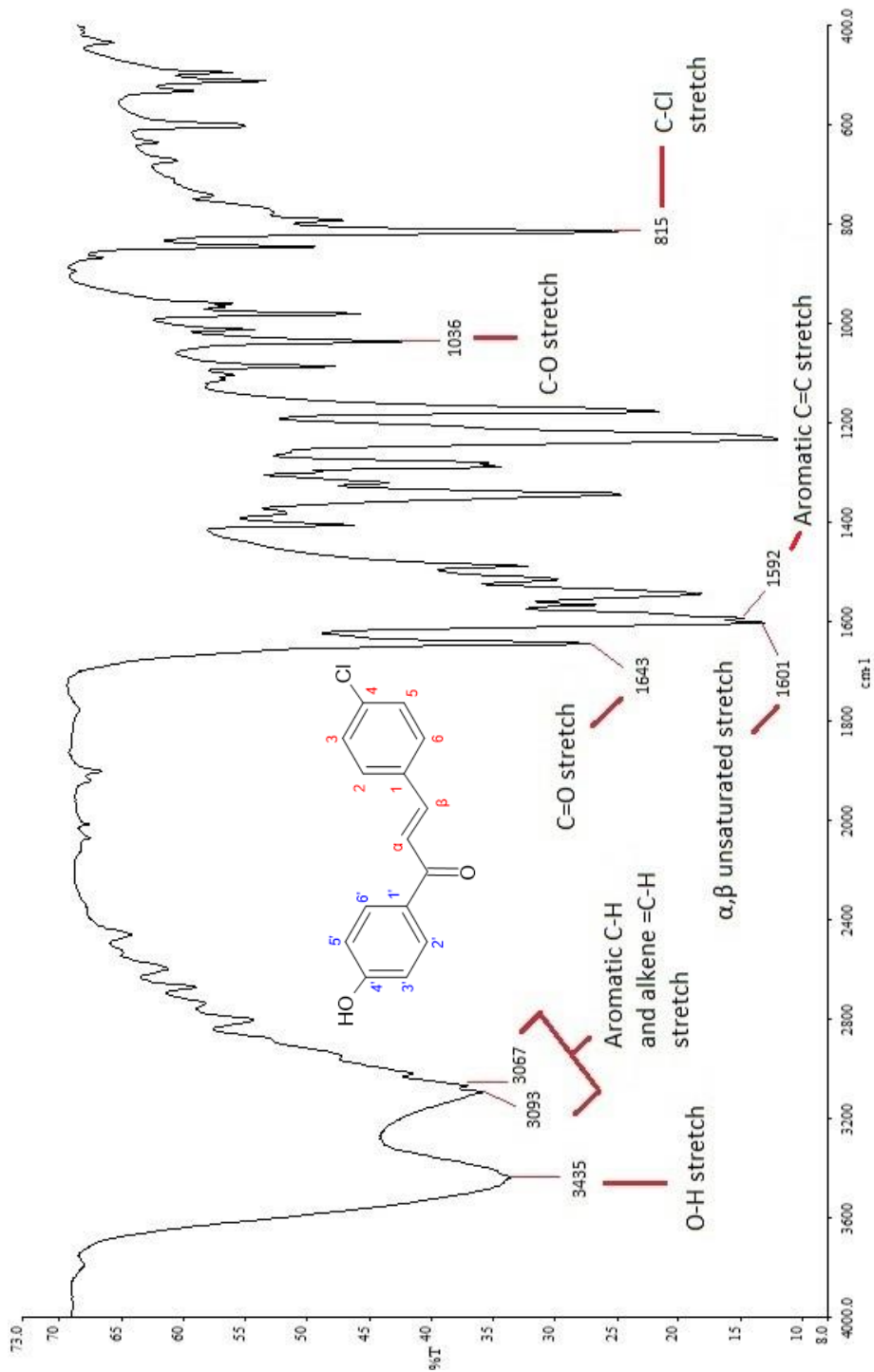


Figure 4.1: FTIR spectrum of CA (KBr).

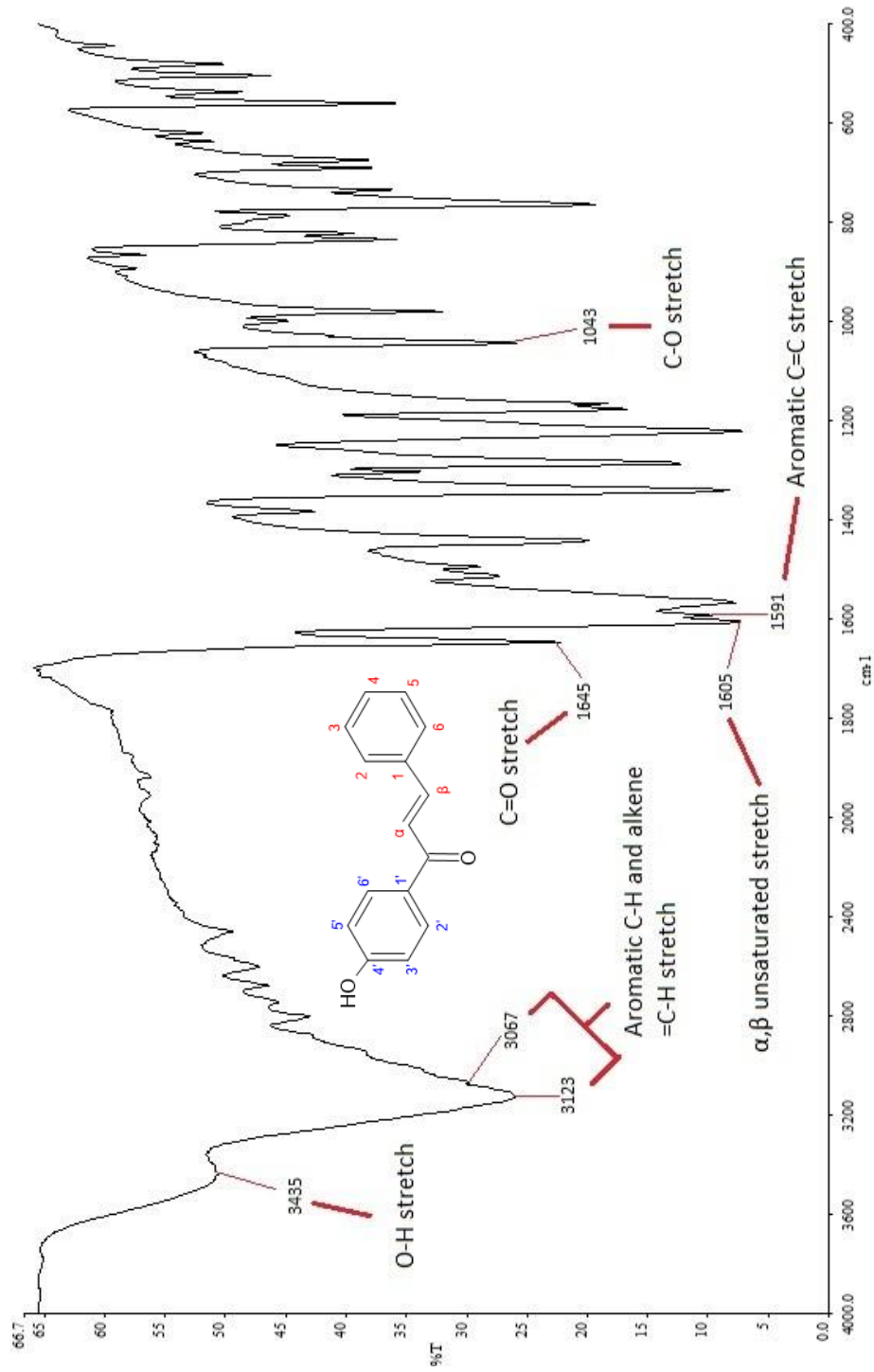


Figure 4.2: FTIR spectrum of CA2 (KBr)..

The characteristic IR absorption bands that were observed in the FTIR spectrum of the Mannich base derivatives are tabulated in Table 4.4. The FTIR spectrum for compound **DA**, **PY** and **PI** are shown in Figure 4.3-4.5, while the spectrum for compound **DA2**, **PY2** and **PI2** are shown in appendix A.

Two additional absorption bands that did not occur in the spectrum of the chalcones include the aliphatic C-H stretch and the C-N stretch, which were due to the newly bonded amine substituent. In the FTIR spectrum of the Mannich bases, O-H stretch occurred at wavenumbers between 3434 and 3437 cm^{-1} . On the other hand, the aliphatic C-H stretch was seen overlapping within the range of 2983 to 2850 cm^{-1} . Moreover, the C=O stretch was observed at wavenumbers between 1652 and 1658 cm^{-1} , while the α , β unsaturated stretch ranged from 1601 to 1613 cm^{-1} . In addition, the aromatic C=C stretch was position between 1588 and 1595 cm^{-1} , while C-N stretch occurred between 1232 and 1284 cm^{-1} . The C-Cl stretch was observed at 814, 815 and 814 cm^{-1} in the spectrum of **DA**, **PY** and **PI**, respectively.

Table 4.4: FTIR spectral data of compound **DA**, **DA2**, **PY**, **PY2**, **PI** and **PI2**.

Compound	IR Absorption Bands, ν (cm ⁻¹)						
	O-H stretch	Aliphatic C-H stretch	C=O stretch	α , β unsaturated stretch	Aromatic C=C stretch	C-N stretch	C-Cl stretch
DA	3437	2983-2855	1654	1613	1590	1271	814
DA2	3434	2976-2851	1654	1612	1588	1277	-
PY	3436	2970-2850	1652	1611	1595	1284	815
PY2	3435	2921-2850	1654	1611	1592	1278	-
PI	3435	2936-2850	1658	1609	1591	1282	814
PI2	3437	2946-2859	1655	1601	1590	1290	-

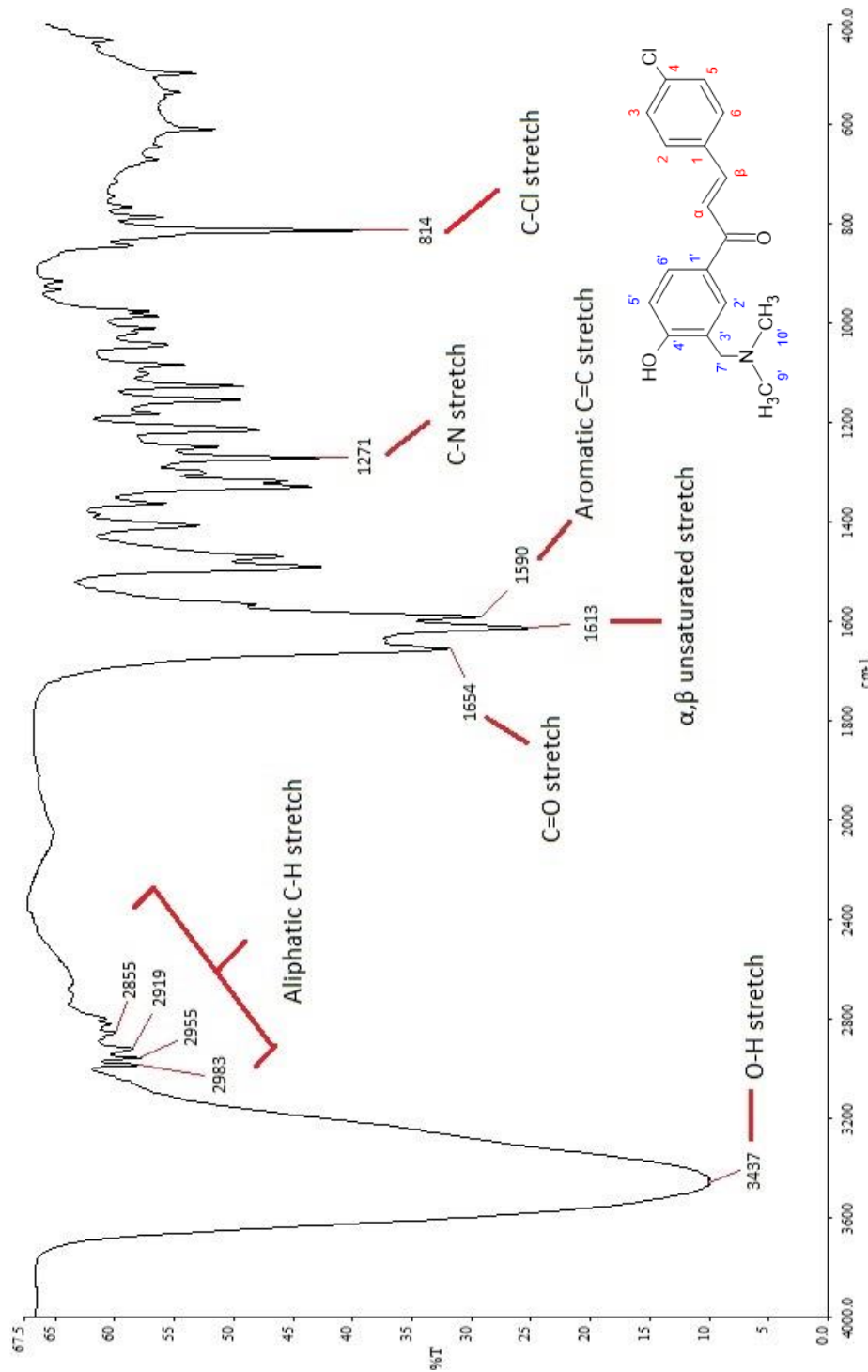


Figure 4.3: FTIR spectrum of DA (KBr)..

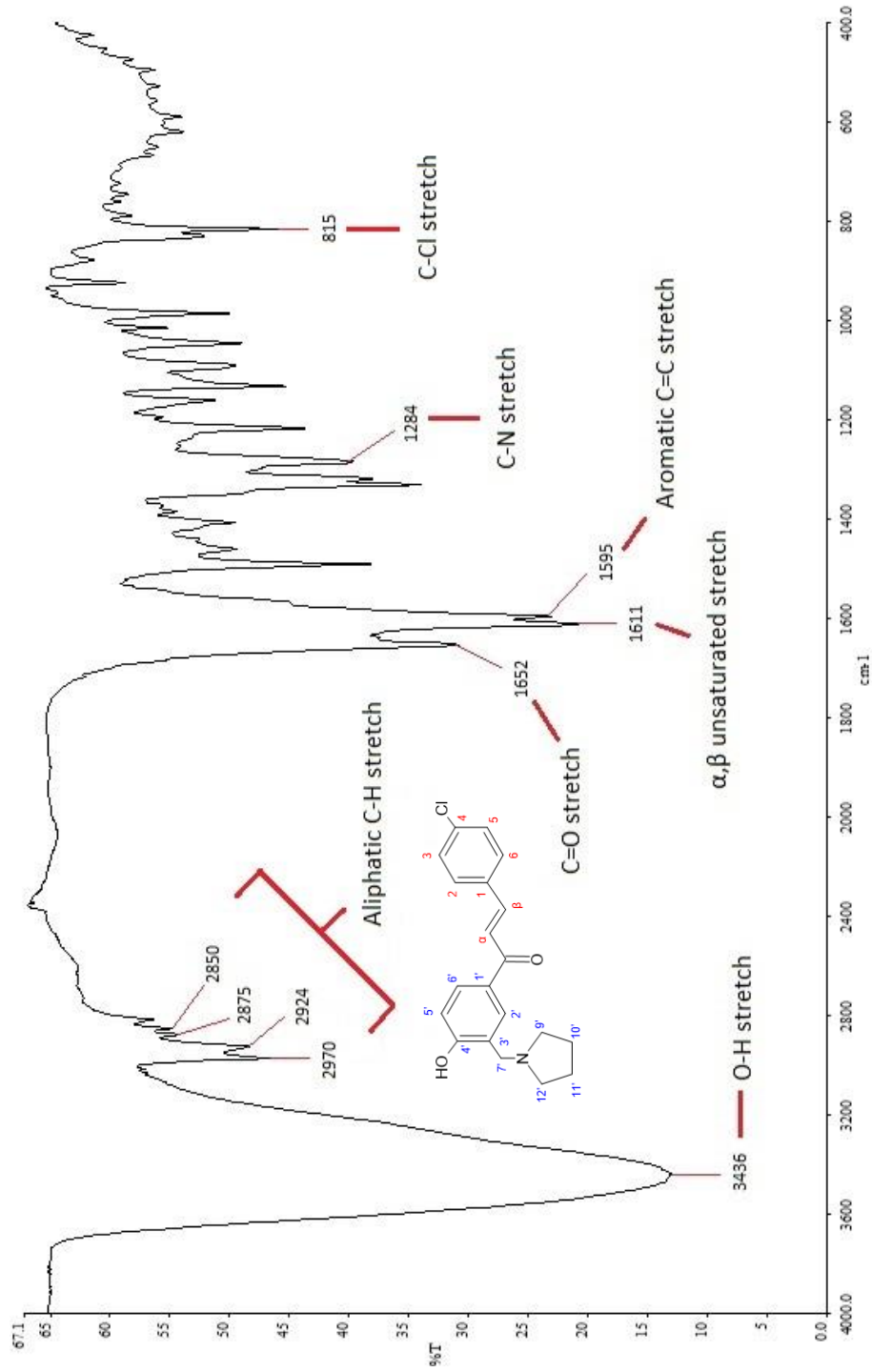


Figure 4.4: FTIR spectrum of PY (KBr)..

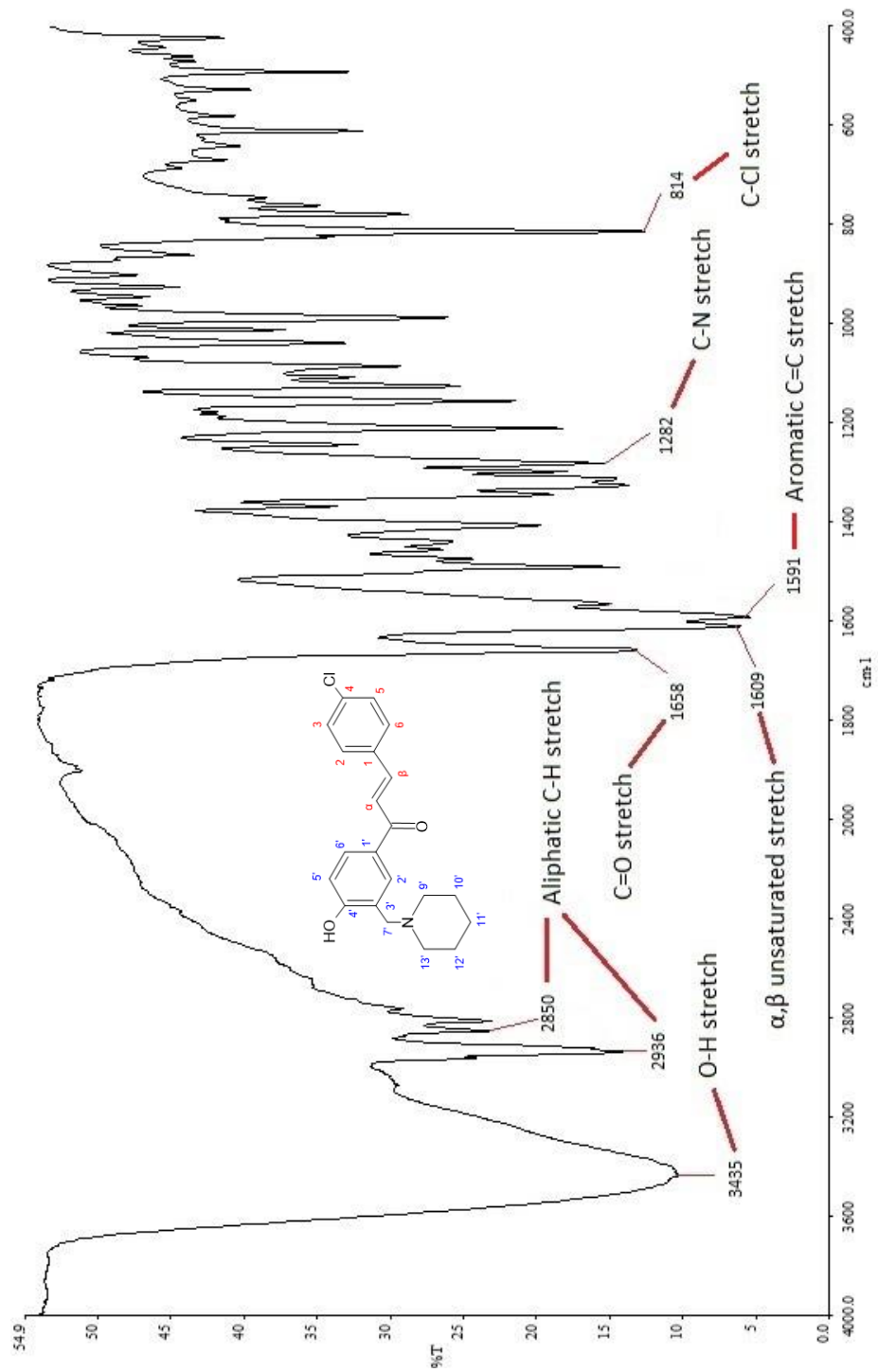


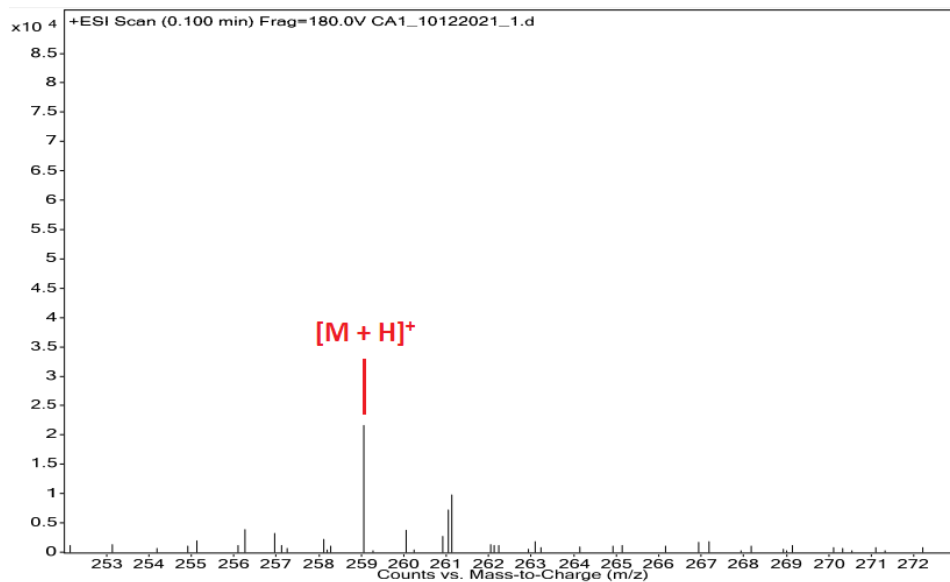
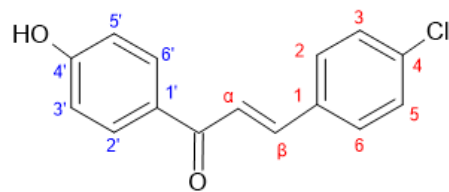
Figure 4.5: FTIR spectrum of PI (KBr)...

4.4 Liquid Chromatography-Mass Spectroscopy (LC-MS)

The molecular formula of the synthesized compounds were confirmed using LC-MS. The LC-MS spectral data of each synthesized compound is tabulated in Table 4.5. The LC-MS spectrum and spectrum identification of compound **CA**, **DA**, **PY** and **PI** are shown in Figure 4.6-4.9. While the LC-MS spectrum and spectrum identification of compound **CA2**, **DA2**, **PY2** and **PI2** are shown in Appendix B. The small peak approximately $m/z = 317$ in the spectrum of DA could be due to the ^{13}C isotope, while the one at $m/z = 318.1076$ could be due to the ^{37}Cl isotope.

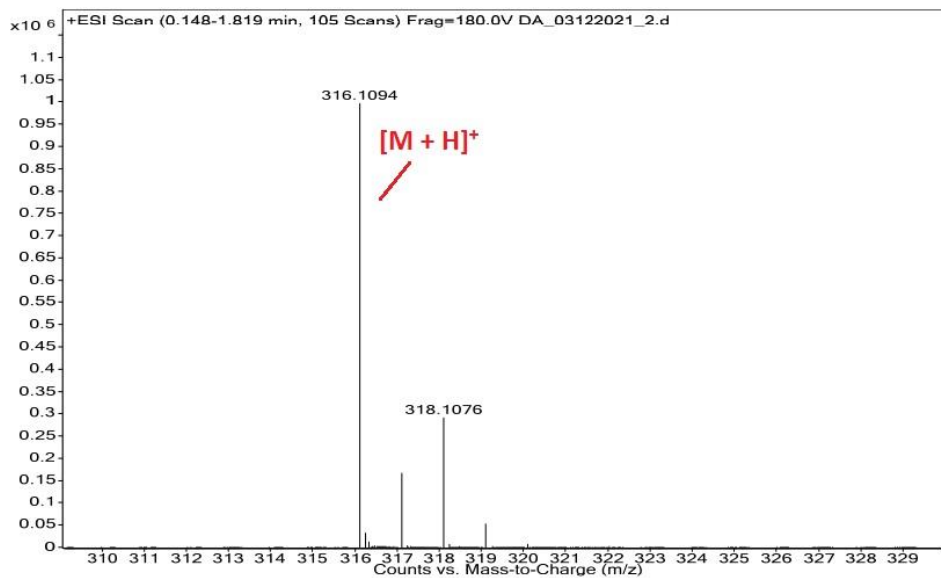
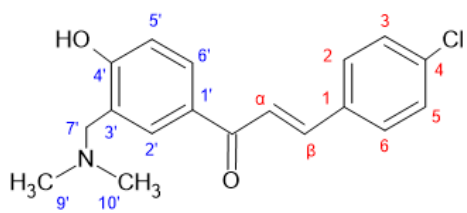
Table 4.5: LC-MS spectral data of the synthesized compounds.

Compound	Molecular Formula	Molecular Weight (g mol ⁻¹)	Molecular Ion Peak (m/z)
CA	C ₁₅ H ₁₁ ClO ₂	Calculated: 258.0448 Measured: 258.0547	259.0520
CA2	C ₁₅ H ₁₂ O ₂	Calculated: 224.0837 Measured: 224.0839	225.0912
DA	C ₁₈ H ₁₈ ClNO ₂	Calculated: 315.1026 Measured: 315.1021	316.1094
DA2	C ₁₈ H ₁₉ NO ₂	Calculated: 281.1416 Measured: 281.1415	282.1488
PY	C ₂₀ H ₂₀ ClNO ₂	Calculated: 341.1183 Measured: 341.1190	342.1263
PY2	C ₂₀ H ₂₁ NO ₂	Calculated: 307.1572 Measured: 307.1582	308.1654
PI	C ₂₁ H ₂₂ ClNO ₂	Calculated: 355.1339 Measured: 355.1342	356.1415
PI2	C ₂₁ H ₂₃ NO ₂	Calculated: 321.1729 Measured: 321.1741	322.1820



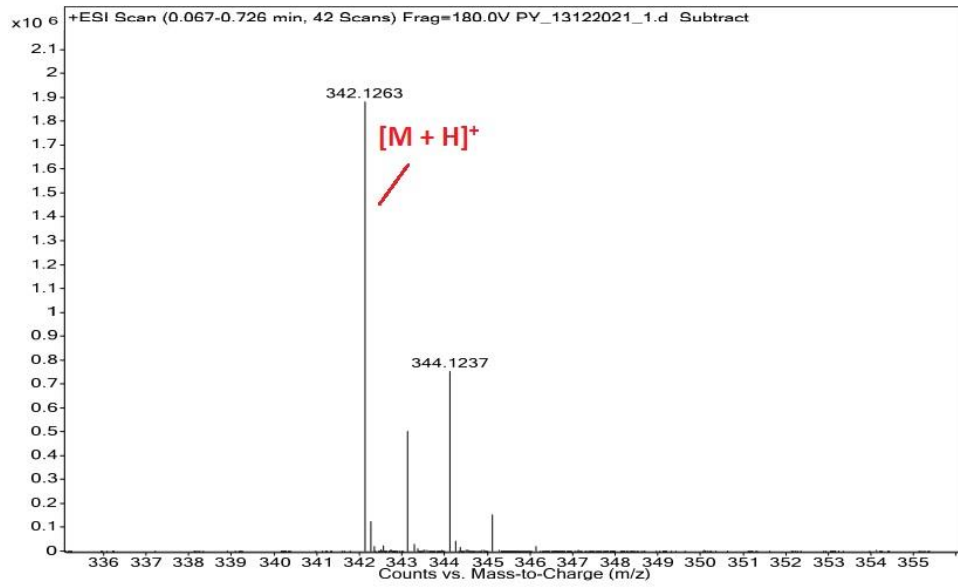
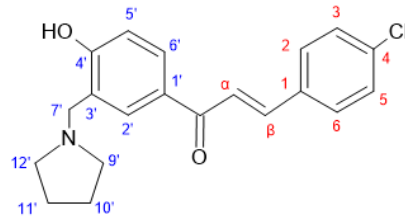
Best	T	Name	Formula	Score	T	Mass	Mass (Tgt)	Miss (DB)	Mass (MFG)	Diff (ppm)	Diff (abs. ppm)
✓			C15 H11 Cl O2	89.01		258.0457			258.0448	-3.83	3.83
	Species	Ion Formula	m/z	Height	Score (MFG)	Score (MFG, MS)	Score (MFG, MS/MS)	Score (MFG, mass)	Score (MFG, abund)	Score (MFG, iso. spacing)	
	(M+H)+	C15 H12 Cl O2	259.052	21586.4	89.01	89.01		92.14	98.98	70.81	
	m/z	m/z (Calc)	Diff (ppm)	Diff (mDa)	Height	Height (Calc)	Height %	Height % (Calc)	Height Sum %	Height Sum% (Calc)	
	259.0531	259.052	-3.93	-1	21586.4	21595.2	100	64	64.3		
	260.0588	260.0564	-13.12	-3.4	3728.7	3666.2	17.3	16.4	11.1	10.6	
	261.0494	261.0495	0.7	0.2	7164.8	7304.8	33.2	33.7	21.2	21.7	
	262.0521	262.0527	2.05	0.5	1255	1168.7	5.8	5.4	3.7	3.5	

Figure 4.6: LC-MS spectrum and spectrum identification of CA.



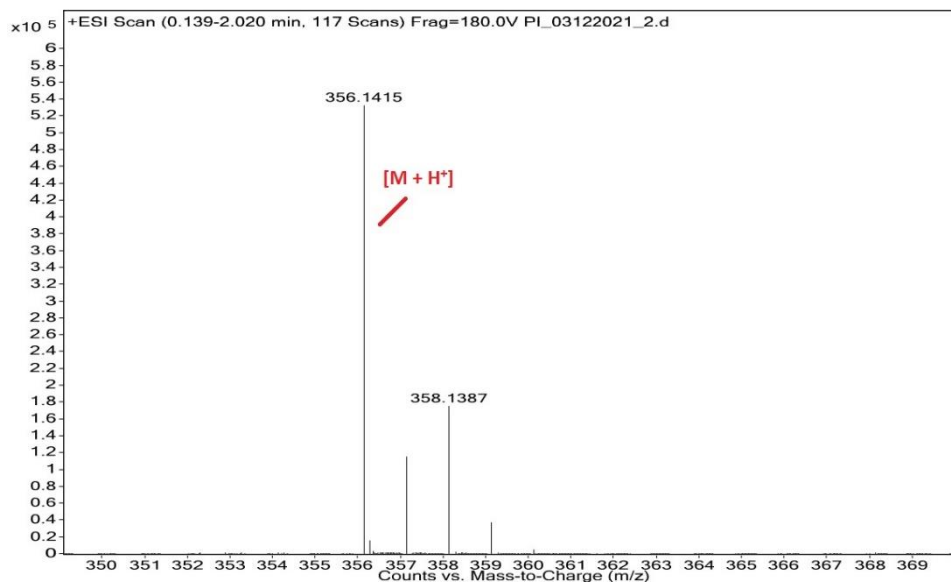
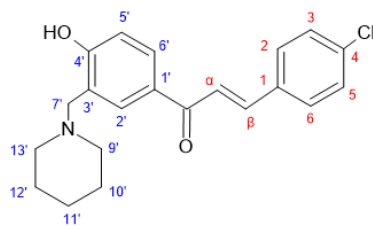
Best	T	Name	Formula	Score	T	Mass	Mass (Tgt)	Mass (DB)	Mass (MFG)	Diff (ppm)	Diff (abs. ppm)
✓			C18 H18 Cl N O2	96.05		315.1021			315.1026	1.49	1.49
	Species	Ion Formula	m/z	Height	Score (MFG)	Score (MFG, MS)	Score (MFG, MS/MS)	Score (MFG, mass)	Score (MFG, abund)	Score (MFG, iso. spacing)	
		[M+H] ⁺	C18 H19 Cl N O2	316.1099	995543.2	96.05	96.05	96.46	89.4	99.22	
m/z	m/z (Calc)	Diff (ppm)	Diff (mDa)	Height	Height (Calc)	Height %	Height % (Calc)	Height Sum %	Height Sum% (Calc)		
316.1094	316.1099	1.52	0.5	995543.2	933491	100	100	65.9	61.8		
317.1128	317.1132	1.01	0.3	166608.2	187896.4	16.7	20.1	11	12.4		
318.1076	318.1076	-0.05	0	290401	320435.3	29.2	34.3	19.2	21.2		
319.1097	319.1105	2.37	0.8	52280.7	61966.4	5.3	6.6	3.5	4.1		
320.1123	320.1132	2.77	0.9	6040.6	7084.5	0.6	0.8	0.4	0.5		

Figure 4.7: LC-MS spectrum and spectrum identification of DA.



Best	Name	Formula	Score	Mass	Mass (Tgt)	Mass (DB)	Mass (MFG)	Diff (ppm)	Diff (abs. ppm)
✓		C20 H20 Cl N O2	95.16	341.119			341.1183	-2.09	2.09
Species	Ion Formula	m/z	Height	Score (MFG)	Score (MFG, MS)	Score (MFG, MS/MS)	Score (MFG, mass)	Score (MFG, abund)	Score (MFG, iso. spacing)
(M+H)+	C20 H21 Cl N O2	342.1255	1879595.5	95.16	95.16		96.73	90.11	98.09
m/z	m/z (Calc)	Diff (ppm)	Diff (mDa)	Height	Height (Calc)	Height %	Height % (Calc)	Height Sum %	Height Sum% (Calc)
342.1263	342.1255	-2.17	-0.7	1879595.5	1996832.1	100	100	56.9	60.4
343.129	343.1288	-0.51	-0.2	501391.2	445583.1	26.7	22.3	15.2	13.5
344.1237	344.1233	-1.25	-0.4	751609	694473.9	40	34.8	22.7	21
345.1267	345.1262	-1.5	-0.5	151457.1	147586.4	8.1	7.4	4.6	4.5
346.1302	346.129	-3.43	-1.2	18171.7	18135.9	1	0.9	0.5	0.5
347.1395	347.1317	-22.62	-7.9	2013.2	1626.2	0.1	0.1	0.1	0

Figure 4.8: LC-MS spectrum and spectrum identification of PY.



Best	✓	Name	Formula	Score	✓	Mass	Mass (Tgt)	Mass (DB)	Mass (MFG)	Diff (ppm)	Diff (abs, ppm)
✓			C21 H22 Cl N O2	97.94		355.1342			355.1339	-0.87	0.87
Species	Ion Formula	m/z	Height	Score (MFG)	Score (MFG, MS)	Score (MFG, MS/MS)	Score (MFG, mass)	Score (MFG, abund)	Score (MFG, iso. spacing)		
(M+H)+	C21 H23 Cl N O2	356.1412	531900.3	97.94	97.94		99.4	98.01	94.94		
m/z	m/z (Calc)	Diff (ppm)	Diff (mDa)	Height	Height (Calc)	Height %	Height % (Calc)	Height Sum %	Height Sum% (Calc)		
356.1415	356.1412	-0.96	-0.3	531900.3	515839.5	100	100	61.7	59.8		
357.1439	357.1445	1.62	0.6	114657.1	120804.8	21.6	23.4	13.3	14		
358.1387	358.139	0.87	0.3	174775.9	180675.4	32.9	35	20.3	20.9		
359.1407	359.1418	3.16	1.1	36460.1	40107.8	6.9	7.8	4.2	4.6		
360.143	360.1447	4.55	1.6	4740.7	5106.6	0.9	1	0.5	0.6		

Figure 4.9: LC-MS spectrum and spectrum identification of PI.

4.5 Nuclear Magnetic Resonance (NMR) Spectroscopy

The structure elucidation of compounds **CA**, **DA**, **PY** and **PI** will be discussed in this thesis, based on their respective NMR spectral data as depicted in Table 4.6 – 4.12. The spectral data of compounds **CA2**, **DA2**, **PY2** and **PI2** are listed in Appendix C, D, E and F, respectively.

4.5.1 Structural Elucidation of 4-Chloro-4'-hydroxychalcone

A total of six characteristic proton signals between 6.8-8.1 ppm were observed in the ^1H NMR spectrum (Figure 4.10 and 4.11) of 4-chloro-4'-hydroxychalcone (**CA**). A pair of doublet peaks observed at 7.87 and 7.61 ppm were attributed to the protons of the unsaturated double bond, $\text{H}\beta$ and $\text{H}\alpha$, respectively. The $\text{H}\alpha$ protons showed chemical shift at upper field region than $\text{H}\beta$ protons was possibly due to the polarization of $\text{C}=\text{C}$ double bond caused by the carbonyl group which resulted in higher electron density at position α (Aksöz and Ertan, 2012). The coupling constants of $\text{H}\alpha$ and $\text{H}\beta$ which are both above 14 Hz indicated that they are in *trans* configuration (Aksöz and Ertan, 2012). The doublets shown at 7.85 ppm corresponded to the aromatic protons H_2 and H_6 , and at 7.46 ppm represented the aromatic protons H_3 and H_5 . In addition, the pair of doublets at 8.03 ppm was assigned to the aromatic protons H_2' and H_6' , and the one at 6.86 ppm indicated the aromatic protons H_3' and H_5' in ring A. The doublets of the aromatic protons H_2' and H_6' appeared in the downfield region as they were deshielded by the electronegative oxygen atom of the carbonyl group.

The ^{13}C NMR spectrum (Figure 4.12 and 4.13) of **CA** showed a total of 11 signals. The signal at the most downfield regions, 187.6 ppm, indicated the carbonyl carbon of $\text{C}=\text{O}$, and at 162.8 ppm indicated the $\text{C}4'$ quaternary carbon. These two carbons were attached to the electronegative oxygen atom of carbonyl and hydroxyl groups, respectively, which resulted in deshielding effect of the atoms and a downfield chemical shift. On the other hand, the characteristic peaks for $\text{C}\alpha$ and $\text{C}\beta$ occurred at 123.4 ppm and 141.8 ppm, respectively. The signals at 135.3, 134.3 and 129.5 ppm corresponded to the quaternary carbons $\text{C}1$, $\text{C}4$ and $\text{C}1'$, respectively. The peak at 130.9 ppm was assigned to $\text{C}2$ and $\text{C}6$, and the peak at 129.5 ppm was attributed to $\text{C}3$ and $\text{C}5$. Lastly, the peak at 131.8 ppm indicated $\text{C}2'$ and $\text{C}6'$ and the peak at 116.0 ppm represented $\text{C}3'$ and $\text{C}5'$.

Six signals were observed in the DEPT-90 spectrum (Figure 4.14), indicating the methine carbons $\text{C}\alpha$, $\text{C}\beta$, $\text{C}2$ and $\text{C}6$, $\text{C}3$ and $\text{C}5$, $\text{C}2'$ and $\text{C}6'$, $\text{C}3'$ and $\text{C}5'$. The remaining carbon signals were not shown as they are all quaternary carbons.

As for the HMQC spectrum (Figure 4.15) of **CA**, a 1-bond coupling could be seen between $\text{C}\alpha$, $\text{C}\beta$, $\text{C}2$, $\text{C}3$, $\text{C}5$, $\text{C}6$, $\text{C}2'$, $\text{C}3'$, $\text{C}5'$, $\text{C}6'$ and their respective protons. In the HMBC spectrum of **CA** (Figure 4.15), one of the characteristic correlations observed was between the carbonyl carbon with $\text{H}\alpha$, $\text{H}\beta$, $\text{H}2'$ and $\text{H}6'$, which indicated the correlations between the α,β -unsaturated carbonyl system and ring A. Besides, a 2-bond coupling

between C1 and the H β and a 4-bond coupling between C2' and H α were also seen, indicating the correlations between the vinylic protons with the aromatic rings. The correlation data was found to be in correspondence to the structure assigned.

The NMR spectral data of the compound **CA** is listed in the Table 4.6 and 4.7, which were in agreement with the literature values reported by Anwar, et al. (2018). Compound 4'-hydroxychalcone (**CA2**) showed similar spectral properties as **CA** as they have identical structural backbones with only difference of the chloro-substituent at position 4 at ring B being replaced by hydrogen in **CA2**. Additional proton signal at position 4 of ring B was shown in the ^1H NMR spectrum of **CA2**. The NMR spectra and spectral data of **CA2** are shown in Appendix C.

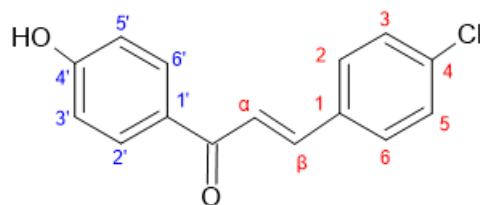


Table 4.6: ^1H , ^{13}C and DEPT NMR spectral data of CA.

Atom Number	^1H (δ_{H} , ppm)	Literature Value (Anwar, et al., 2018)	^{13}C (δ_{C} , ppm)	Literature Value (Anwar, et al., 2018)	DEPT
C=O	-	-	187.6	190.5	C
α	7.61 (d, J = 15.88 Hz)	7.69 (d, J = 15.60 Hz)	123.4	123.8	CH
β	7.87 (d, J = 14.04 Hz)	7.76 (d, J = 15.60 Hz)	141.8	143.6	CH
1	-	-	135.3	137.3	C
2 & 6	7.85 (d, J = 8.56 Hz)	7.72 (d, J = 8.45 Hz)	130.9	130.9	CH
3 & 5	7.46 (d, J = 8.52 Hz)	7.43 (d, J = 8.45 Hz)	129.5	130.3	CH
4	-	-	134.3	135.4	C
1'	-	-	129.5	131.1	C
2' & 6'	8.03 (d, J = 8.52 Hz)	8.02 (d, J = 9.10 Hz)	131.8	132.6	CH
3' & 5'	6.86 (d, J = 8.52 Hz)	6.89 (d, J = 9.10 Hz)	116.0	116.6	CH
4'	-	-	162.8	164.2	C

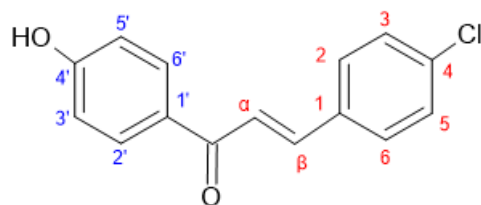


Table 4.7: $^1\text{H} - ^{13}\text{C}$ correlations in CA.

Carbon Number	Proton Number			
	HMQC	HMBC		
	1J	2J	3J	4J
C=O	-	H α	H β , H2', H6'	-
C α	H α	H β	-	-
C β	H β	H α	H2, H6	-
C1	-	H β , H2, H6	H α , H3, H5	-
C2	H2	H3	H β	-
C3	H3	-	-	-
C4	-	H3, H5	H2, H6	-
C5	H5	-	-	-
C6	H6	H5	H β	-
C1'	-	H2', H6'	H5'	-
C2'	H2'	-	-	H α
C3'	-	-	-	-
C4'	-	H5'	H2', H6', H7'	-
C5'	H5'	-	-	-
C6'	H6'	-	H2'	H α
C7'	H7'	-	H2', H9', H10'	-
C9' & C10'	H9' or H10'	-	H7'	-

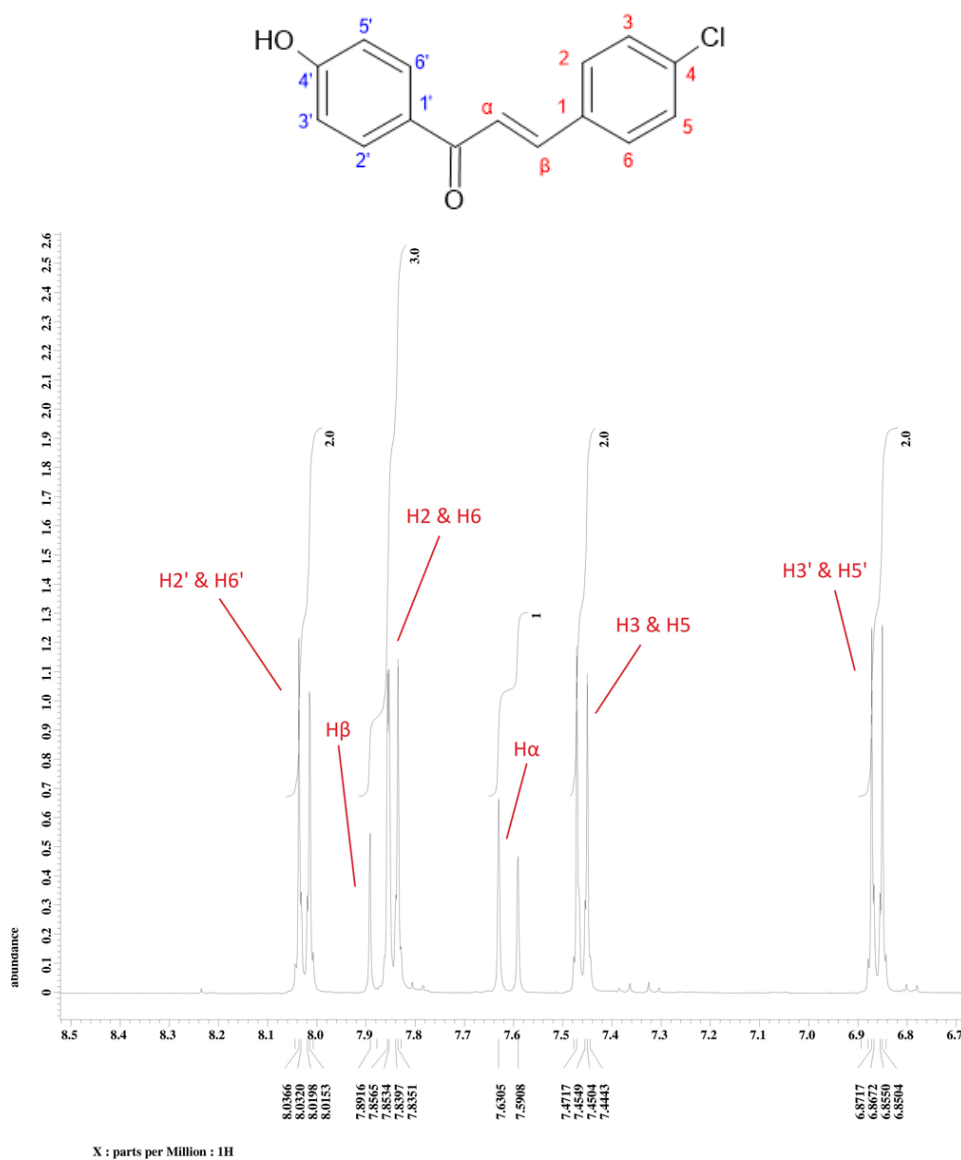


Figure 4.10: Expanded (downfield region) ^1H NMR spectrum of 4-chloro-4'-hydroxychalcone (CA) (400 MHz, DMSO-d_6).

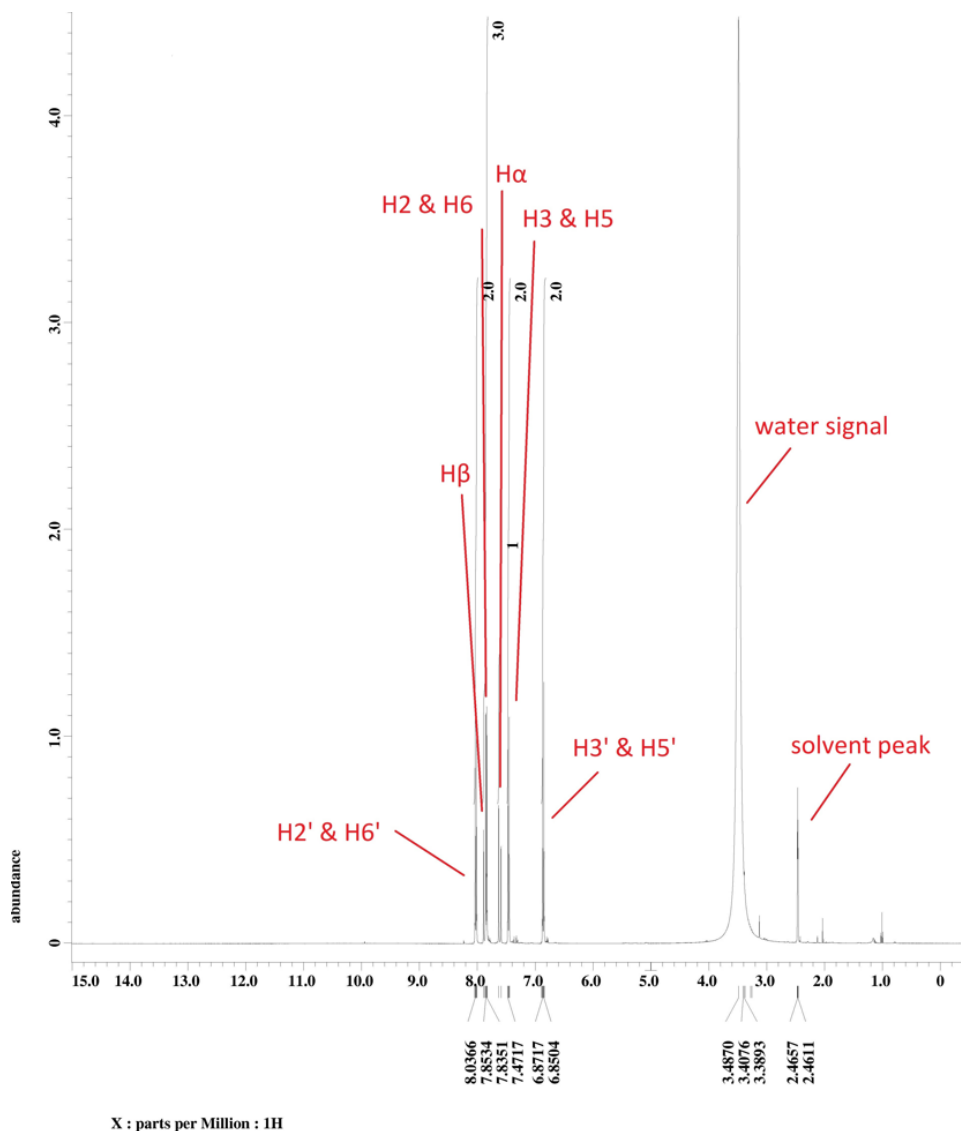
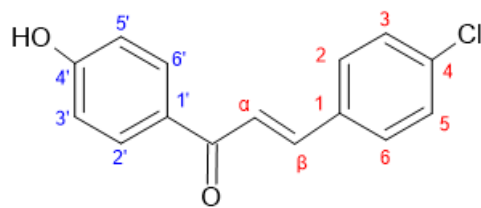


Figure 4.11: ^1H NMR spectrum of 4-chloro-4'-hydroxychalcone (CA) (400 MHz, DMSO-d_6).

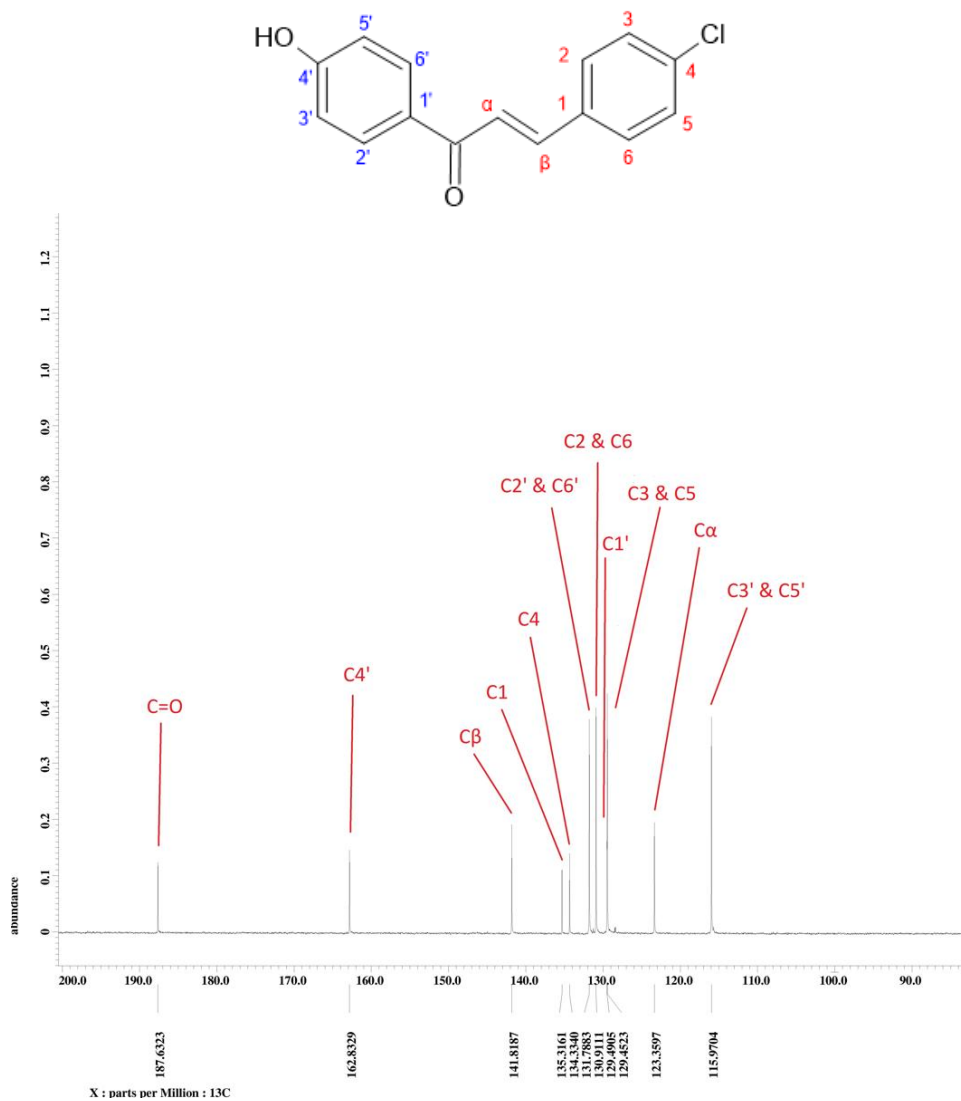


Figure 4.12: Expanded (downfield region) ^{13}C NMR spectrum of 4-chloro-4'-hydroxychalcone (CA) (100 MHz, DMSO-d_6).

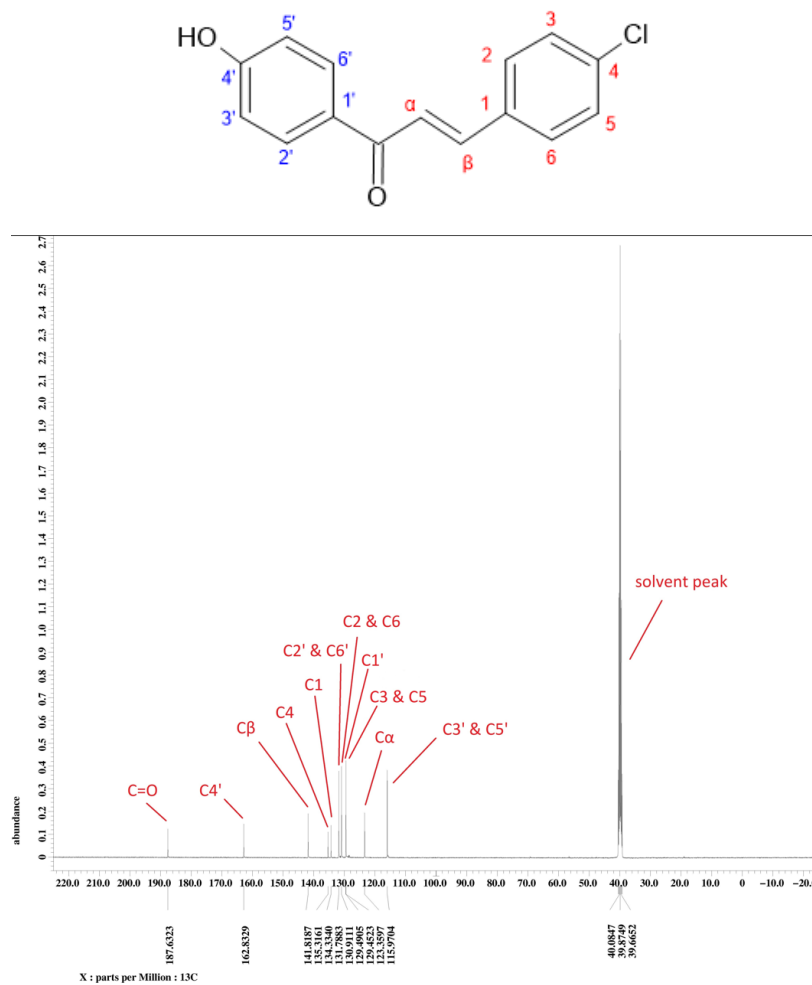


Figure 4.13: ^{13}C NMR spectrum of 4-chloro-4'-hydroxychalcone (CA) (100 MHz, DMSO- d_6).

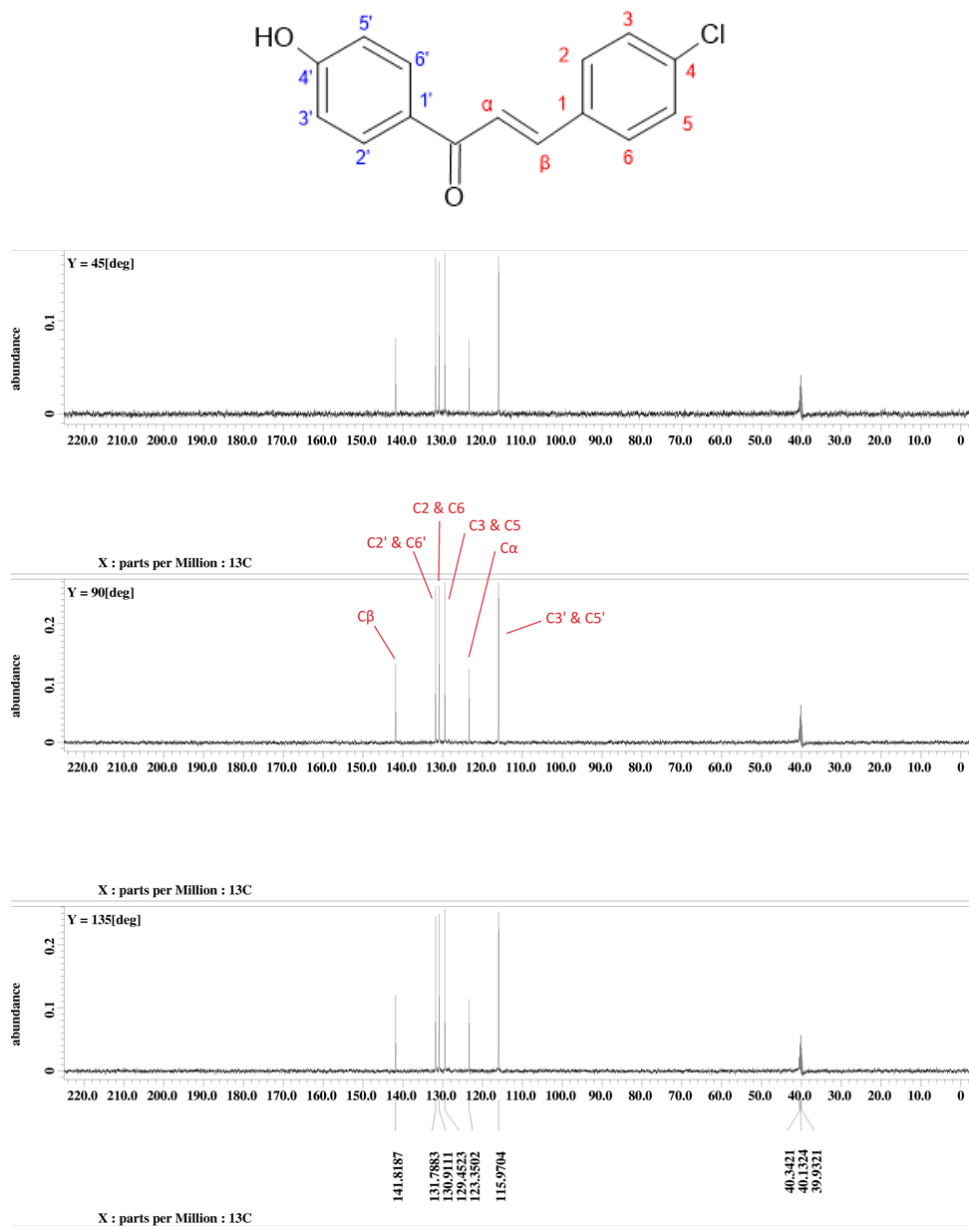


Figure 4.14: DEPT NMR spectrum of 4-chloro-4'-hydroxychalcone (CA).

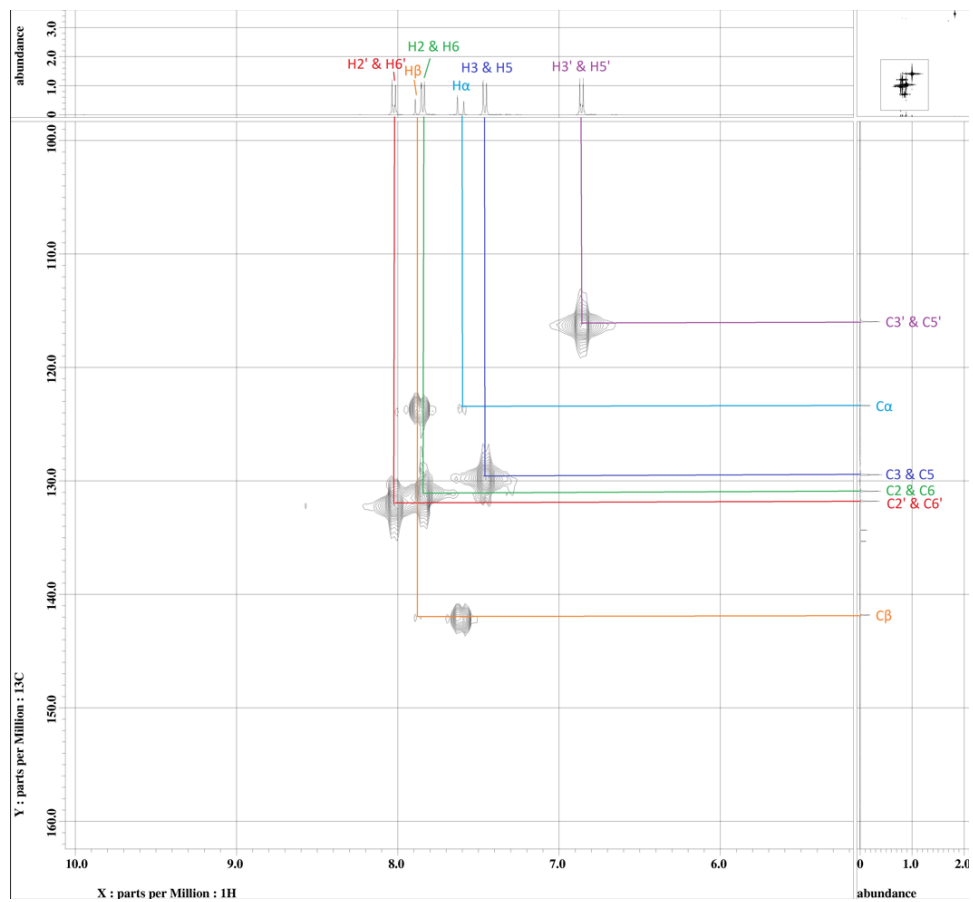
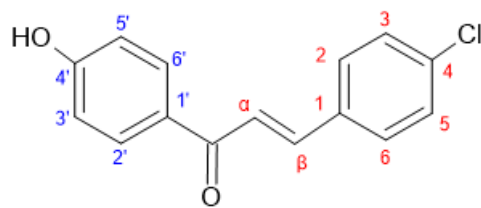


Figure 4.15: Expanded (downfield region) HMQC spectrum of 4-chloro-4'-hydroxychalcone (CA).

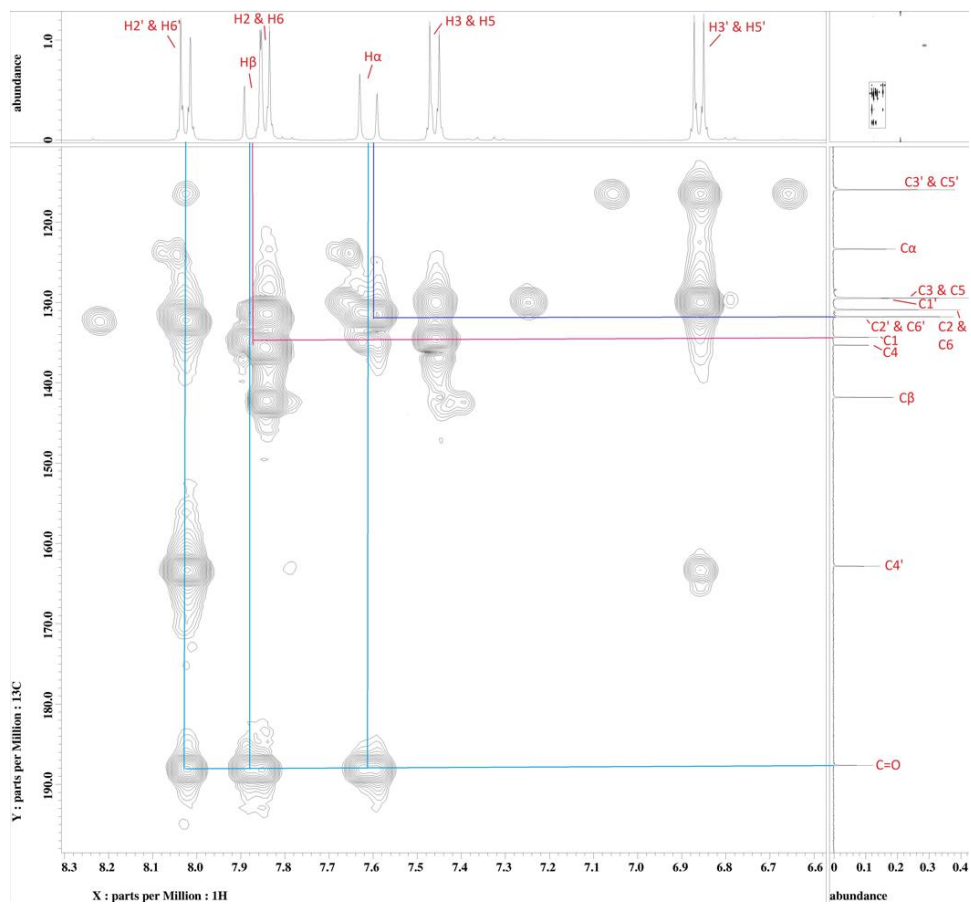
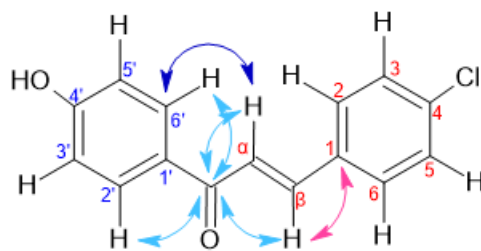


Figure 4.16: Expanded (downfield region) HMBC spectrum of 4-chloro-4'-hydroxychalcone (CA).

4.5.2 Structural Elucidation of 4-Chloro-4'-hydroxy-3'-dimethylaminomethylchalcone

In the ^1H NMR spectrum (Figure 4.17 and 4.18) of 4-chloro-4'-hydroxy-3'-dimethylaminomethylchalcone (**DA**), the six signals attributed to the aromatic protons in the structure occurred within the region 6.8-7.8 ppm. The doublets attributed to the vinylic protons $\text{H}\alpha$ and $\text{H}\beta$ were observed at 7.51 and 7.72 ppm, respectively. The coupling constant of 15.6 Hz for both $\text{H}\alpha$ and $\text{H}\beta$ indicated the vinylic protons are in *trans* configuration. The peaks corresponded to $\text{H}2'$ and $\text{H}\beta$ showed overlapping within the region 7.70-7.75 ppm. Additionally, a doublet of doublets corresponded to $\text{H}6'$ was observed at 7.90 ppm. The coupling constant of $\text{H}6'$ with the hydroxyl proton attached at *meta* position was 2.28 Hz, while with the $\text{H}5'$ proton attached at *ortho* position was 8.68 Hz. The protons of the amine substituent occurred in the upfield region, whereby the singlet peak attributed to $\text{H}7'$ occurred at 3.74 ppm, and the singlet peak corresponded to $\text{H}9'$ and $\text{H}10'$ occurred at 2.36 ppm.

A total of 13 carbon signals were shown in the ^{13}C NMR spectrum (Figure 4.19 and 4.20) of **DA**. Two additional carbon signals that were not observed in the spectrum of **CA** were attributed to the newly bonded amine substituent. The carbon signal for $\text{C}7'$ was positioned at 62.6 ppm and for $\text{C}9'$ and $\text{C}10'$ was at 44.5 ppm. As for the DEPT NMR spectrum (Figure 4.21) of **DA**, two additional carbon signals could be seen in the DEPT-135 spectrum, which were due to the amine substituent. The signal observed at

62.6 ppm was assigned to the methylene carbon C7', while the one at 44.5 was assigned to the methyl carbons C9' and C10'.

The HMQC spectrum (Figure 4.22) of **DA** showed 1-bond couplings between C α , C β , C2, C3, C5, C6, C2', C3', C5', C6', C7', C9' and C10' with their respective protons. Characteristic correlations that were observed in the HMBC spectrum (Figure 4.23) include 3-bond couplings between the carbonyl carbon with H2' and H6', and between C β with H2 and H6. These correlations indicated the correlations between ring A, the α,β -unsaturated carbonyl system and ring B. Furthermore, a 3-bond coupling was observed between C4' with H7', and between C7' with H2', indicated that the amine group was substituted at the position 3' of ring A.

The NMR spectral data of the compound **DA** is listed in the Table 4.8 and 4.9. The compound 4'-hydroxy-3'-dimethylaminomethylchalcone (**DA2**) showed similar spectral properties as **DA** as they possess identical structural backbones with only difference of the substituent at position 4 of ring B. The NMR spectra and spectral data of **DA2** are shown in Appendix D.

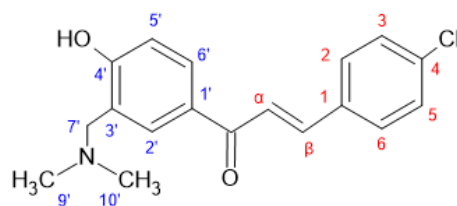


Table 4.8: ^1H , ^{13}C and DEPT NMR spectral data of **DA**.

Atom Number	^1H (δ_{H} , ppm)	^{13}C (δ_{C} , ppm)	DEPT
C=O	-	188.3	C
α	7.51 (d, $J = 15.6$)	122.4	CH
β	7.72 (d, $J = 15.6$)	142.2	CH
1	-	133.8	C
2 & 6	7.56 (d, $J = 8.72$)	129.6	CH
3 & 5	7.37 (d, $J = 8.72$)	129.3	CH
4	-	136.2	C
1'	-	129.4	C
2'	7.75 (d, $J = 1.84$)	130.5	CH
3'	-	116.2	C
4'	-	163.6	C
5'	6.88 (d, $J = 8.24$)	116.2	CH
6'	7.90 (dd, $J = 8.68, 2.28$)	130.5	CH
7'	3.74 (s)	62.6	CH ₂
9' & 10'	2.36 (s)	44.5	CH ₃

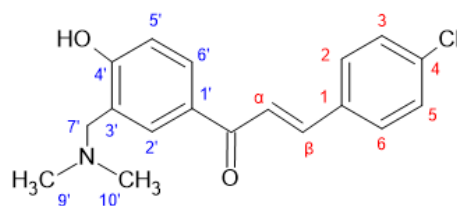


Table 4.9: $^1\text{H} - ^{13}\text{C}$ correlations in DA.

Carbon Number	Proton Number			
	HMQC	HMBC		
	1J	2J	3J	4J
C=O	-	H α	H β , H2', H6'	-
C α	H α	H β	-	-
C β	H β	H α	H2, H6	-
C1	-	H β , H2, H6	H α , H3, H5	-
C2	H2	H3	H β	-
C3	H3	-	-	-
C4	-	H3, H5	H2, H6	-
C5	H5	-	-	-
C6	H6	H5	H β	-
C1'	-	H2', H6'	H5'	-
C2'	H2'	-	-	-
C3'	-	-	-	-
C4'	-	H5'	H2', H6', H7'	-
C5'	H5'	-	-	-
C6'	H6'	-	H2'	-
C7'	H7'	-	H2', H9', H10'	-
C9' & C10'	H9' or H10'	-	H7'	-

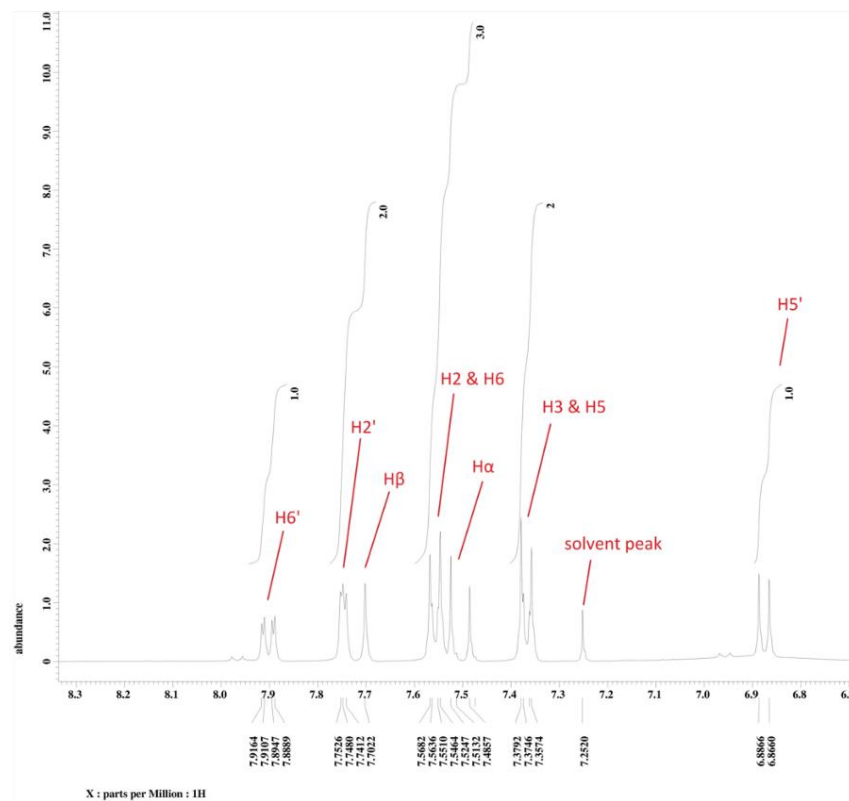
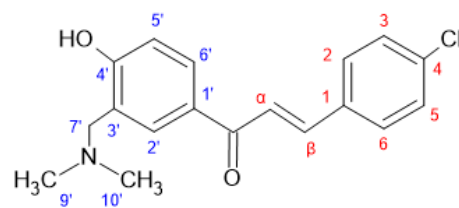


Figure 4.17: Expanded (downfield region) ^1H NMR spectrum of 4-chloro-4'-hydroxy-3'-dimethylaminomethylchalcone (**DA**) (400 MHz, CDCl_3).

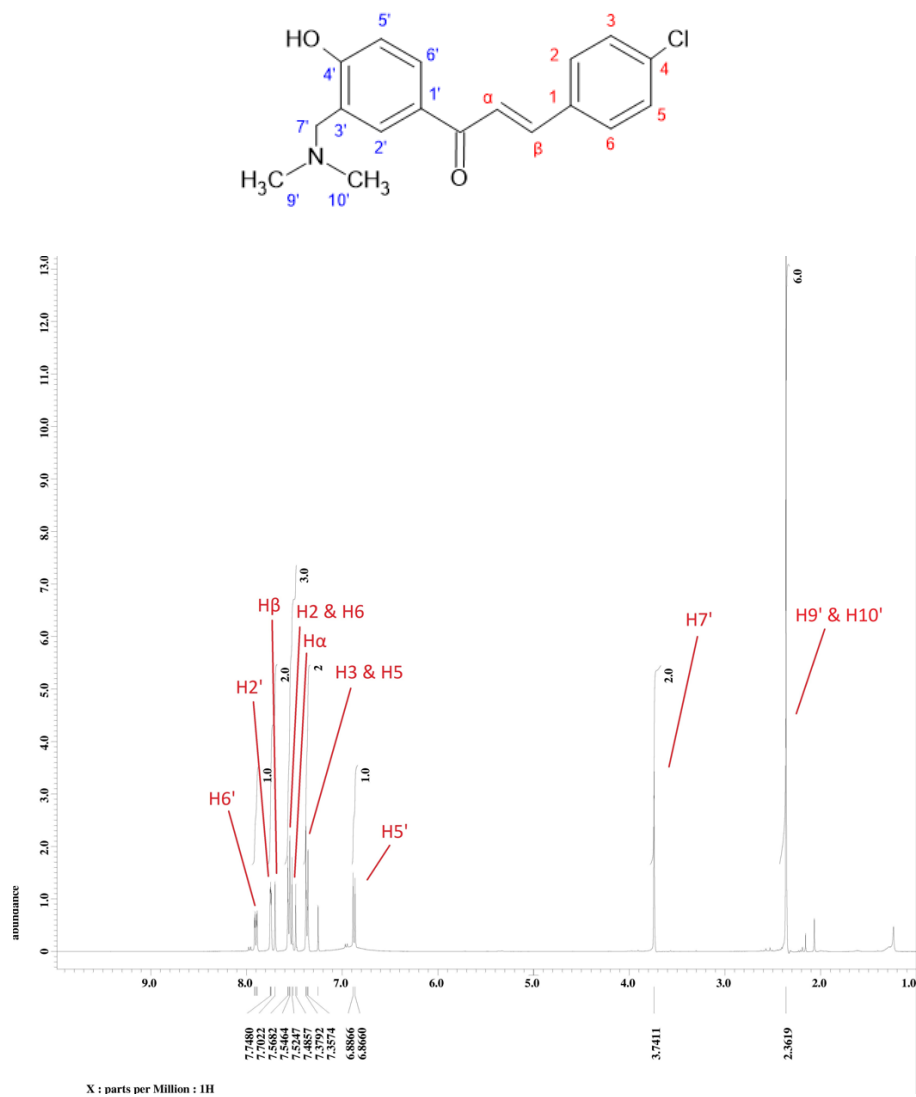


Figure 4.18: ¹H NMR spectrum of 4-chloro-4'-hydroxy-3'-dimethylaminomethylchalcone (**DA**) (400 MHz, CDCl₃).

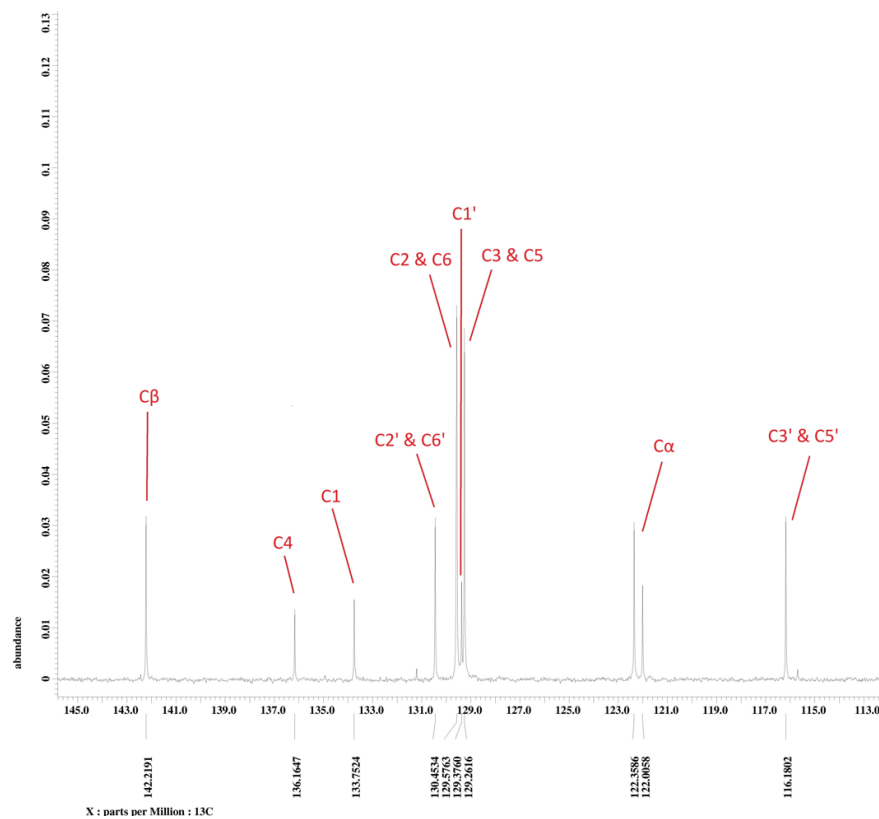
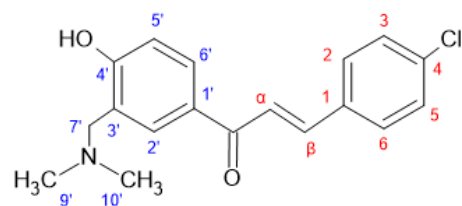


Figure 4.19: Expanded (downfield region) ^{13}C NMR spectrum of 4-chloro-4'-hydroxy-3'-dimethylaminomethylchalcone (**DA**) (100 MHz, CDCl_3).

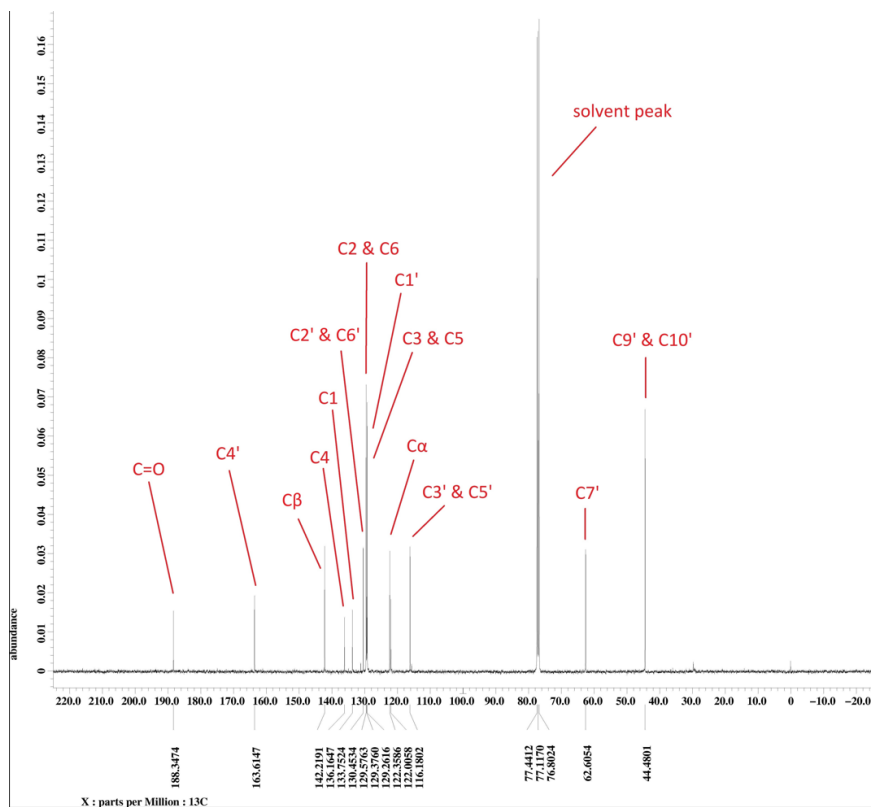
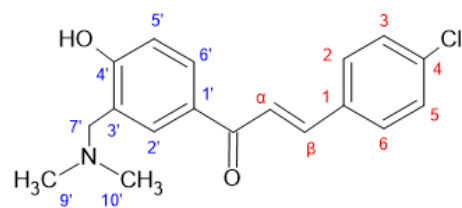


Figure 4.20: ^{13}C NMR spectrum of 4-chloro-4'-hydroxy-3'-dimethylaminomethylchalcone (**DA**) (100 MHz, CDCl_3).

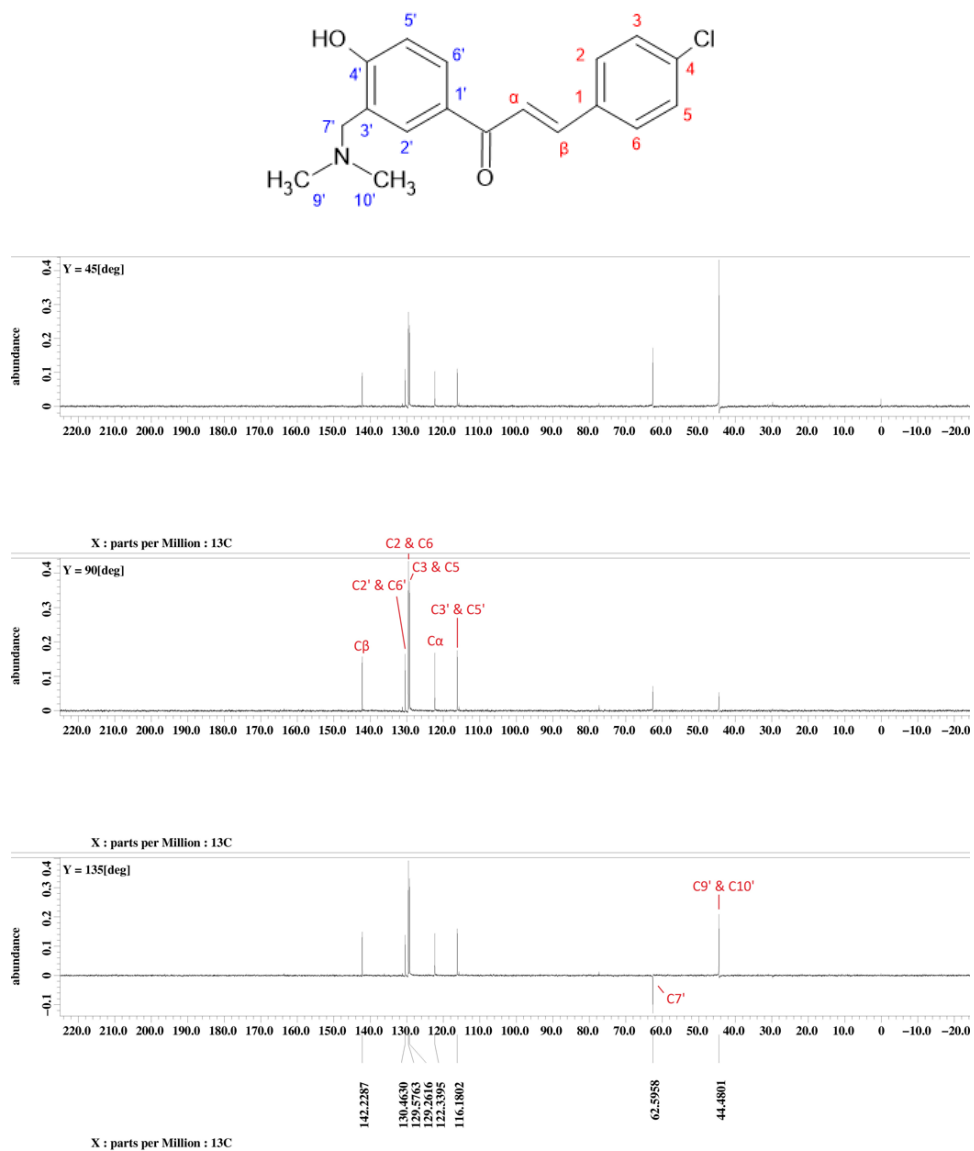


Figure 4.21: DEPT NMR spectrum of 4-chloro-4'-hydroxy-3'-dimethylaminomethylchalcone (**DA**).

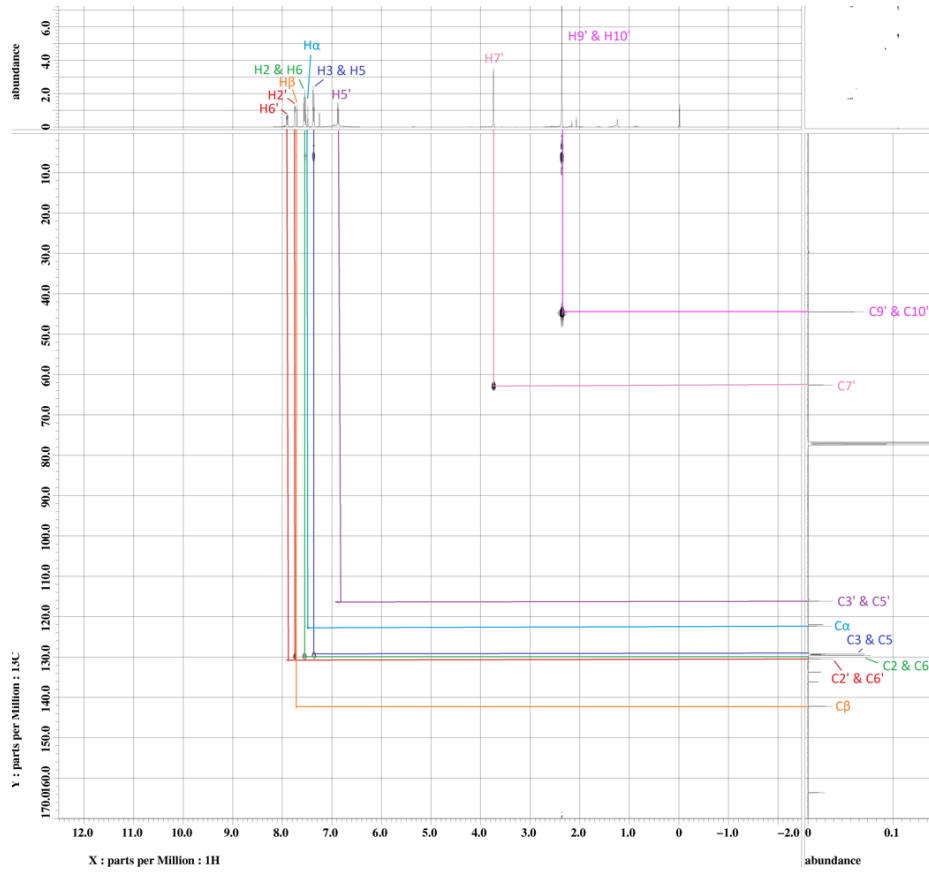
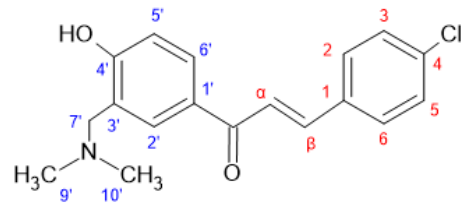


Figure 4.22: HMQC NMR spectrum of 4-chloro-4'-hydroxy-3'-dimethylaminomethylchalcone (**DA**).

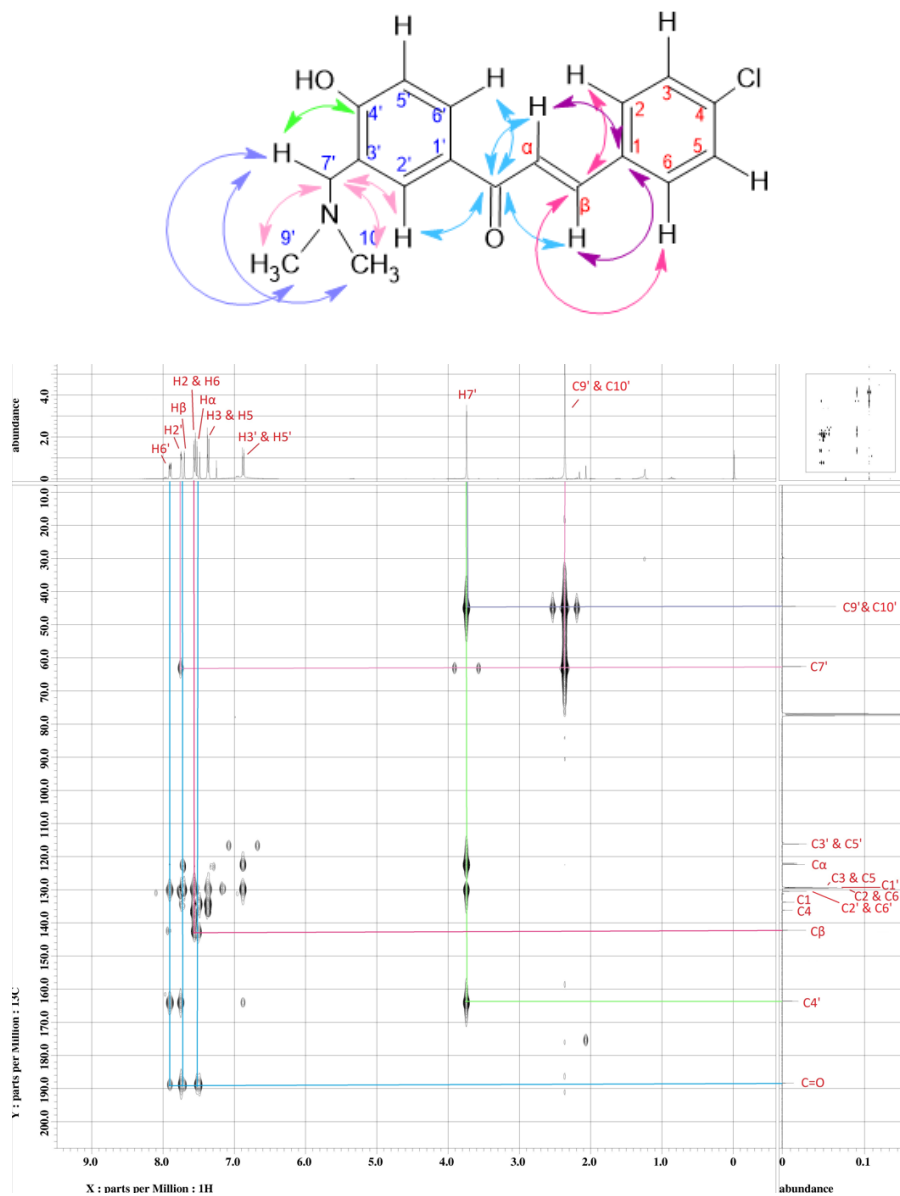


Figure 4.23: HMBC NMR spectrum of 4-chloro-4'-hydroxy-3'-dimethylaminomethylchalcone (**DA**).

4.5.3 Structural Elucidation of 4-chloro-4'-hydroxy-3'-pyrrolidinomethylchalcone

Based on the ^1H NMR spectrum (Figure 4.24) of 4-chloro-4'-hydroxy-3'-pyrrolidinomethylchalcone (**PY**), the six signals attributed to the aromatic protons in the structure occurred within the region 6.8-7.8 ppm as well. The doublets attributed to vinylic protons $\text{H}\alpha$ and $\text{H}\beta$ were observed at 7.51 and 7.72 ppm, respectively. Additionally, the doublet of doublets corresponded to $\text{H6}'$ was observed at 7.90 ppm, with the coupling constants of 2.44 Hz for the coupling with *meta*-benzylic proton and 8.56 Hz for *ortho*-benzylic proton. The proton peaks attributed to the amine substituent include the singlet at 3.92 ppm which was assigned to $\text{H7}'$, singlet at 2.69 ppm corresponded to $\text{H9}'$ and $\text{H12}'$, and the singlet at 1.88 ppm which represented $\text{H10}'$ and $\text{H11}'$.

A total of 14 carbon signals were shown in the ^{13}C NMR spectrum (Figure 4.25) of **PY**. The carbon signals attributed to the amine substituent are the signal at 58.6 ppm which indicated $\text{C7}'$, at 53.5 ppm which corresponded to $\text{C9}'$ and $\text{C12}'$, and at 23.7 ppm which represented $\text{C10}'$ and $\text{C11}'$. $\text{C7}'$, $\text{C9}'$ and $\text{C12}'$ occurred at lower field regions than $\text{C10}'$ and $\text{C11}'$ was due to the deshielding effect of the electronegative nitrogen atom. The proton and carbon spectral data of **PY** were in accordance to those as reported by Hieu, et al. (2012). As for the DEPT NMR spectrum (Figure 4.26) of **PY**, the signals for methylene carbons of $\text{C7}'$, $\text{C9}'$ and $\text{C12}'$, $\text{C11}'$ and $\text{C10}'$ were shown in the DEPT-135 NMR spectrum.

1-bond couplings were observed in the HMQC spectrum (Figure 4.27) of **PY** between C_{α} , C_{β} , C2, C3, C5, C6, C2', C3', C5', C6', C7', C9' and C10' with their respective protons. Likewise, 3-bond correlations could be seen between the carbonyl carbon with H2' and H6', and between C_{β} with H2 and H6 in the HMBC spectrum (Figure 4.28) of **PY**. These correlations indicated the core structure of the chalcone. Apart from that, a 3-bond coupling was observed between C7' and H2', and between C9' and C12' with H7', indicating the correlation between the amine substituent and ring A.

The NMR spectral data of the compound **PY** is listed in the Table 4.10 and 4.11. The compound 4'-hydroxy-3'-pyrrolidinomethylchalcone (**PY2**) showed similar spectral properties as **PY** as they possess identical structural backbones with only difference of the substituent at position 4 of ring B. The NMR spectra and spectral data of **PY2** are shown in Appendix E.

Table 4.10: ^1H , ^{13}C and DEPT NMR spectral data of PY.

Atom Number	^1H (δ_{H} , ppm)	Literature Value (Hieu, et al., 2012)	^{13}C (δ_{C} , ppm)	Literature Value (Hieu, et al., 2012)	DEPT
C=O	-	-	188.4	188.2	C
α	7.51 (d, $J = 15.88$ Hz)	7.54 (d, $J = 15.5$ Hz)	122.4	122.4	CH
β	7.72 (d, $J = 15.84$ Hz)	7.74 (d, $J = 15.5$ Hz)	142.2	142.0	CH
1	-	-	133.8	133.6	C
2 & 6	7.56 (d, $J = 8.56$ Hz)	7.58 (d, $J = 8.5$ Hz)	129.6	129.4	CH
3 & 5	7.37 (d, $J = 8.52$ Hz)	7.38 (d, ($J = 8.5$ Hz)	129.3	129.2	CH
4	-	-	136.1	136.0	C
1'	-	-	129.1	129.1	C
2'	7.76 (d, $J = 1.84$ Hz)	7.77 (d, $J = 2$ Hz)	130.4	130.2	CH
3'	-	-	116.1	117.2	C
4'	-	-	163.8	163.5	C
5'	6.87 (d, $J = 8.52$ Hz)	6.88 (d, $J = 8$ Hz)	116.1		CH
6'	7.89 (dd, $J = 2.44$ Hz, 8.56 Hz)	7.92 (dd, $J = 2.5$ Hz, 8.5 Hz)	130.4	130.2	CH
7'	3.92 (s)	3.92 (s)	58.6	58.5	CH ₂
9' & 12'	2.69 (s)	2.68 (s)	53.5	53.4	CH ₂
10' & 11'	1.88 (s)	1.88 (m)	23.7	23.6	CH ₂

Table 4.11: $^1\text{H} - ^{13}\text{C}$ correlations in PY.

Carbon Number	Proton Number			
	HMQC	HMBC		
	1J	2J	3J	4J
C=O	-	H α	H β , H2', H6'	-
C α	H α	-	-	-
C β	H β	H α	H2, H6	-
C1	-	H β	H α , H3, H5	-
C2	H2	-	H6	-
C3	H3	-	H5	-
C4	-	H3, H5	H2, H6	-
C5	H5	-	H3	H β
C6	H6	-	H2	-
C1'	-	H2', H6'	H5'	-
C2'	H2'	-	-	-
C3'	-	-	-	-
C4'	-	H5'	H2', H6'	-
C5'	H5'	-	-	-
C6'	H6'	-	-	-
C7'	H7'	-	H2'	-
C9' & C12'	H9' or H12'	H10' or H11'	H7'	-
C10' & C11'	H10' or H11'	-	-	-

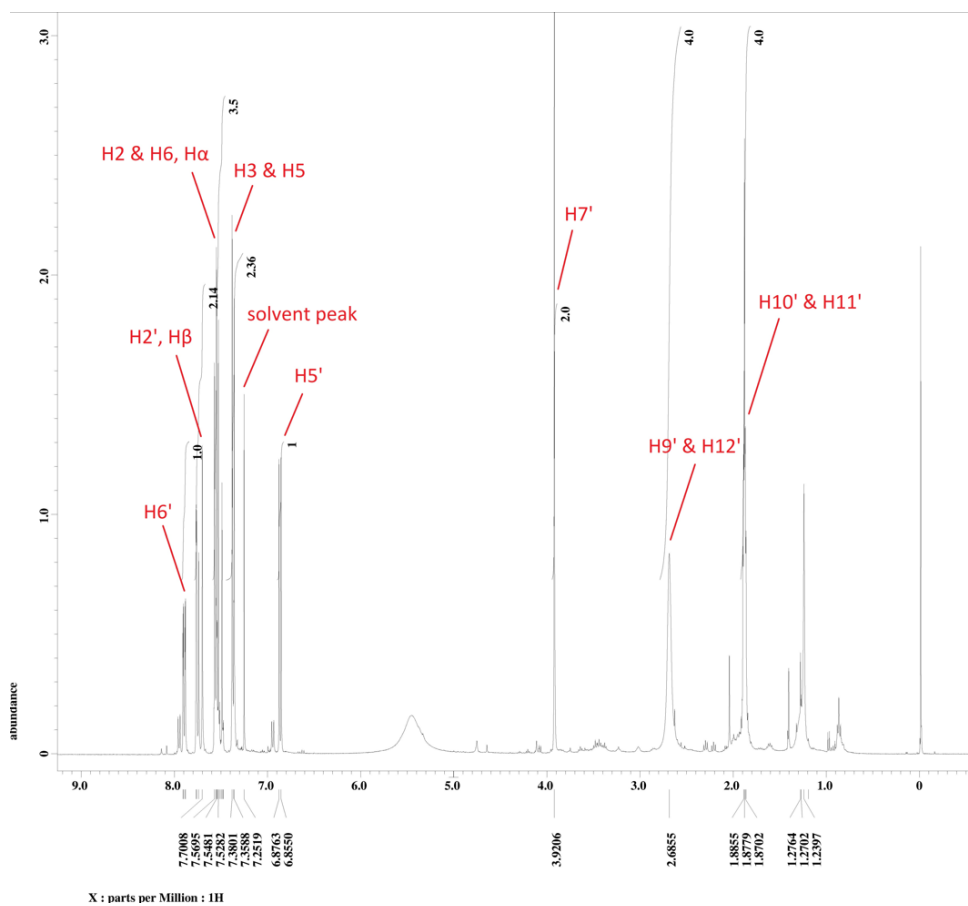
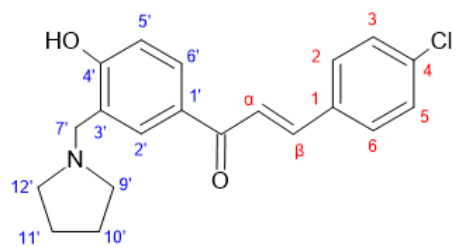


Figure 4.24: ^1H NMR spectrum of 4-chloro-4'-hydroxy-3'-pyrrolidinomethylchalcone (**PY**) (400 MHz, CDCl_3).

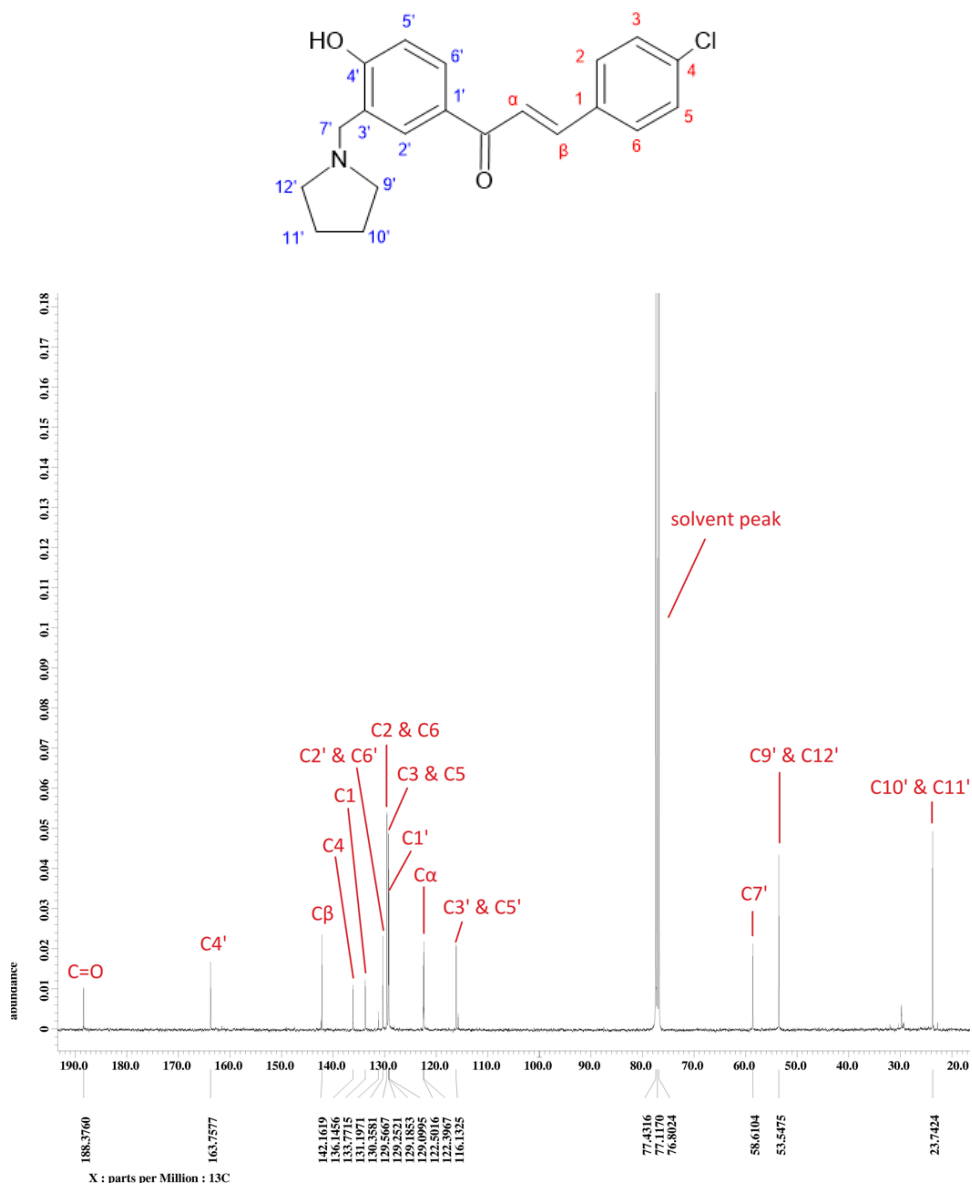


Figure 4.25: ^{13}C NMR spectrum of 4-chloro-4'-hydroxy-3'-pyrrolidinomethylchalcone (PY) (100 MHz, CDCl_3).

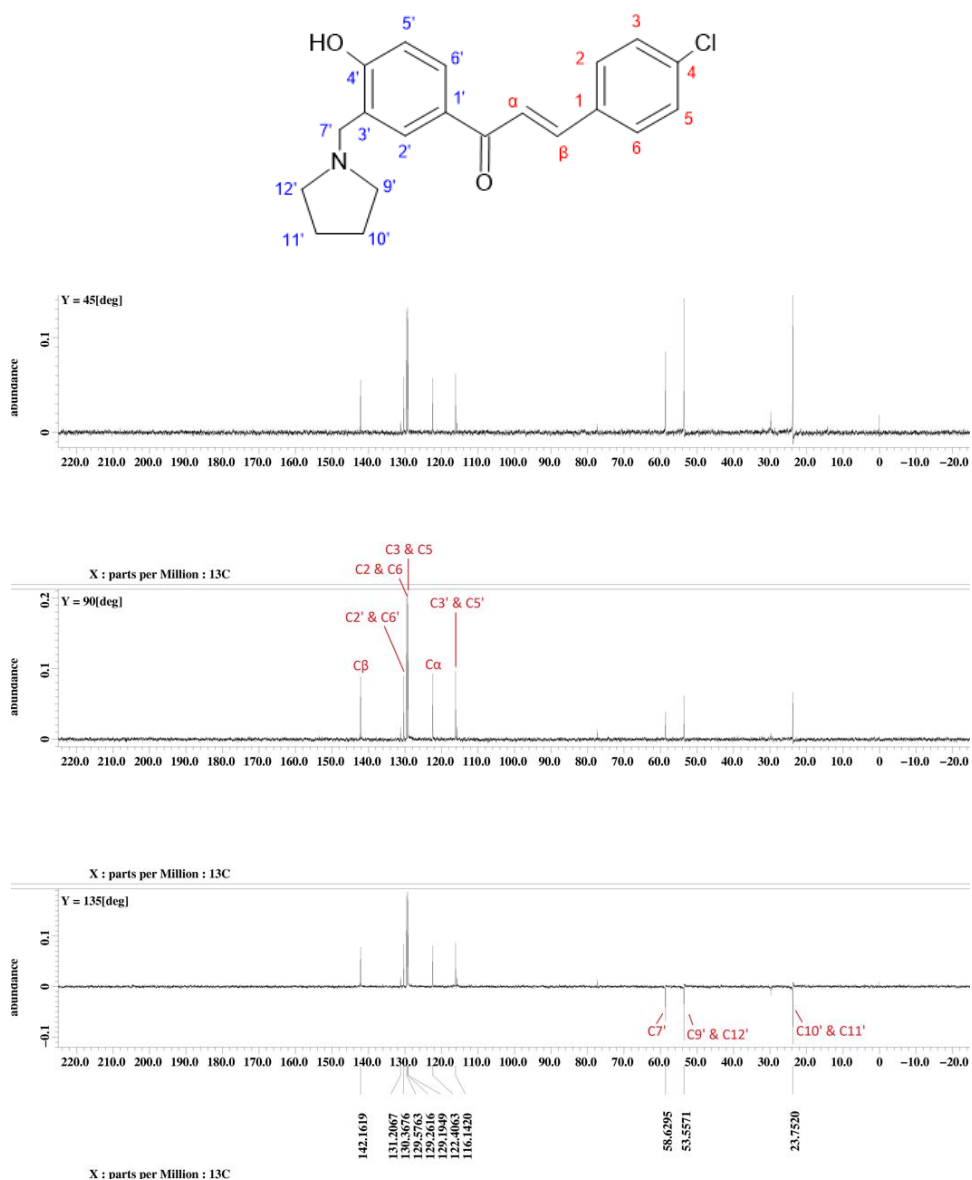


Figure 4.26: DEPT NMR spectrum of 4-chloro-4'-hydroxy-3'-pyrrolidinomethylchalcone (**PY**).

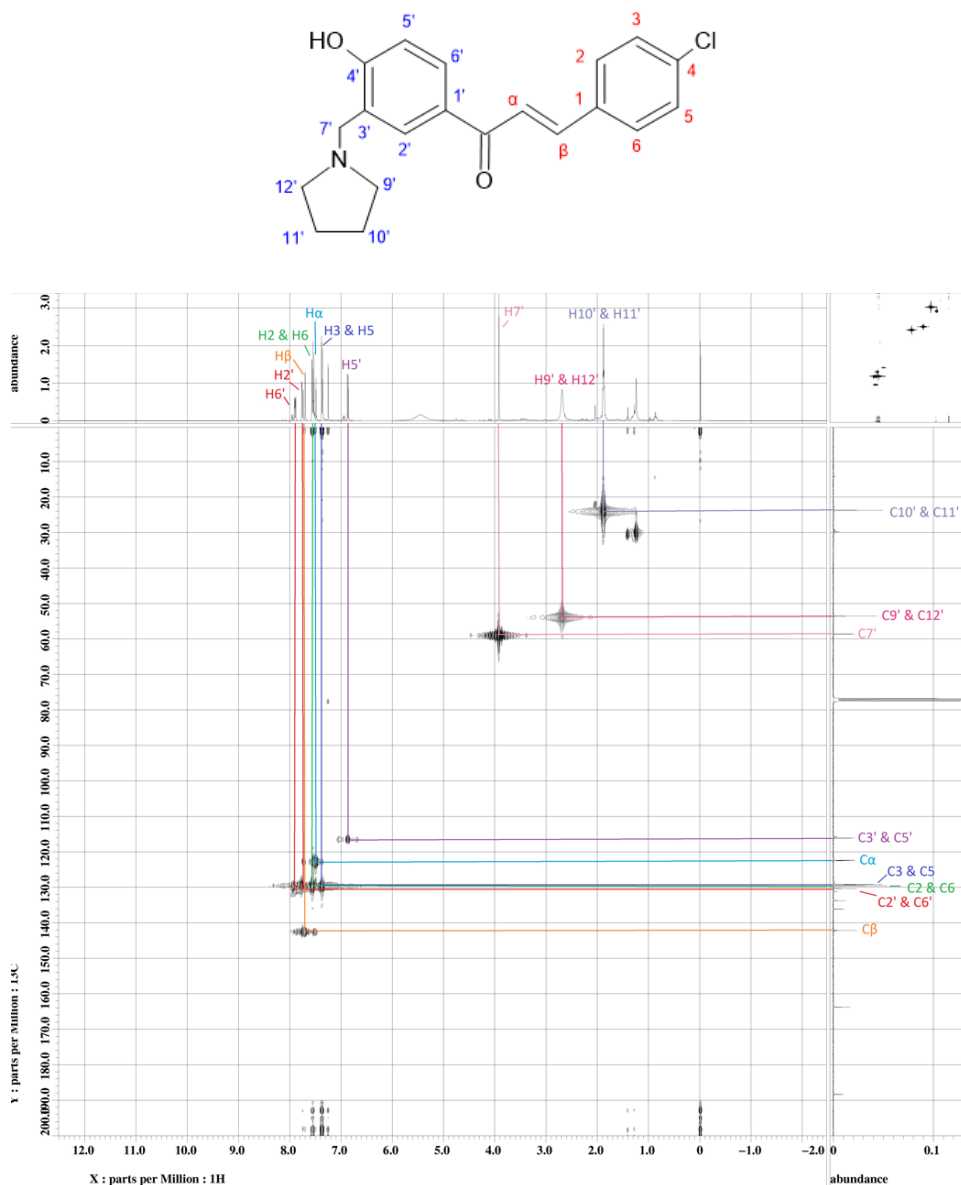


Figure 4.27: HMQC NMR spectrum of 4-chloro-4'-hydroxy-3'-pyrrolidinomethylchalcone (**PY**),

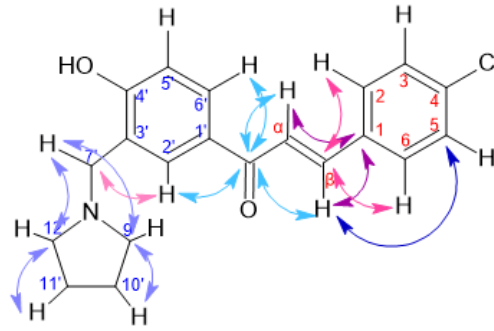


Figure 4.28: HMBC NMR spectrum of 4-chloro-4'-hydroxy-3'-pyrrolidinomethylchalcone (**PY**).

4.5.4 Structural Elucidation of 4-chloro-4'-hydroxy-3'-piperidinomethylchalcone

Based on the ^1H NMR spectrum (Figure 4.29) of 4-chloro-4'-hydroxy-3'-piperidinomethylchalcone (**PI**), the six signals attributed to the aromatic protons in the structure occurred within the region 6.8-7.4 ppm. The doublets attributed to vinylic protons $\text{H}\alpha$ and $\text{H}\beta$ were observed at 7.50 and 7.72 ppm, respectively, with coupling constant of 15.88 Hz. Additionally, the doublet of doublets corresponded to $\text{H}6'$ was observed at 7.88 ppm, with the coupling constants of 2.44 Hz for the coupling with *meta*-benzylic proton and 9.16 Hz for *ortho*-benzylic proton. The proton peaks attributed to the amine substituent include the singlet at 3.75 ppm which was assigned to $\text{H}7'$, the triplets at 1.98 ppm corresponded to $\text{H}9'$ and $\text{H}13'$, triplets at 1.24 ppm which represented $\text{H}10'$ and $\text{H}12'$ and multiplets at 1.66 ppm which were assigned to $\text{H}11'$. A total of 15 carbon signals were shown in the ^{13}C NMR spectrum (Figure 4.30) of **PI**. The carbon signals attributed to the amine substituent are the signal at 61.9 ppm which indicated $\text{C}7'$, at 25.8 ppm which corresponded to $\text{C}9'$ and $\text{C}13'$, at 23.9 ppm which represented $\text{C}10'$ and $\text{C}12'$, and at 25.5 ppm was assigned to $\text{C}11'$.

The spectral data of compound **PI** is listed in Table 4.12. The compound 4'-hydroxy-3'-piperidinomethylchalcone (**PI2**) showed similar spectral properties as **PI** as they possess identical structural backbones with only difference of the substituent at position 4 of ring B. The NMR spectra and spectral data of **PI2** are shown in Appendix F.

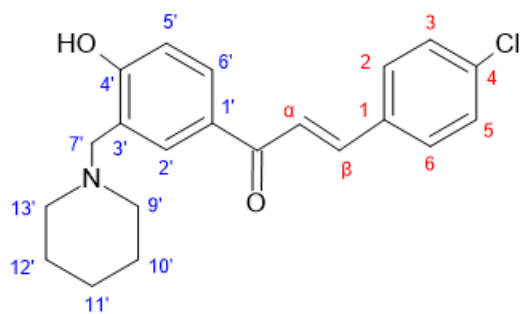


Table 4.12: ^1H and ^{13}C NMR spectral data of **PI**.

Atom Number	^1H (δ_{H} , ppm)	^{13}C (δ_{C} , ppm)
C=O	-	188.3
α	7.50 (d, $J = 15.88$ Hz)	122.4
β	7.72 (d, $J = 15.88$ Hz)	142.1
1	-	133.8
2 & 6	7.56 (d, $J = 8.56$ Hz)	129.6
3 & 5	7.37 (d, $J = 8.56$ Hz)	129.4
4	-	136.1
1'	-	129.7
2'	7.74 (s)	130.2
3'	-	116.1
4'	-	163.7
5'	6.85 (d, $J = 8.56$ Hz)	116.1
6'	7.88 (dd, $J = 2.44$ Hz, 9.16 Hz)	130.2
7'	3.75 (s)	61.9
9' & 13'	1.98 (t)	25.8
10' & 12'	1.24 (t)	23.9
11'	1.66 (m)	25.5

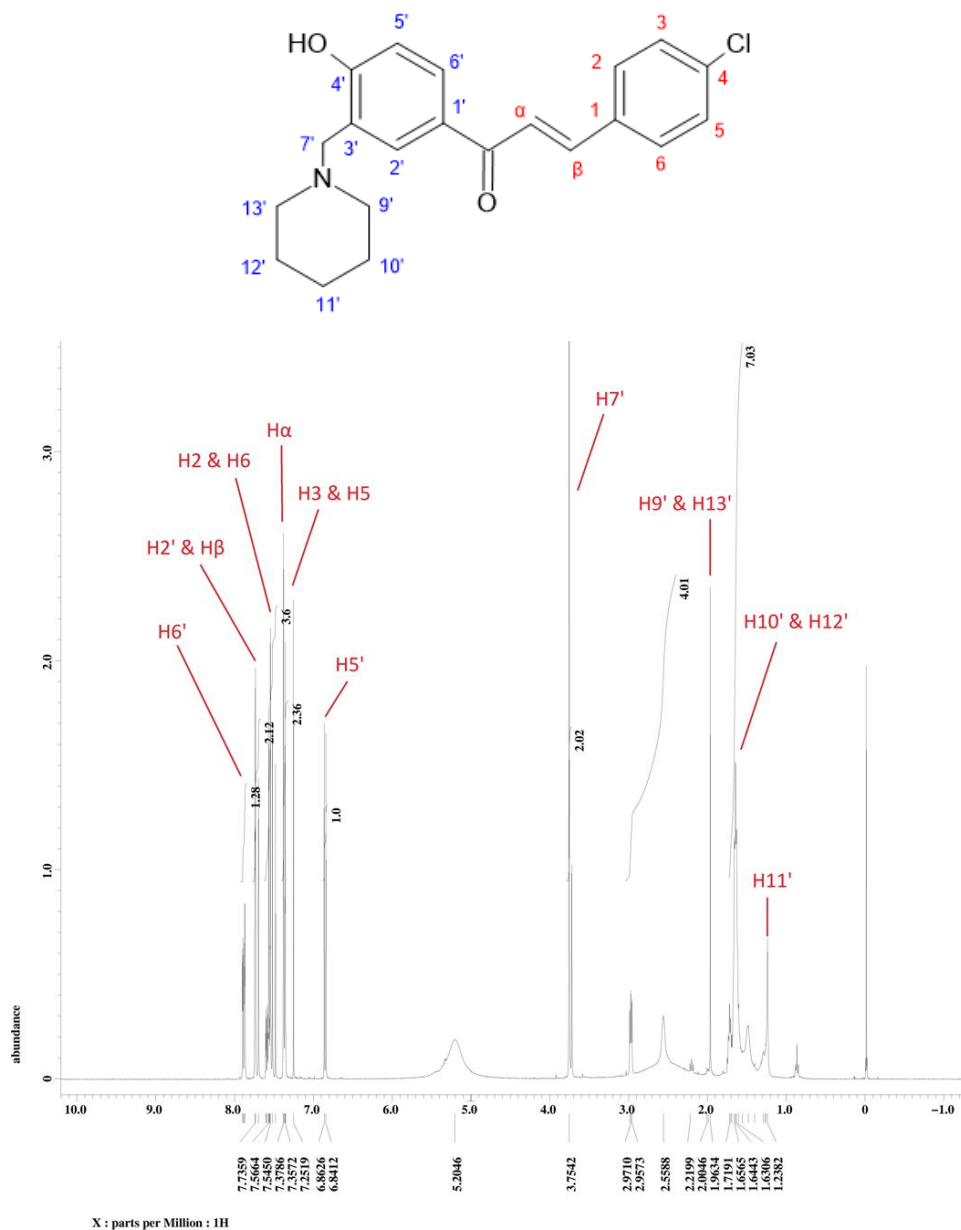


Figure 4.29: ^1H NMR spectrum of 4-chloro-4'-hydroxy-3'-piperidinomethylchalcone (**PI**) (400 MHz, CDCl_3).

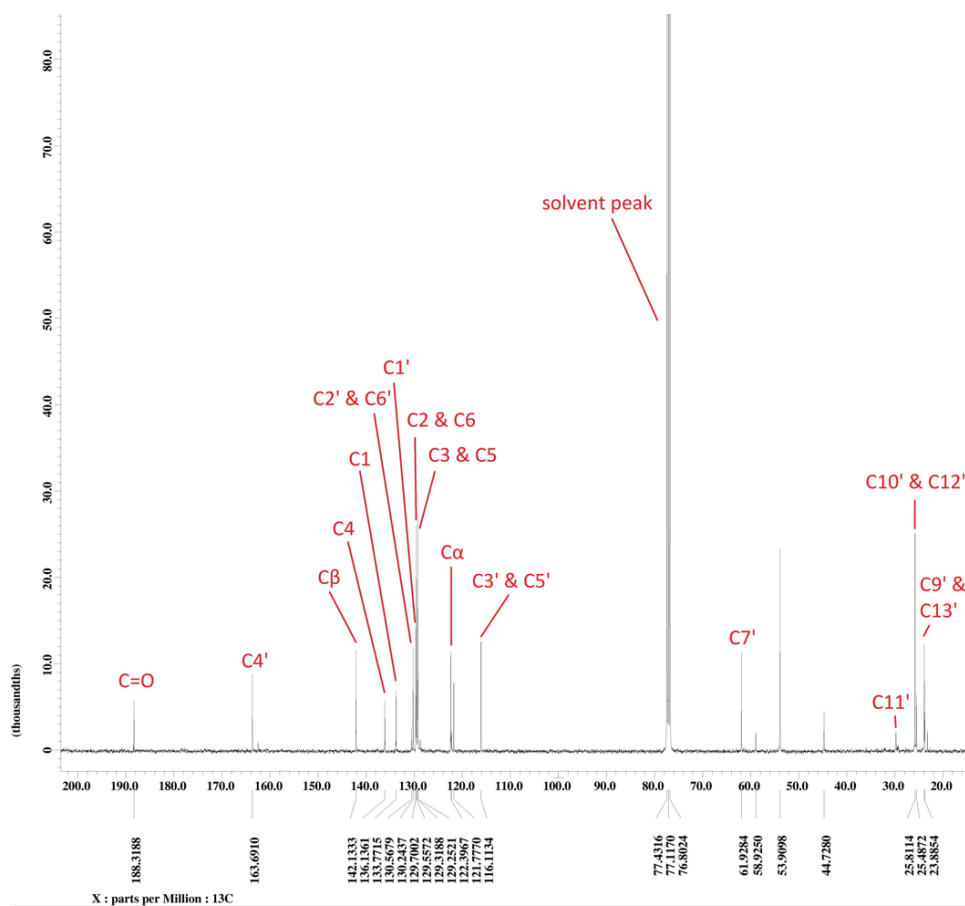
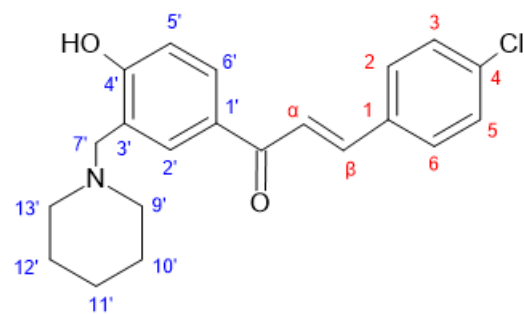


Figure 4.30: ¹³C NMR spectrum of 4-chloro-4'-hydroxy-3'-piperidinomethylchalcone (**PI**) (100 MHz, CDCl₃).

4.6 DPPH Radical Scavenging Capacity Assay

The percentage of DPPH radical scavenging of each synthesized compound at concentrations ranged from 7.8 to 1000 ppm is shown in Table 4.13 and 4.14.

Table 4.13: % DPPH radical scavenging of compounds **CA**, **CA2**, **DA** and **DA2** at different concentrations.

Concentration (ppm)	% DPPH Radical Scavenging			
	CA	CA2	DA	DA2
1000	38.68	37.98	36.69	36.18
500	26.83	26.48	25.58	27.65
250	15.33	14.98	17.57	19.90
125	3.83	2.79	13.70	16.02
62.5	0.70	1.74	10.08	9.04
31.25	0.70	0.70	7.24	8.53
15.625	0.35	2.09	4.91	4.13
7.8125	0	0	3.88	2.07

Table 4.14: % DPPH radical scavenging of compounds **PY**, **PY2**, **PI** and **PI2** at different concentrations.

Concentration (ppm)	% DPPH Radical Scavenging			
	PY	PY2	PI	PI2
1000	64.60	63.57	39.02	40.42
500	47.80	41.86	25.78	24.04
250	33.59	33.85	13.94	17.77
125	22.22	23.77	10.80	13.59
62.5	14.21	16.54	10.45	11.85
31.25	10.08	10.59	9.76	10.10
15.625	5.94	8.53	9.41	9.41
7.8125	3.88	4.13	8.01	9.06

A graph of percentage of DPPH radical scavenging against concentration of the compounds, as shown in Figure 4.31, was plotted to obtain the IC₅₀ value, which is the minimum concentration required to scavenge 50 % of the DPPH free radicals, of each compound. The IC₅₀ values of the compounds are tabulated in Table 4.15.

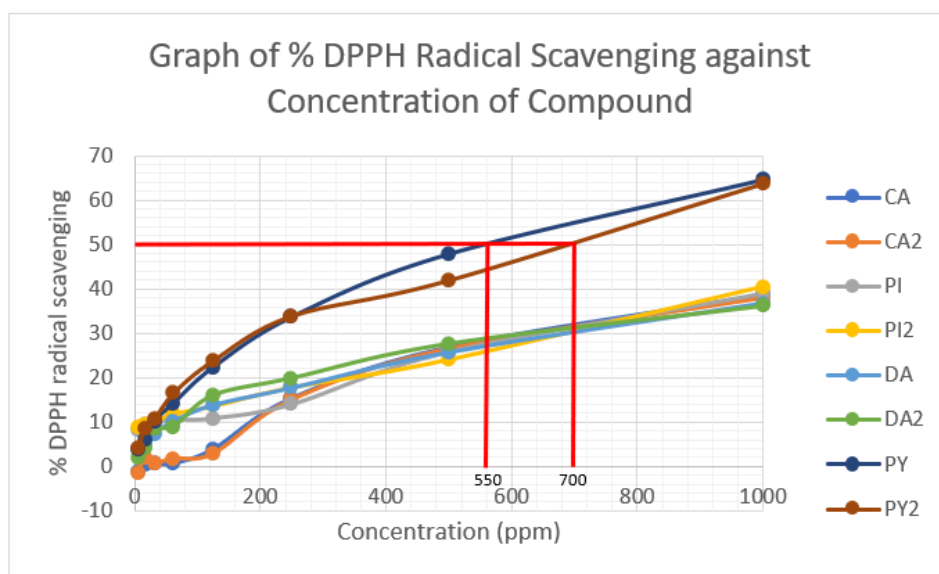


Figure 4.31: Graph of % DPPH radical scavenging against concentration of the chalcone and Mannich base derivatives.

Table 4.15: IC₅₀ values of the synthesized chalcones and their Mannich base derivatives.

Compound	IC ₅₀ value
CA	>1000
CA2	>1000
DA	>1000
DA2	>1000
PY	550
PY2	700
PI	>1000
PI2	>1000

Ascorbic acid was used as the positive control in this study due to its strong antioxidant properties. As the antioxidant capacity of ascorbic acid is much higher than that of the chalcone and Mannich base derivatives, the ascorbic acid was prepared at lower concentrations in the range of 0.2 to 25 ppm. Table 4.16 shows the percentage of DPPH radical scavenging by ascorbic acid at different concentrations, and Figure 4.32 shows the graph of percentage of DPPH radical scavenging against concentration of ascorbic acid.

Table 4.16: % DPPH radical scavenging of ascorbic acid at different concentrations.

Concentration (ppm)	% DPPH Radical Scavenging
25	82.69
12.5	80.10
6.25	79.85
3.125	38.24
1.5625	21.19
0.78125	10.34
0.39063	4.91
0.19531	2.58

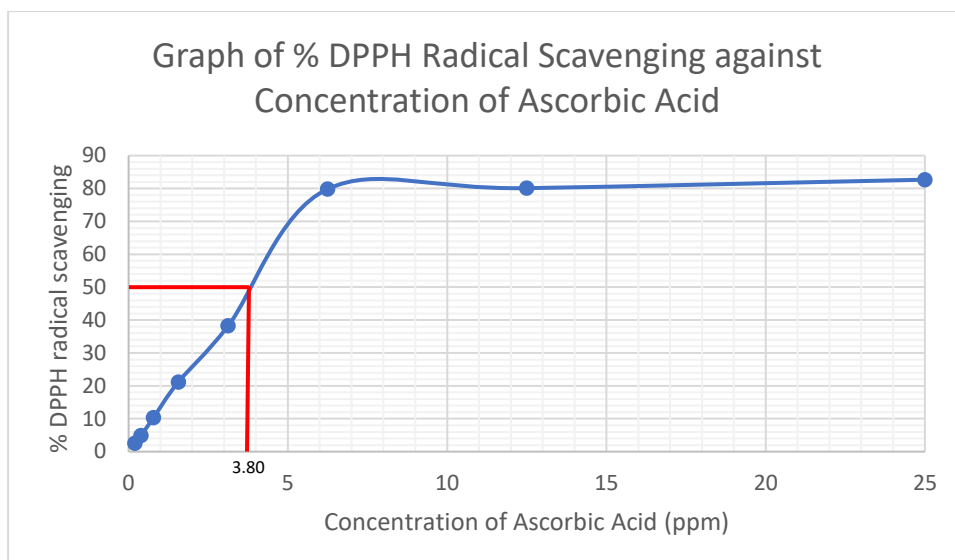


Figure 4.32: Graph of % DPPH radical scavenging against concentration of ascorbic acid.

Based on the results, the Mannich base derivatives generally showed better antioxidant activity than their chalcone parent compounds. At the lowest concentration, both of the chalcone derivatives showed zero antioxidant activity, while all Mannich base derivatives showed antioxidant activity despite the low percentages of DPPH radical scavenging. Besides, the IC_{50} values for the Mannich bases **PY** and **PY2** were recorded at 550 and 700 ppm, respectively, while the IC_{50} values for other compounds occurred at concentrations of above 1000 ppm. This has proven that the Mannich base derivatives are able to demonstrate improved biological activities of their parent chalcone compounds (Bernades, et al., 2017; Reddy, et al., 2008).

Furthermore, the results had also revealed that the chloro-substituent at position 4 of ring B had improved the antioxidant activity of the compounds

as the IC₅₀ value for **PY** was recorded at a lower concentration than **PY2**. In other words, lower concentration of **PY** was required to scavenge 50 % of the DPPH free radicals than **PY2**. On the other hand, the IC₅₀ value for ascorbic acid was recorded at 3.80 ppm. This indicates that the antioxidant activity of the chalcone and Mannich base derivatives is relatively much weaker than ascorbic acid.

CHAPTER 5

CONCLUSION

5.1 Conclusion

In this work, two intermediate compounds, 4-chloro-4'-hydroxychalcone and 4'-hydroxychalcone derivatives were successfully synthesized through Claisen-Schmidt condensation. Moreover, a total of six chalcone Mannich base derivatives were successfully synthesized through Mannich reaction, namely 4-chloro-4'-hydroxy-3'-dimethylaminomethylchalcone (**DA**), 4'-hydroxy-3'-dimethylaminomethylchalcone (**DA2**), 4-chloro-4'-hydroxy-3'-pyrrolidinomethylchalcone (**PY**), 4'-hydroxy-3'-pyrrolidinomethylchalcone (**PY2**), 4-chloro-4'-hydroxy-3'-piperidinomethylchalcone (**PI**) and 4'-hydroxy-3'-piperidinomethylchalcone (**PI2**).

The synthesized compounds were characterized using FTIR, LC-MS and NMR spectroscopy analysis. Some of the characteristic absorption bands observed in the FTIR spectra of the chalcone derivatives include the C=O stretch, α , β unsaturated stretch and aromatic C=C stretch which represented the core structure of the chalcones. While the formation of the Mannich bases could be indicated by the aliphatic C-H and C-N stretches in the FTIR spectra, as well as the methylene peak in the NMR spectra of the Mannich bases. The molecular formulae of the compounds were further confirmed through LC-MS spectroscopy.

Additionally, the antioxidant activity of the synthesized compounds was also studied using the DPPH antioxidant assay test. Generally, the Mannich bases showed improved antioxidant activity over their corresponding chalcone parent compounds. Nevertheless, only notable antioxidant activity was shown by the Mannich bases substituted with pyrrolidine (**PY** and **PY2**). The IC₅₀ values of the compound **PY** and **PY2** were recorded at 550 and 700 ppm, respectively. This indicated that the antioxidant activity of chalcone derivatives can be improved through structure modification.

5.2 Further Studies

The effect of position or nature of substituents on the antioxidant activity of the chalcone and Mannich base derivatives can be further studied by synthesizing chalcones with different acetophenone or benzaldehyde starting materials or synthesizing the Mannich bases using different secondary amines.

Furthermore, the Claisen-Schmidt condensation reaction can be carried out using the green synthesis methods, such as microwave-assisted or grinding methods, in order to achieve better yield with shorter reaction time and a more environmentally friendly approach.

Last but not least, the synthesized compounds can be tested for different biological activities, such as cytotoxicity and antibacterial activity.

REFERENCES

- Aksöz, B.E. and Ertan, R., 2012. Spectral properties of chalcones II. *FABAD Journal of Pharmaceutical Sciences*, pp. 37(4), pp. 205-216.
- Amole, L.K., Bello, I.A. and Oyewale, A.O., 2019. Synthesis, characterization and biological evaluation of three derivatives of 2-hydroxychalcones. *Journal of Applied Sciences and Environmental Management*, 23(4), pp. 647-653.
- Anwar, C., Prasetyo, Y.D., Matsjeh, S., Haryadi, W., Sholikhah, E.N. and Nendrowati, 2018. Synthesis of chalcone derivatives and their *in vitro* anticancer test against breast (T47D) and colon (WiDr) cancer cell line. *Indonesian Journal of Chemistry*, 18(7), pp. 102-107.
- Attarde, M., Vora, A., Varghese, A. and Kachwala, Y., 2014. Synthesis and evaluation of chalcone derivatives for its alpha amylase inhibitory activity. *Organic Chemistry An Indian Journal*, 10(5), pp. 192-204.
- Bala, S., Sharma, N., Kajal, A., Kamboj, S. and Saini, V., 2014. Mannich bases: an important pharmacophore in present scenario. *International Journal of Medicinal Chemistry*, 14, pp. 1-15.
- Behrendorff, J., Vickers, C.E., Chrysanthopoulos, P. and Nielsen, L.K., 2013. 2,2-Diphenyl-1-picrylhydrazyl as a screening tool for recombinant monoterpene biosynthesis. *Microbial Cell Factories*, 12(1), pp. 76-87.
- Bernades, A., Pérez, C.N., Mayer, M., da Silva, C.C., Martins, F.T. and Perjési, P., 2017. Study of reactions of two Mannich bases derived of 4'-hydroxychalcones with glutathione by RP-TLC, RP-HPLC and RP-HPLC-ESI-MS analysis. *Journal of the Brazilian Chemical Society*, 28(6), pp. 1048-1062.
- Hieu, B.T., Thuy, L.T., Thuy, V.T., Tien, H.X., Chinh, L.V., Hoang, V.D. and Vu, T.K., 2012. *Bulletin of the Korean Chemical Society*, 33(5), pp. 1586-1592.
- Koçyiğit, Ü.M., Gezegen, H. and Taslimi, P., 2020. Synthesis, characterization, and biological studies of chalcone derivatives containing Schiff bases: Synthetic derivatives for the treatment of epilepsy and Alzheimer's disease. *Archiv der Pharmazie*, 353(12), pp. 1-11.
- Kostopoulou, I., Tzani, A., Polyzos, N., Karadendrou, M., Kritsi, E., Pontiki, E., Liargkova, T., Hadjipavlou-Litina, D., Zoumpoulakis, P. and Detsi, A., 2021. Exploring the 2'-hydroxy-chalcone framework for the development of dual antioxidant and soybean lipoxygenase inhibitory agents. *Molecules*, 26, pp. 2777-2801.

Kristanti, A.N., Suwito, H., Aminah, N.S., Haq, K.U., Hardiyanti, H.D., Anggraeni, H., Faiza, N., Anto, R.S. and Muharromah, S., 2020. Synthesis of some chalcone derivatives, in vitro and in silico toxicity evaluation. *Rasayan Journal of Chemistry*, 13(1), pp. 654-662.

Leopoldini, M., Marino, T., Russo, N. and Toscano, M., 2004. Antioxidant properties of phenolic compounds: H-atom versus electron transfer mechanism. *The Journal of Physical Chemistry*, 108(22), pp. 4916-4922.

Marinescu, M., Cintează, L.O., Marton, G.L., Chifiriuc, M., Popa, M., Stănculescu, L., Zălaru, C. and Stavarache, C., 2020. Synthesis, density functional theory study and in vitro antimicrobial evaluation of new benzimidazole Mannich bases. *BMC Chemistry*, 14(1):45.

Merck, 2022. *1-(4-Hydroxyphenyl)-3-phenyl-prop-2-en-1-one*. [online] Available at: <<https://www.sigmaaldrich.com/MY/en/product/ambeedinc/ambh2d6f6d8a?context=bbe>> [Accessed 15 April 2022].

Minatel, I.O., Borges, C.V., Ferreira, M.I., Gomez, H.A., Chen, C.O. and Lima, G.P., 2017. Phenolic compounds: functional properties, impact of processing and bioavailability. In: M. Soto-Hernandez, M. Palma-Tenango and M.R. Garcia-Mateos, eds. *Phenolic Compounds – Biological Activity*. London: IntechOpen.

Prabhakar, V., Iqbal, H. and Balasubramanian, R., 2019. Antioxidant studies on monosubstituted chalcone derivatives – understanding substituent effects. *Pakistan Journal of Pharmaceutical Sciences*, 29(1), pp. 165-171.

Rammohan, A., Reddy, J.S., Sravya, G., Rao, C.N. and Zyryanov, G.V., 2020. Chalcone synthesis, properties and medicinal applications: a review. *Environmental Chemistry Letter*, 18, pp. 433-458.

Rashdan, S.A., Hassan, A.M., Mandeel, Q.A., Alasfoor, N.M. and Dawood, Z.H., 2018. Synthesis of substituted chalcones and investigation of their biological activities. *Journal of Chemistry and Biochemistry*, 6(1), pp. 1-8.

Reddy, M.V.B., Su, C., Chiou, W., Liu, Y., Chen, R.Y., Bastow, K.F., Lee, K. and Wu, T., 2008. Design, synthesis, and biological evaluation of Mannich bases of heterocyclic chalcone analogs as cytotoxic agents. *Bioorganic & Medicinal Chemistry*, 16, pp. 7358-7370.

Rozmer, Z. Bernades, A., Pérez, C.N. and Perjési, P. Study on the interaction of 4'-hydroxychalcones and their Mannich derivatives with calf thymus DNA by TLC and spectroscopic methods, a DNA cleavage study. *The Open Medicinal Chemistry Journal*, 14, pp. 122-131.

Sökmen, M. and Khan, M.A., 2017. The antioxidant activity of some curcuminoids and chalcones. *Inflammopharmacology*, 24, pp. 81-86.

Sreedhar, N.Y., Jayapal, M.R., Prasad, K.S. and Prasad, P.R., 2010. Synthesis and characterization of 4-hydroxy chalcones using PEG-400 as a recyclable solvent. *Research Journal of Pharmaceutical, Biological and Chemical Sciences*, 1(4), pp. 480-485.

Susanti, V.H.E. and Setyowati, W.A.E., 2019. Synthesis and characterization of some bromochalcones derivatives. In: *3rd International Conference on Advanced Materials for Better Future 2018*. Indonesia, 15-16 October 2018. Bristol, United Kingdom: IOP Publishing. Available at: <<https://iopscience.iop.org/article/10.1088/1757-899X/578/1/012002/pdf#:~:text=Chalcone%20synthesis%20can%20be%20carried,an%20acidic%20or%20alkaline%20atmosphere.>> [Accessed 15 April 2022].

Syahri, J., Nasution, H., Nurohmah, B.A., Purwono, B., Yuanita, E., Zakaria, N.H. and Hassan, N.I., 2020. Design, synthesis and biological evaluation of aminoalkylated chalcones as antimalarial agent. *Sains Malaysiana*, 49(11), pp. 2667-2677.

The Royal Society of Chemistry, 2017. *Solvent-free aldol condensation reactions: synthesis of chalcone derivatives*. [online] Available at: <<http://www.rsc.org/suppdata/books/184973/9781849739634/bk9781849739634-chapter%204.2.2.pdf>> [Accessed 15 April 2022].

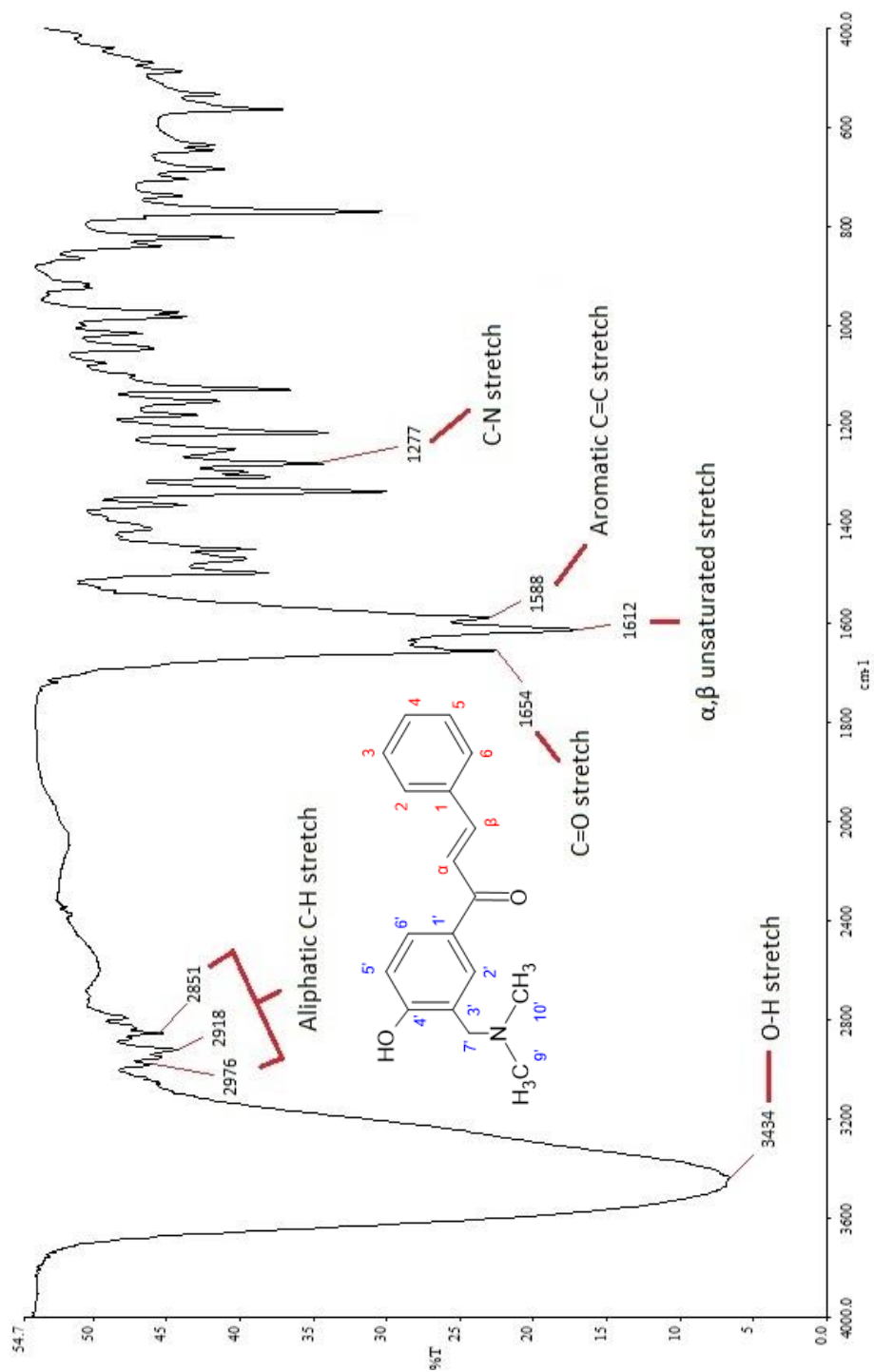
Vutturi, A.V., 2011. *Mannich reaction*. [online] Available at: <<https://www.adichemistry.com/organic/namedreactions/mannich/mannich-reaction-1.html>> [Accessed 15 April 2022].

Xue, Y., Zheng, Y., Zhang, L., Wu, W., Yu, D. and Liu, Y., 2013. Theoretical study on the antioxidant properties of 2'-hydroxychalcones: H-atom vs. electron transfer mechanism. *Journal of Molecular Modeling*, 19, pp. 3851-3862.

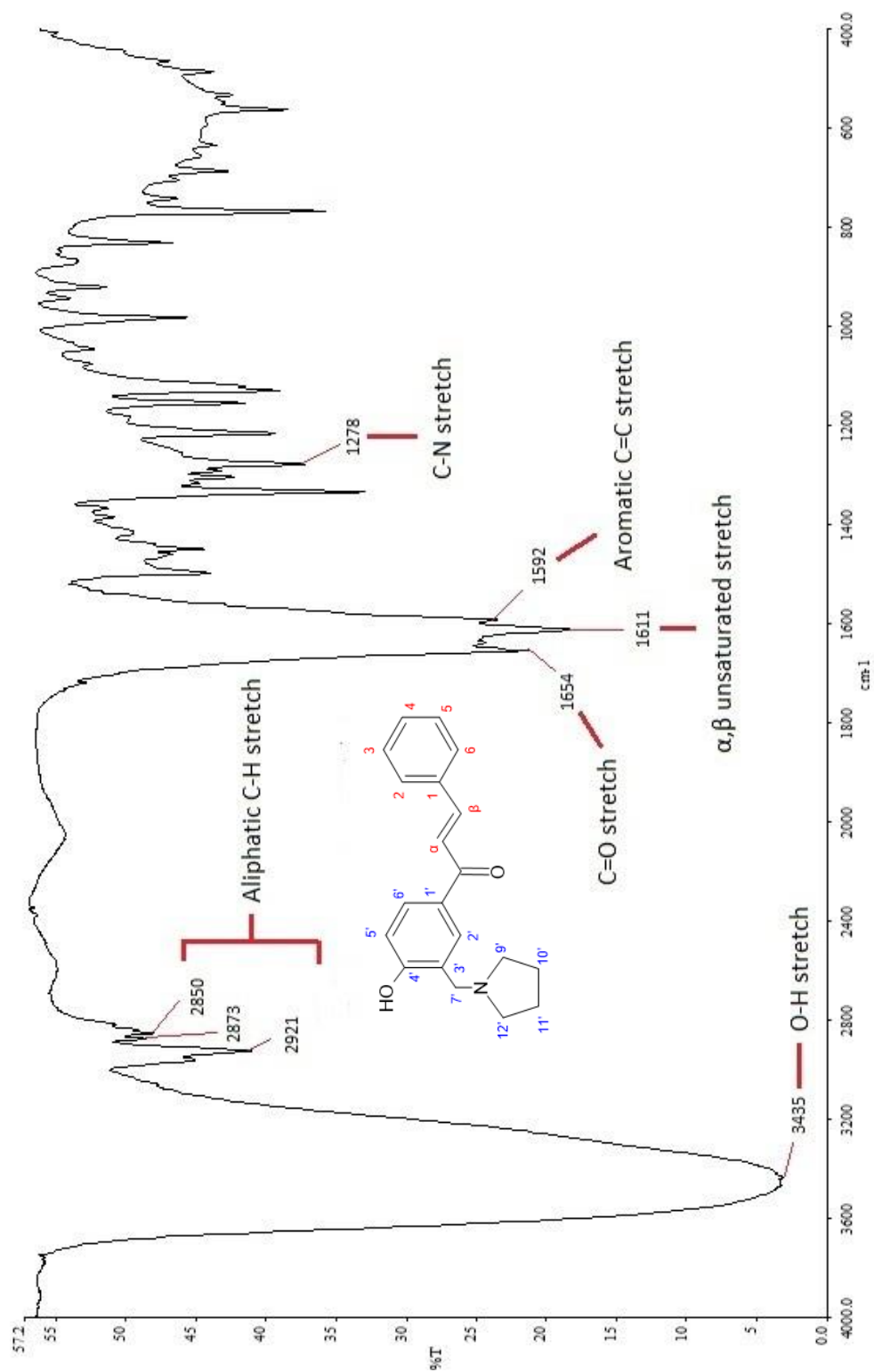
Zhang, X., Song, Q., Cao, Z., Li, Y., Tian, C., Yang, Z., Zhang, H. and Deng, Y., 2019. Design, synthesis and evaluation of chalcone Mannich base derivatives as multifunctional agents for the potential treatment of Alzheimer's disease. *Bioorganic Chemistry*, 87, pp. 395-408.

APPENDICES

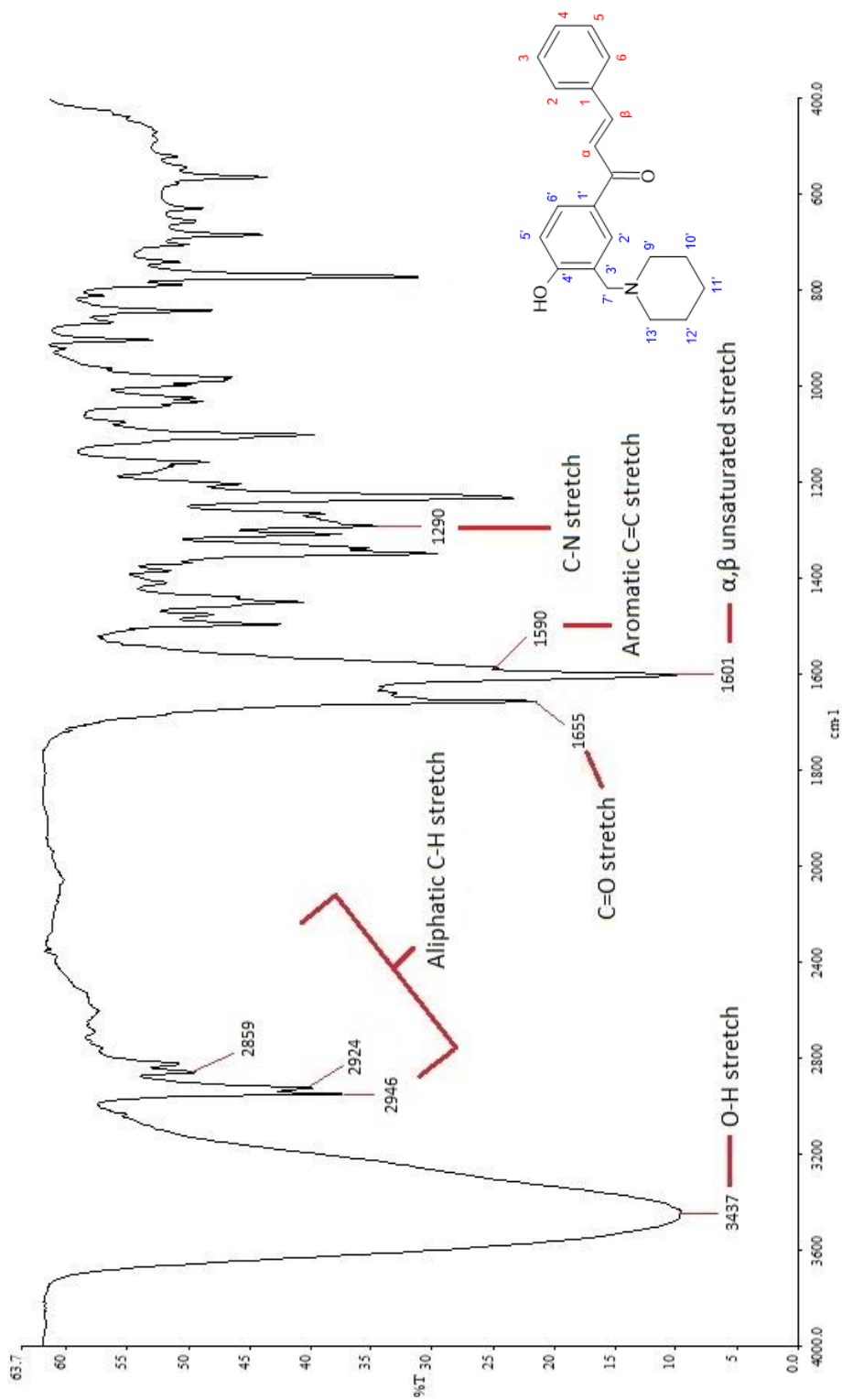
APPENDIX A



Appendix A1: FTIR spectrum of DA2 (KBr).

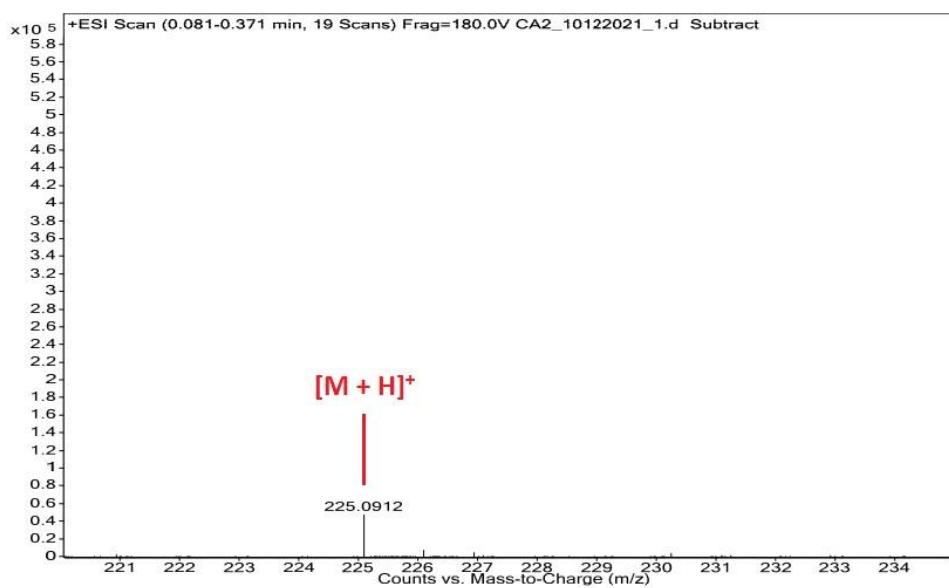
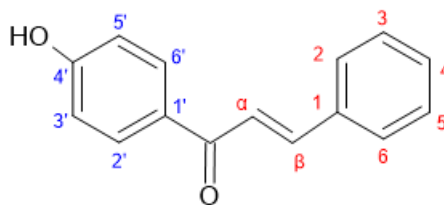


Appendix A2: FTIR spectrum of PY2 (KBr)..



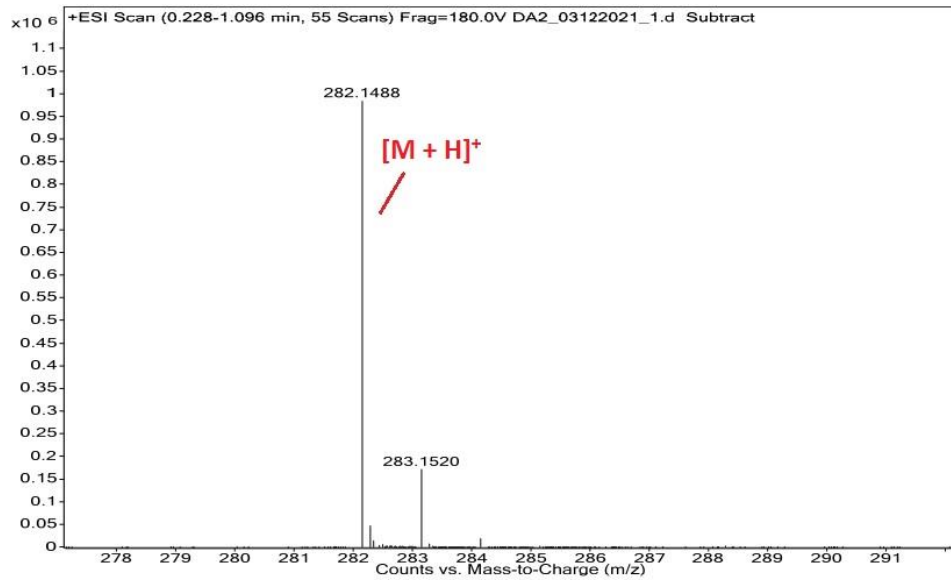
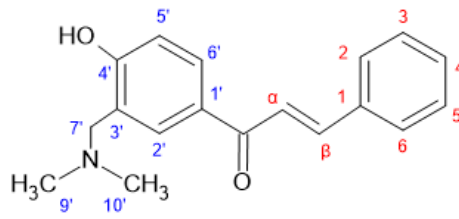
Appendix A3: FTIR spectrum of PI2 (KBr)..

APPENDIX B



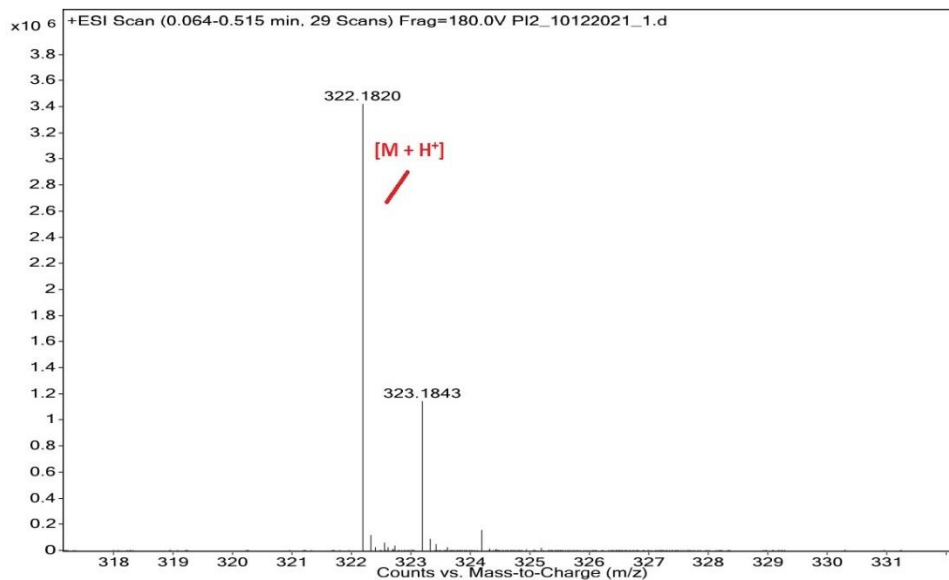
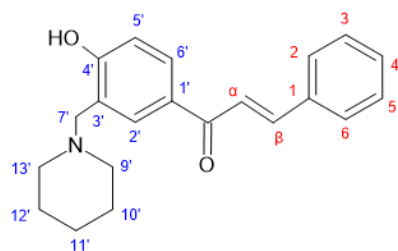
Best	Name	Formula	Score	Mass	Mass (Tgt)	Mass (DB)	Mass (MFG)	Diff (ppm)	Diff (abs. ppm)
✓		C15 H12 O2	86.5	224.0839			224.0837	-0.84	0.84
Species	Ion Formula	m/z	Height	Score (MFG)	Score (MFG, MS)	Score (MFG, MS/MS)	Score (MFG, mass)	Score (MFG, abund)	Score (MFG, iso. spacing)
(M+H) ⁺	C15 H13 O2	225.091	47105.3	86.5	86.5		99.67	93.56	51.7
m/z	m/z (Calc)	Diff (ppm)	Diff (mDa)	Height	Height (Calc)	Height %	Height % (Calc)	Height Sum %	Height Sum% (Calc)
225.0912	225.091	-0.92	-0.2	47105.3	46692.9	100	100	85.3	84.6
226.0884	226.0944	26.31	5.9	6733.4	7680.7	14.3	14.3	12.2	13.9
227.1035	227.0972	-27.8	-6.3	1275.3	782.6	2.7	1.7	2.3	1.4
228.117	228.0998	-75.38	-17.2	101.9	59.7	0.2	0.1	0.2	0.1

Figure B1: LC-MS spectrum and spectrum identification of CA2.



Best	1	Name	Formula	Score	1	Mass	Mass (Tgt)	Mass (DB)	Mass (MFG)	Diff (ppm)	Diff (abs. ppm)
✓			C18 H19 N O2	98.16		281.1415			281.1416	0.15	0.15
Species	Ion Formula	m/z	Height	Score (MFG)	Score (MFG, MS)	Score (MFG, MS/MS)	Score (MFG, mass)	Score (MFG, abund)	Score (MFG, iso. spacing)		
[M+H] ⁺	C18 H20 N O2	282.1489	982711.8	98.16	98.16		99.99	93.7	99.84		
m/z	m/z (Calc)	Diff (ppm)	Diff (mDa)	Height	Height (Calc)	Height %	Height % (Calc)	Height Sum %	Height Sum% (Calc)		
282.1488	282.1489	0.15	0	982711.8	956305.7	100	100	83.9	81.7		
283.152	283.1521	0.55	0.2	170349.2	192598.6	17.3	20.1	14.5	16.4		
284.154	284.155	3.39	1	18154.8	22311.5	1.8	2.3	1.6	1.9		

Figure B2: LC-MS spectrum and spectrum identification of DA2.



Best	Name	Formula	Score	Mass	Mass (Tgt)	Mass (DB)	Mass (MFG)	Diff (ppm)	Diff (abs. ppm)
✓		C21 H23 N O2	76.06	321.1747			321.1729	-5.73	5.73
Species	Ion Formula	m/z	Height	Score (MFG)	Score (MFG, MS)	Score (MFG, MS/MS)	Score (MFG, mass)	Score (MFG, abund)	Score (MFG, iso. spacing)
(M+H) ⁺	C21 H24 N O2	322.1802	3416851.3	76.06	76.06		79.14	56.19	93.76
m/z	m/z (Calc)	Diff (ppm)	Diff (mDa)	Height	Height (Calc)	Height %	Height % (Calc)	Height Sum %	Height Sum% (Calc)
322.182	322.1802	-5.83	-1.9	3416951.3	3729546.6	100	100	72.3	78.9
323.1843	323.1834	-2.53	-0.8	11399563.5	873854.3	33.4	23.4	24.1	18.5
324.1875	324.1864	-3.17	-1	155019.3	113095.9	4.5	3	3.3	2.4
325.1902	325.1892	-3.11	-1	15497.7	10635	0.5	0.3	0.3	0.2

Figure B3: LC-MS spectrum and spectrum identification of **PI2**.

APPENDIX C

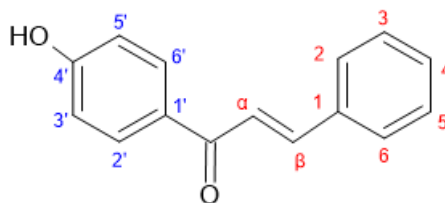


Table C1: ^1H , ^{13}C and DEPT NMR spectral data of **CA2**.

Atom Number	^1H (δ_{H} , ppm)	^{13}C (δ_{C} , ppm)	DEPT
C=O	-	187.8	C
α	7.86 (d, $J = 15.6$ Hz)	122.6	CH
β	7.64 (d, $J = 15.6$ Hz)	143.3	CH
1	-	135.4	C
2 & 6	7.81 (m)	129.4	CH
3 & 5	7.40 (m)	129.2	CH
4	7.40 (m)	130.9	CH
1'	-	129.6	C
2' & 6'	8.03 (d, $J = 8.24$ Hz)	131.7	CH
3' & 5'	6.87 (d, $J = 8.72$ Hz)	116.0	CH
4'	-	162.7	C

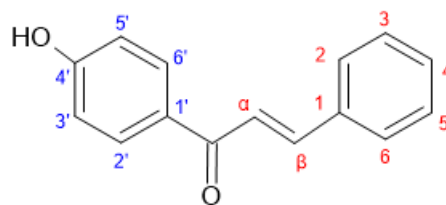


Table C2: $^1\text{H} - ^{13}\text{C}$ correlations in CA2.

Carbon Number	Proton Number			
	HMQC	HMBC		
	1J	2J	3J	4J
C=O	-	H α	H β , H2', H6'	-
C α	H α	-	-	-
C β	H β	H α	H2, H6	H3, H5
C1	-	H β , H2, H6	H α , H3, H5	-
C2	H2	H β	-	-
C3	H3	H2	-	-
C4	H4	-	H2, H6	-
C5	H5	H6	-	-
C6	H6	-	H β	-
C1'	-	-	-	-
C2'	H2'	-	-	-
C3'	H3'	H2'	H5'	-
C4'	-	H3', H5'	H2', H6'	-
C5'	H5'	H6'	H3'	-
C6'	H6'	-	-	-

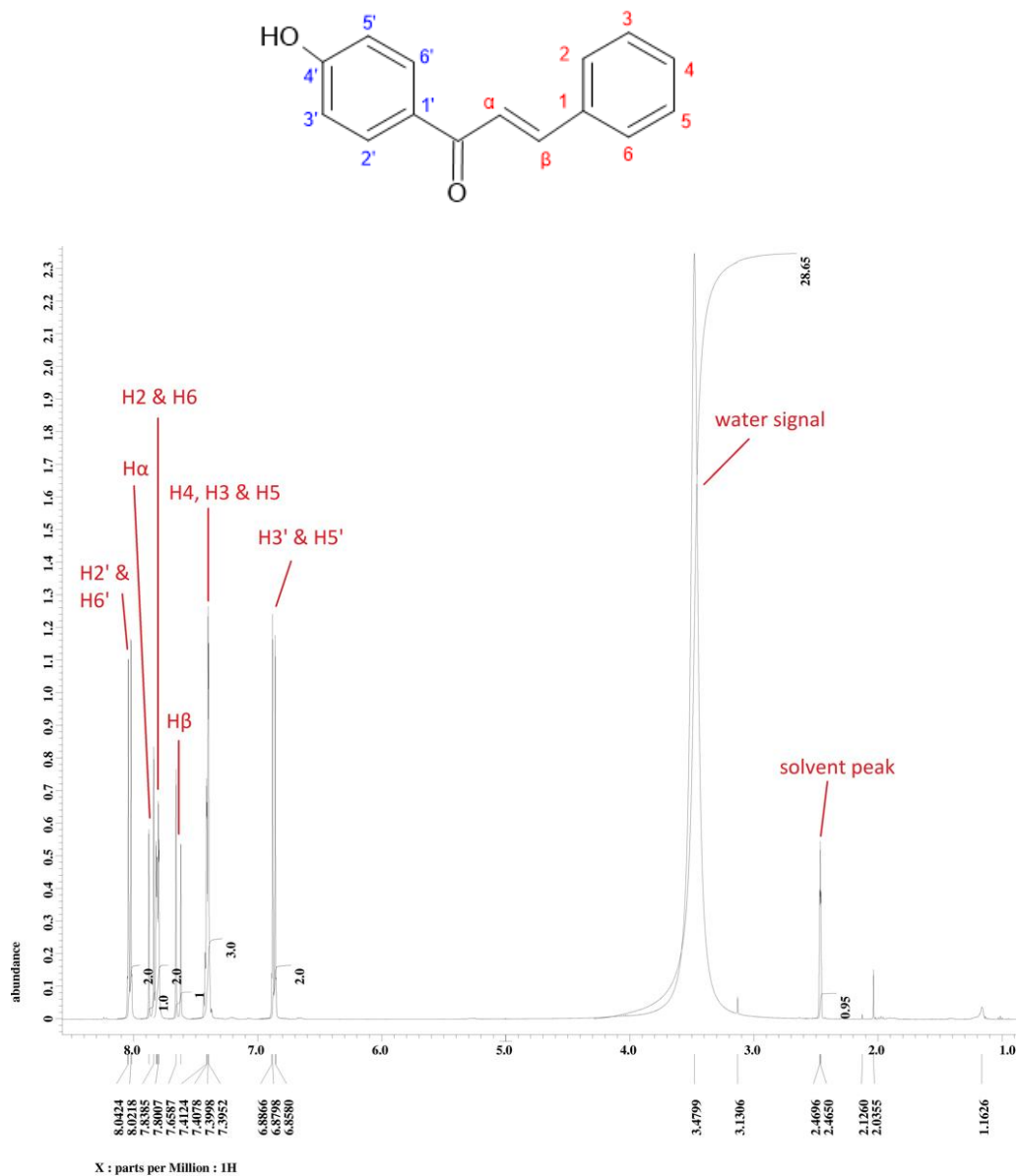


Figure C1: Expanded (downfield region) ^1H NMR spectrum of 4'-hydroxychalcone (CA2) (400 MHz, DMSO- d_6).

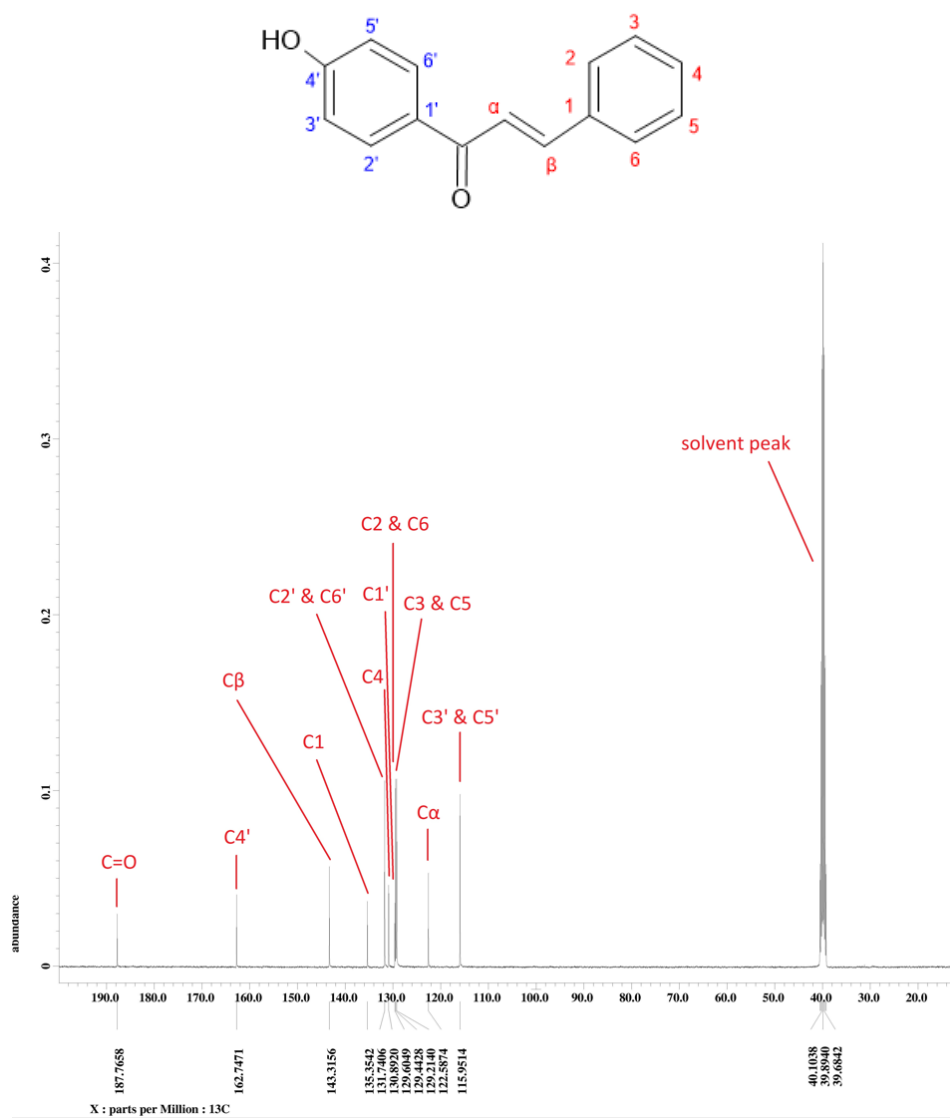


Figure C2: ^{13}C NMR spectrum of 4'-hydroxychalcone (CA2) (100 MHz, DMSO- d_6).

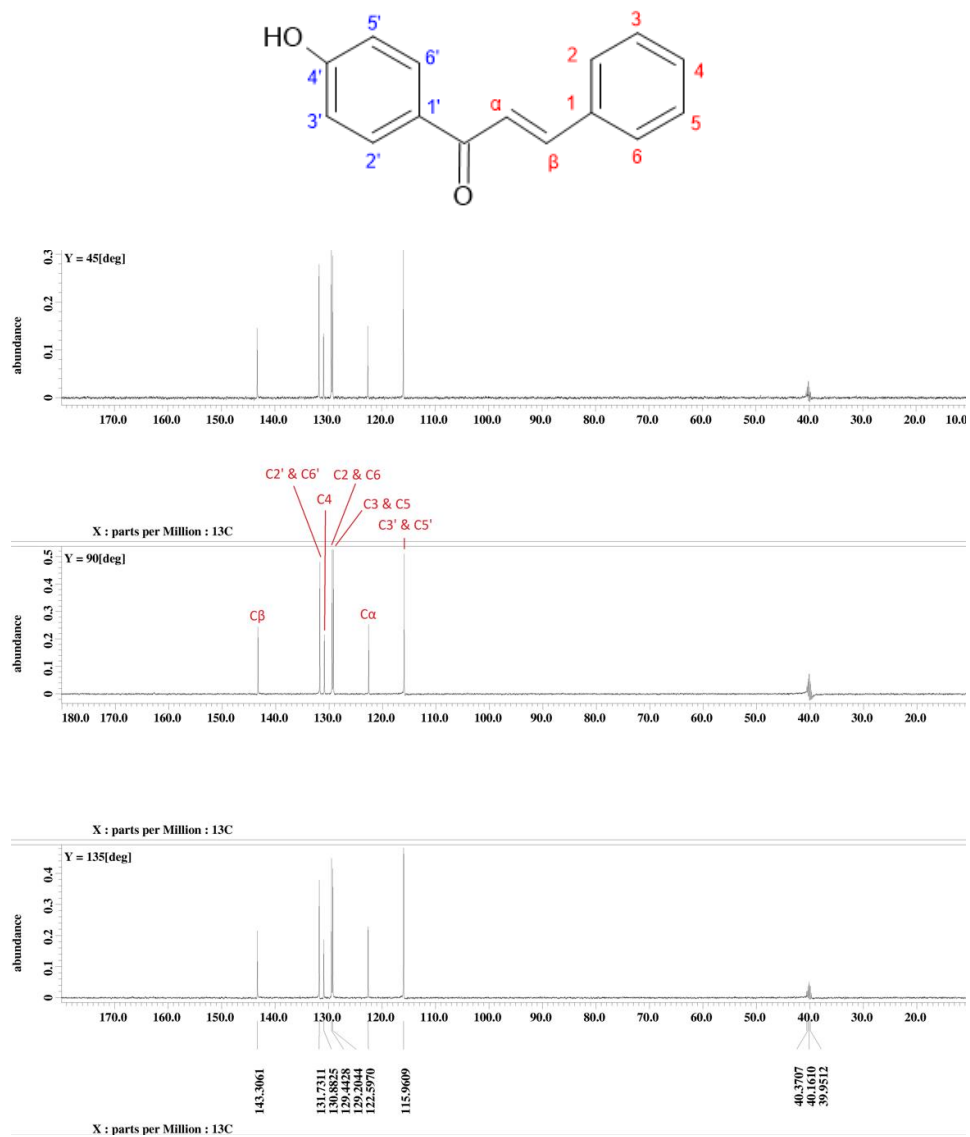


Figure C3: DEPT NMR spectrum of 4'-hydroxychalcone (CA2).

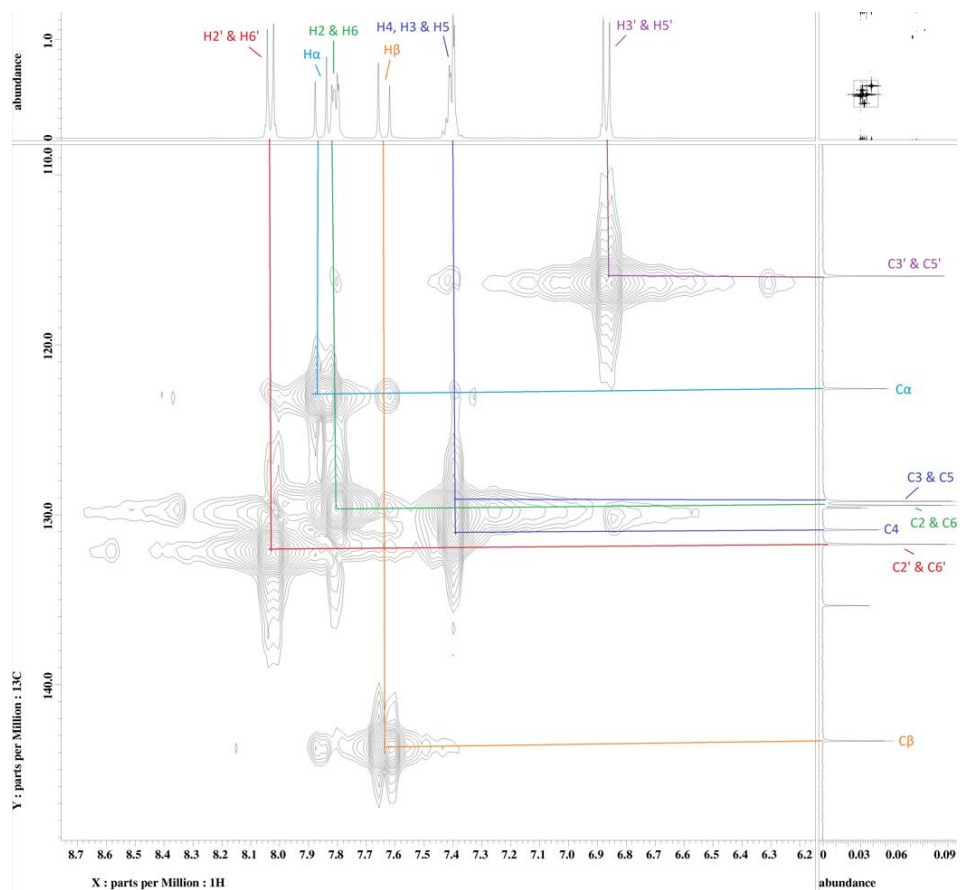
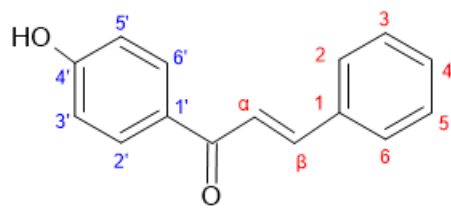


Figure C4: HMQC NMR spectrum of 4'-hydroxychalcone (CA2).

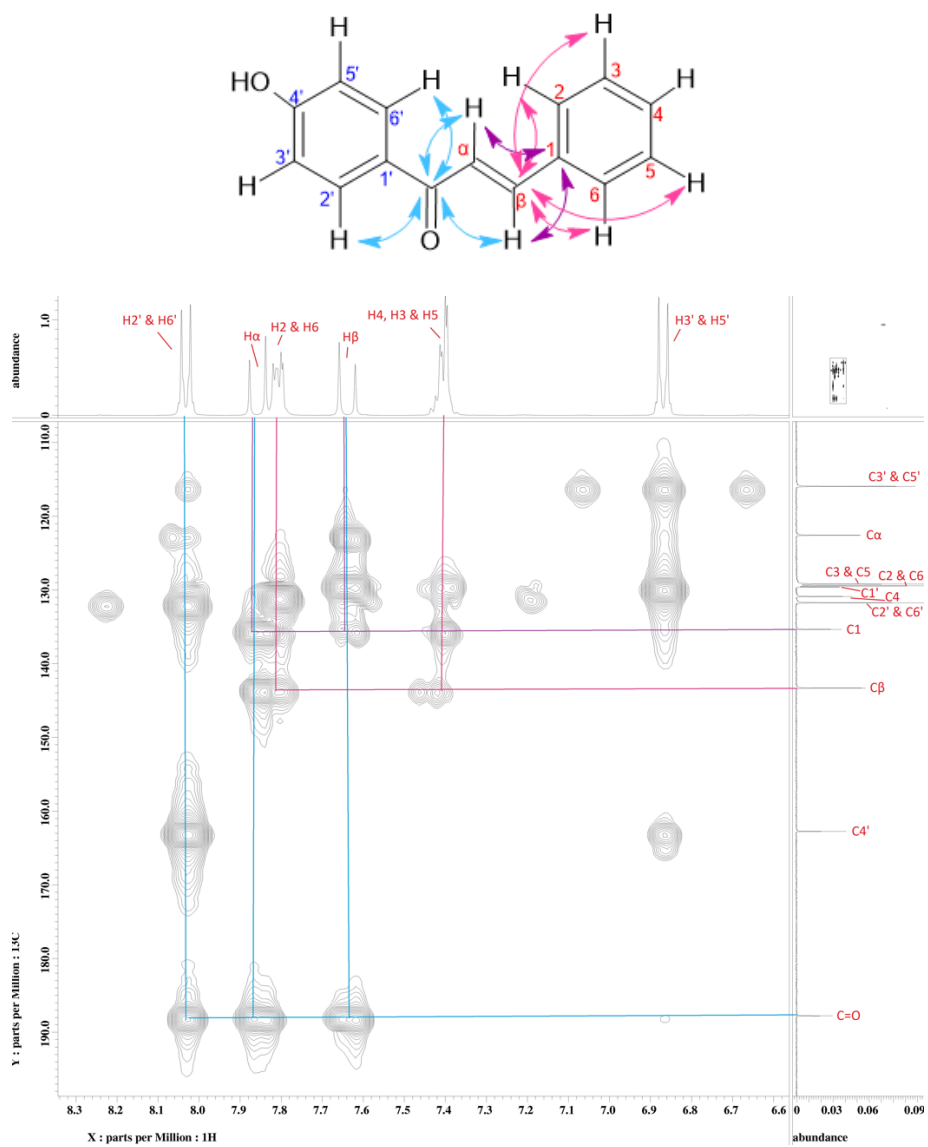


Figure C5: Expanded (downfield region) HMBC NMR spectrum of 4'-hydroxychalcone (**CA2**).

APPENDIX D

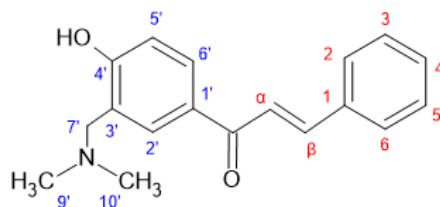


Table D1: ^1H , ^{13}C and DEPT NMR spectral data of **DA2**.

Atom Number	^1H (δ_{H} , ppm)	^{13}C (δ_{C} , ppm)	DEPT
C=O	-	188.7	C
α	7.54 (d, $J = 15.88$)	121.9	CH
β	7.78 (t, $J = 15.88$)	143.8	CH
1	-	135.3	C
2 & 6	7.63 (m)	128.4	CH
3 & 5	7.40 (m)	129.0	CH
4	7.40 (m)	129.6	CH
1'	-	130.4	C
2'	7.78 (t, $J = 15.88$)	130.4	CH
3'	-	116.1	CH
4'	-	163.5	C
5'	6.88 (d, $J = 8.56$)	116.1	CH
6'	7.92 (dd, $J = 2.44, 8.56$)	130.4	CH
7'	3.74 (s)	62.6	CH ₂
9' & 10'	2.36 (s)	44.5	CH ₃

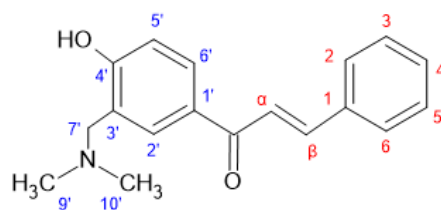


Table D2: $^1\text{H} - ^{13}\text{C}$ correlations in **DA2**.

Carbon Number	Proton Number			
	HMQC	HMBC		
	1J	2J	3J	4J
C=O	-	H α	H β , H2', H6'	-
C α	H α	-	-	-
C β	H β	H α	H2, H6	-
C1	-	H β	H α , H3, H5	-
C2	H2	H3	H β , H4	-
C3	H3	-	-	-
C4	H4	-	H2, H6	-
C5	H5	-	-	H β
C6	H6	H5	H β , H4	-
C1'	-	H2', H6'	H5'	-
C2'	H2'	-	-	-
C3'	-	-	-	-
C4'	-	H5'	H2', H6', H7'	-
C5'	H5'	-	-	-
C6'	H6'	-	-	-
C7'	H7'	-	H2', H9', H10'	-
C9' & C10'	H9' or H10'	-	H7'	-

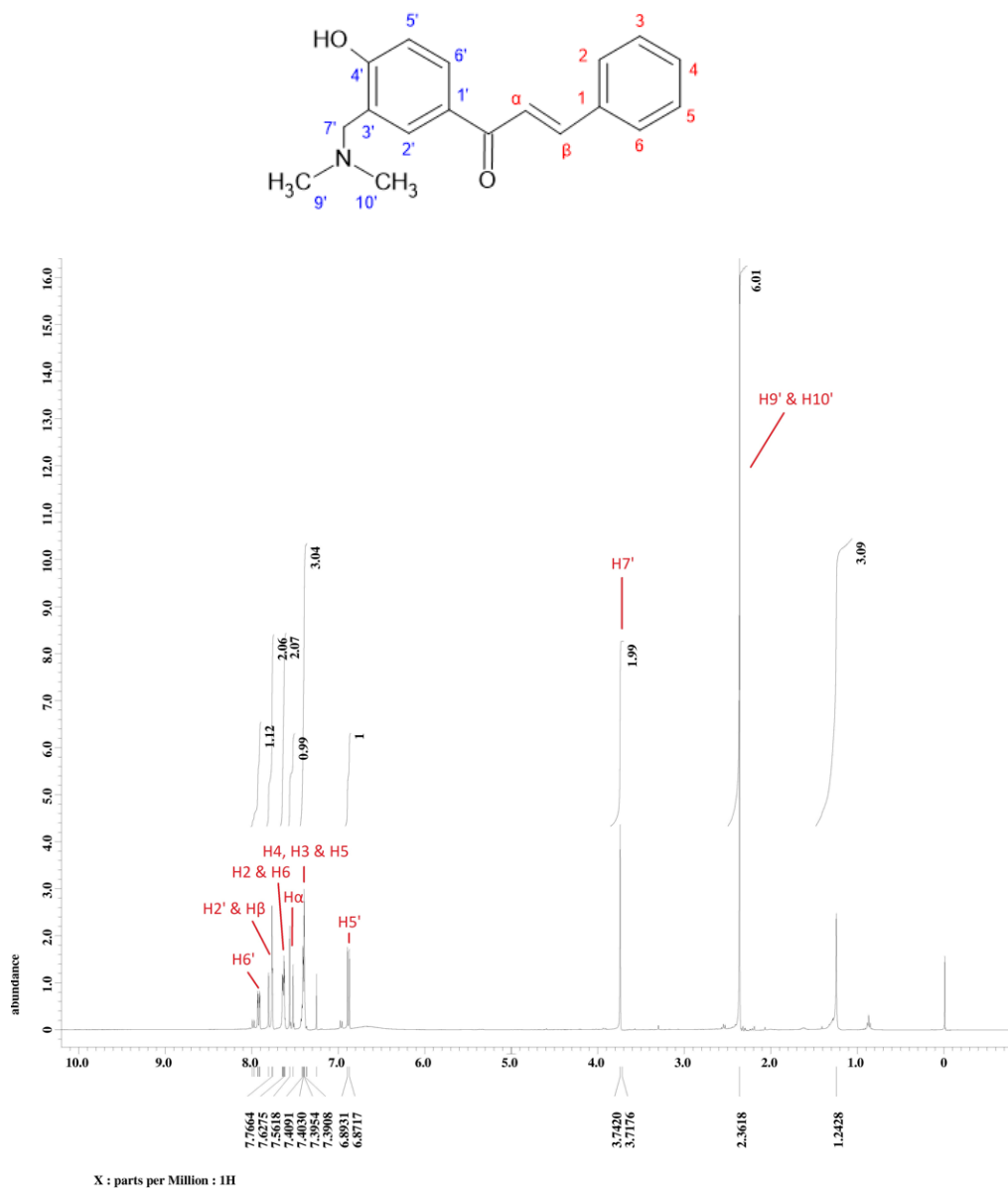


Figure D1: ¹H NMR spectrum of 4'-hydroxy-3'-dimethylaminomethylchalcone (**DA2**) (400 MHz, CDCl₃).

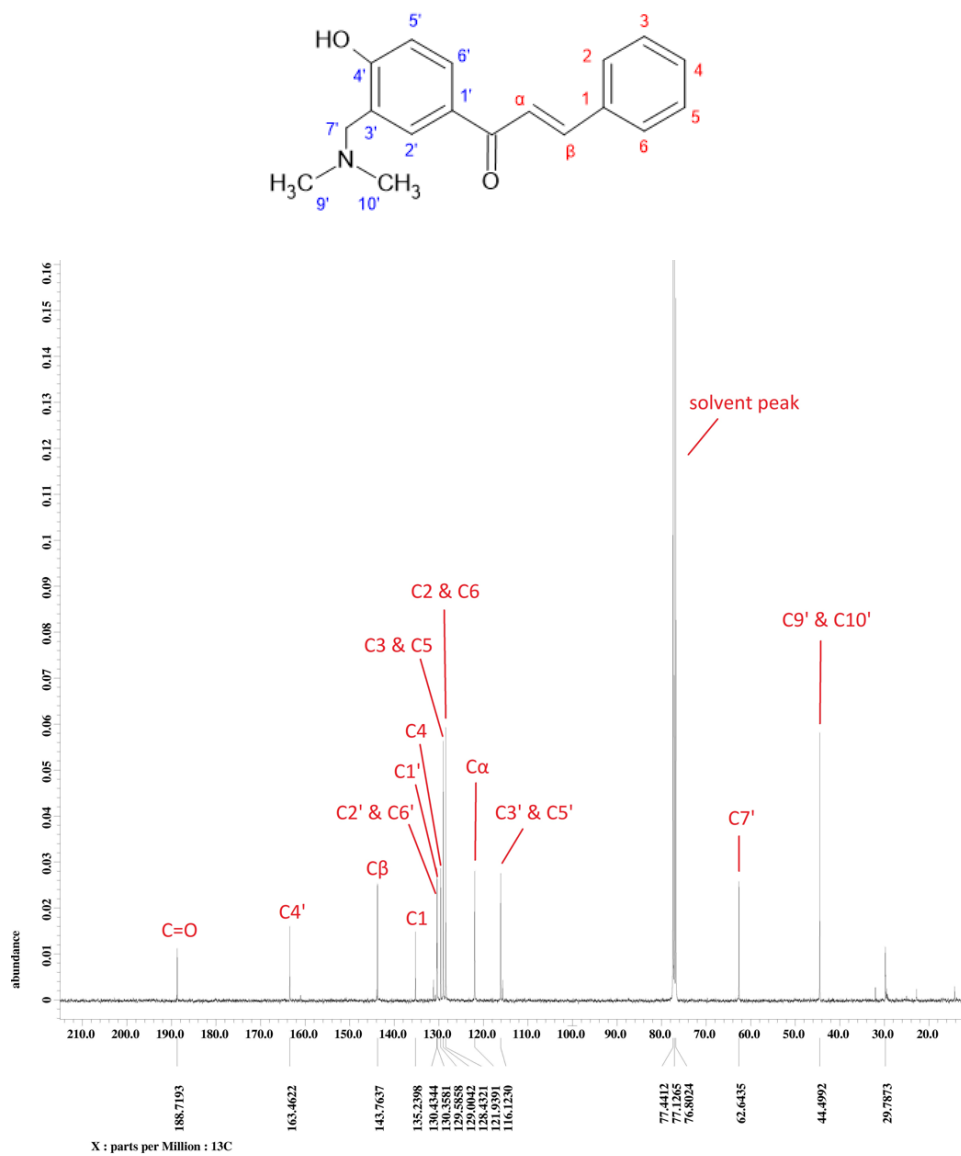


Figure D2: ¹³C NMR spectrum of 4'-hydroxy-3'-dimethylaminomethylchalcone (**DA2**) (100 MHz, CDCl₃).

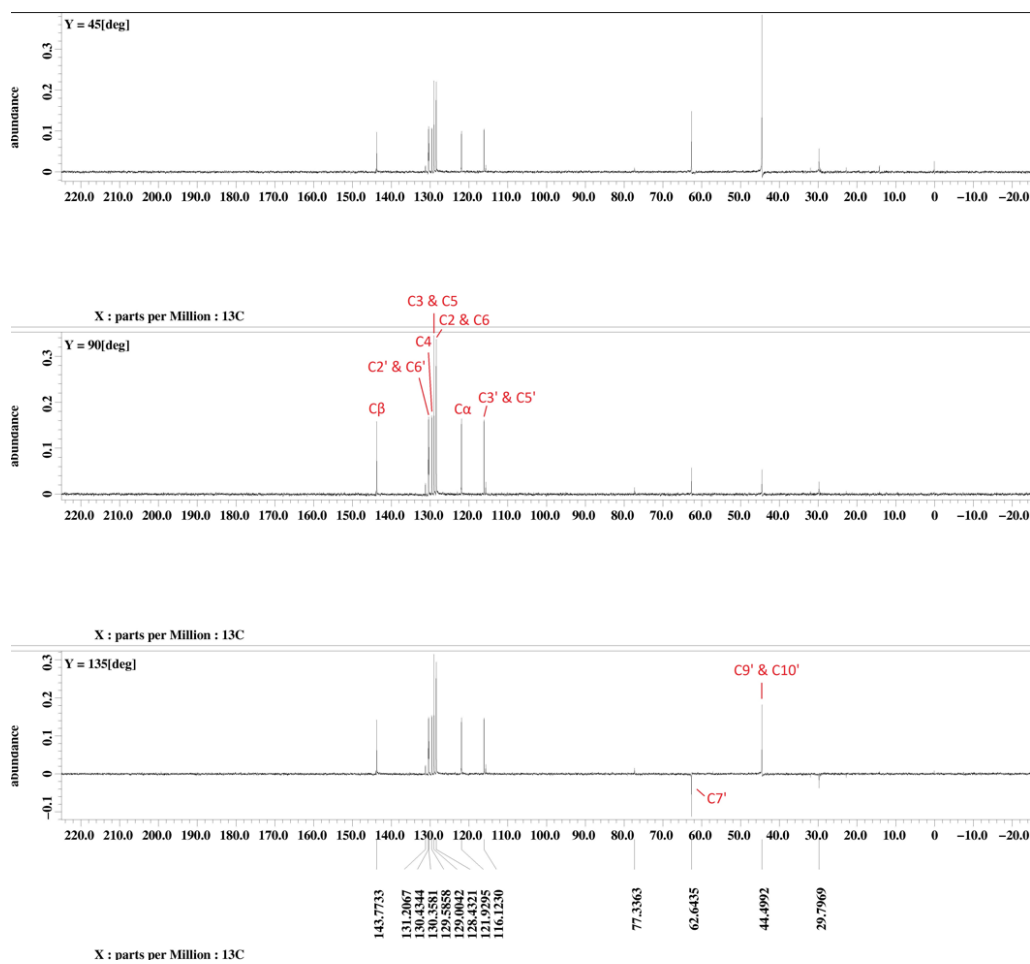
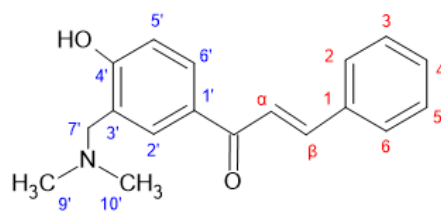


Figure D3: DEPT NMR spectrum of 4'-hydroxy-3'-dimethylaminomethylchalcone (**DA2**).

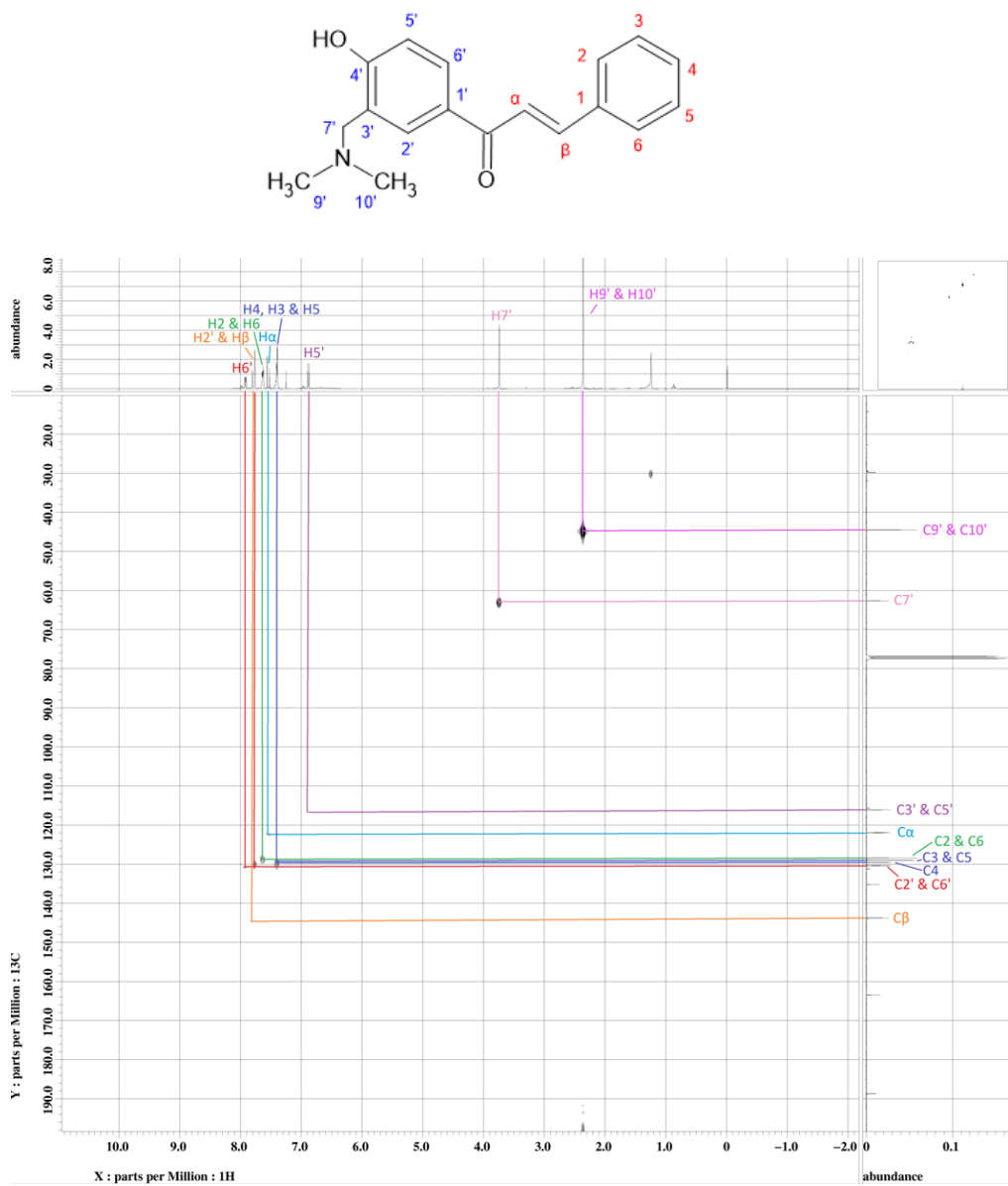


Figure D4: HMQC NMR spectrum of 4'-hydroxy-3'-dimethylaminomethylchalcone (DA2).

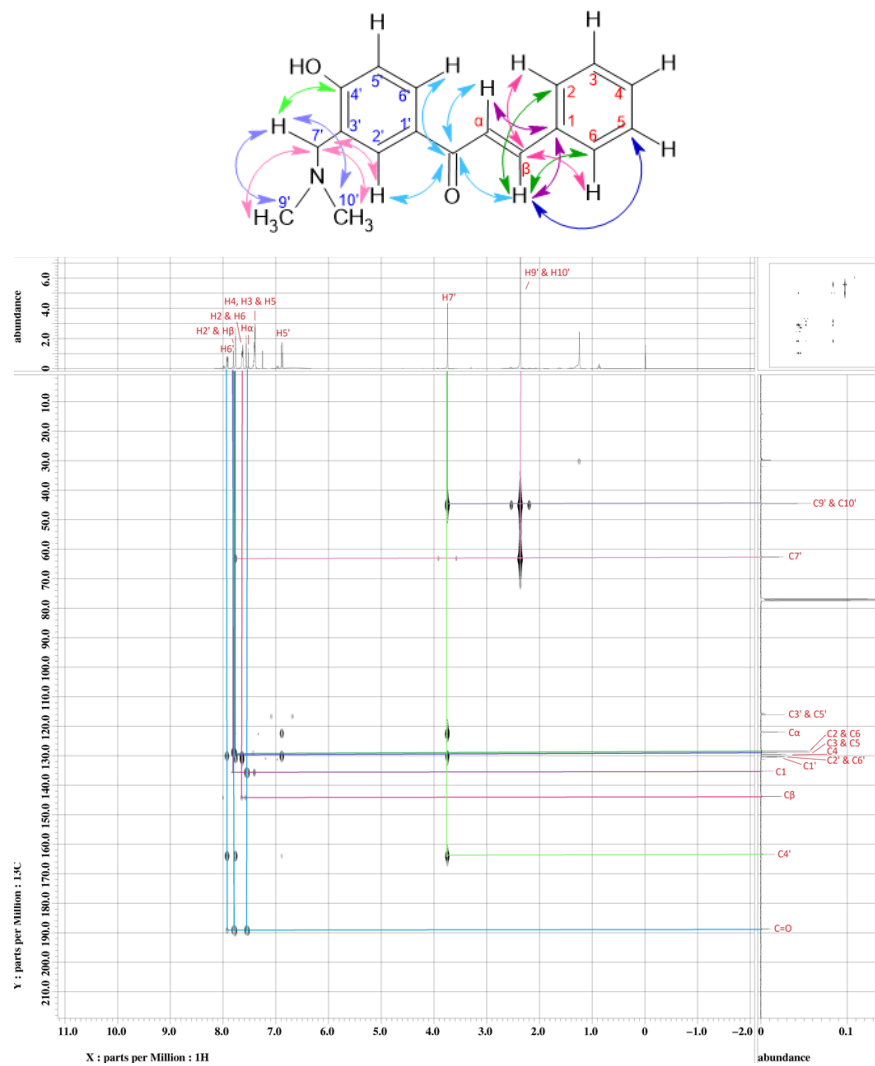


Figure D5: HMBC NMR spectrum of 4'-hydroxy-3'-dimethylaminomethylchalcone (**DA2**).

APPENDIX E

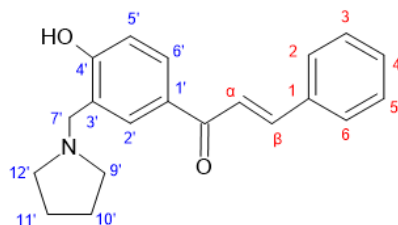


Table E1: ^1H , ^{13}C and DEPT NMR spectral data of **PY2**.

Atom Number	^1H (δ_{H} , ppm)	^{13}C (δ_{C} , ppm)	DEPT
C=O	-	188.7	C
α	7.55 (d, $J = 15.88$)	122.0	CH
β	7.78 (q, $J = 15.88$)	143.7	CH
1	-	135.3	C
2 & 6	7.64 (m)	128.4	CH
3 & 5	7.40 (m)	129.0	CH
4	7.40 (m)	129.2	CH
1'	-	129.4	C
2'	7.78 (q, $J = 15.88$)	130.3	CH
3'	-	116.1	C
4'	-	163.6	C
5'	6.87 (d, $J = 8.56$)	116.1	CH
6'	7.91 (dd, $J = 8.56$)	130.3	CH
7'	3.92 (s)	58.6	CH ₂
9' & 12'	2.68 (s)	53.6	CH ₂
10' & 11'	1.88 (s)	23.7	CH ₂

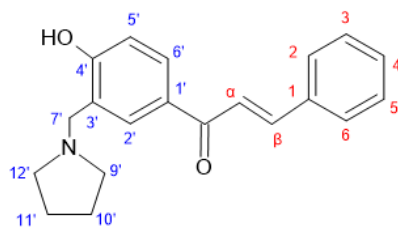


Table E2: $^1\text{H} - ^{13}\text{C}$ correlations in **PY2**.

Carbon Number	Proton Number			
	HMQC	HMBC		
	1J	2J	3J	4J
C=O	-	H α	H β , H2', H6'	-
C α	H α	H β	-	-
C β	H β	H α	H2, H6	-
C1	-	H β	H α , H3, H5	-
C2	H2	-	-	-
C3	H3	H4	-	-
C4	H4	H3, H5	-	-
C5	H5	H4	-	H β
C6	H6	-	-	-
C1'	-	H2', H6'	H5'	-
C2'	H2'	-	-	-
C3'	-	-	-	-
C4'	-	H5'	H2', H6'	-
C5'	H5'	-	-	-
C6'	H6'	-	-	-
C7'	H7'	-	H2'	-
C9' & C12'	H9' or H12'	H10' or H11'	H7'	-
C10' & C11'	H10' or H11'	-	-	-

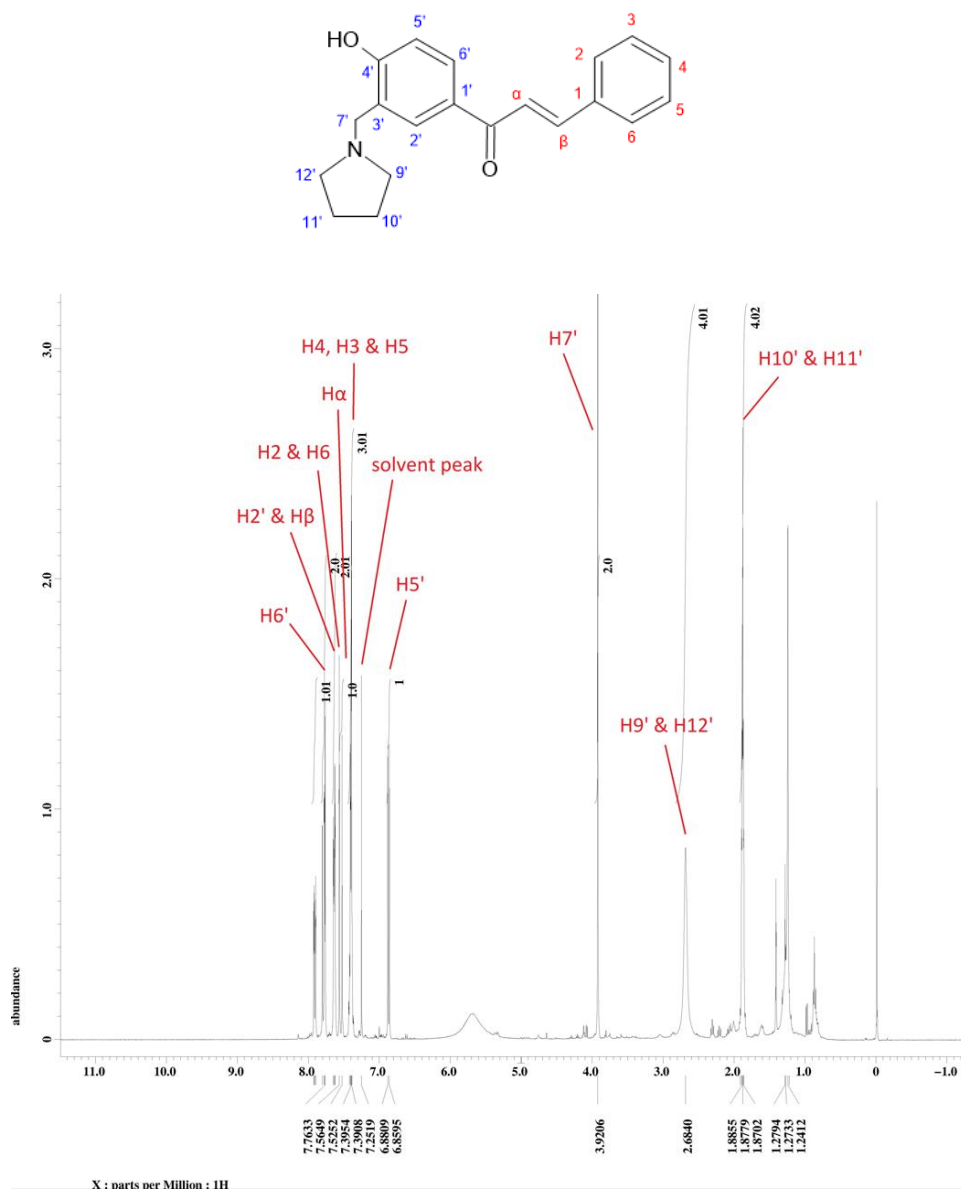
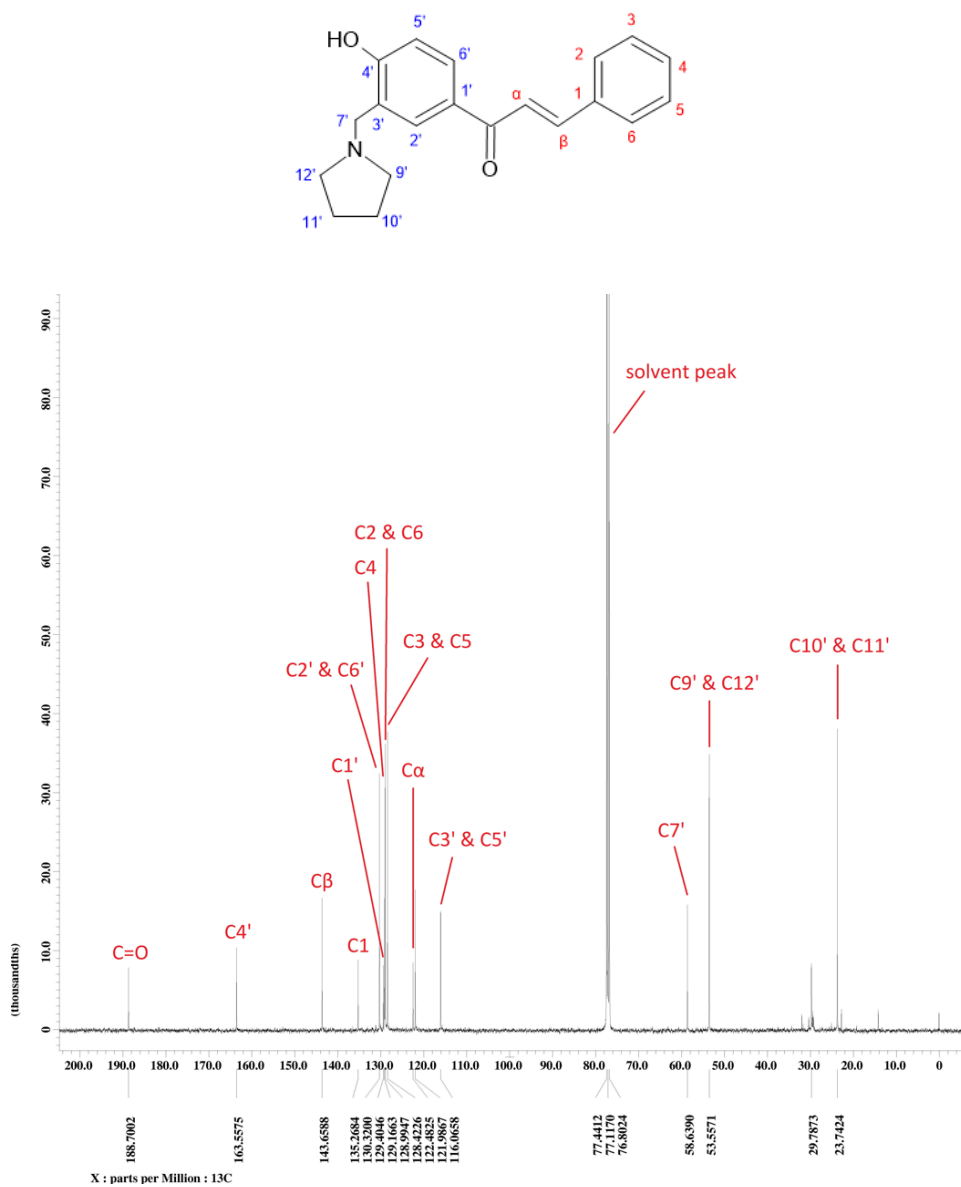


Figure E1: ¹H NMR spectrum of 4'-hydroxy-3'-pyrrolidinomethylchalcone (**PY2**) (400 MHz, CDCl₃).



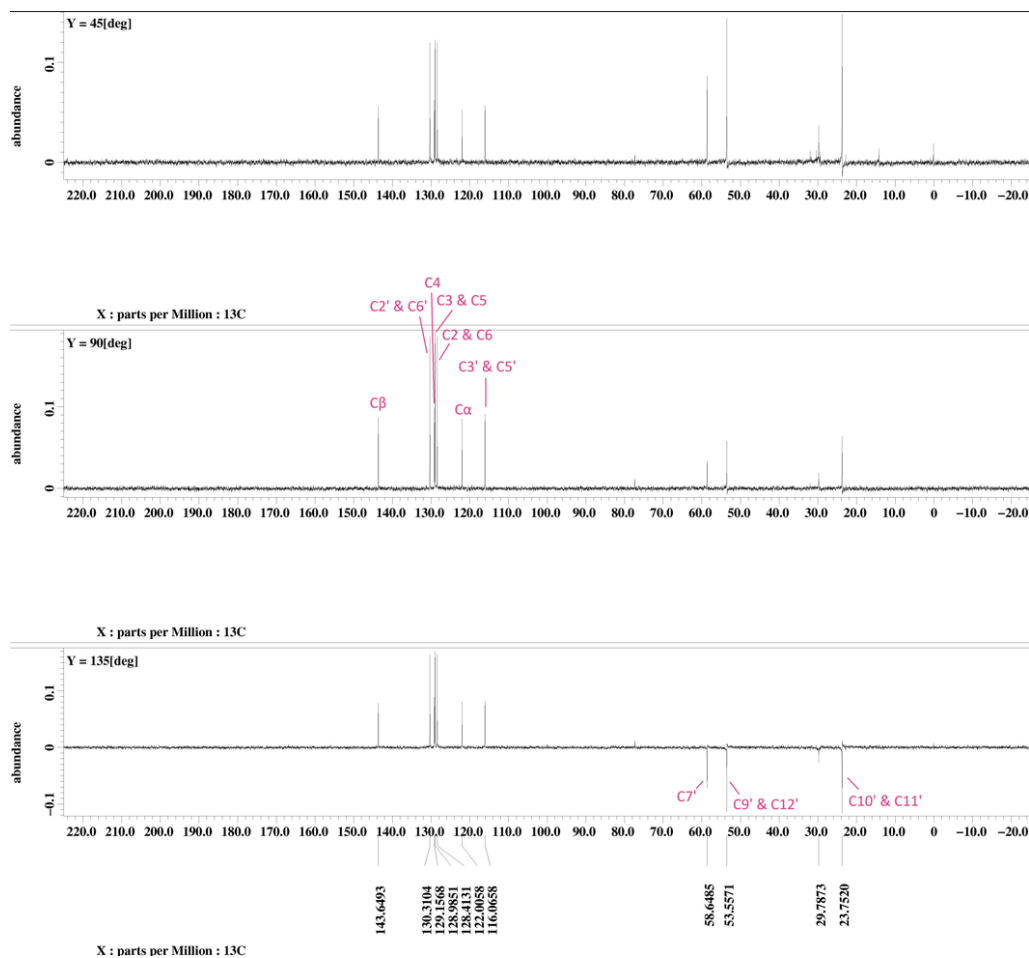
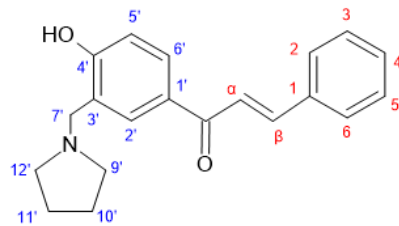


Figure E3: DEPT NMR spectrum of 4'-hydroxy-3'-pyrrolidinomethylchalcone (PY2)

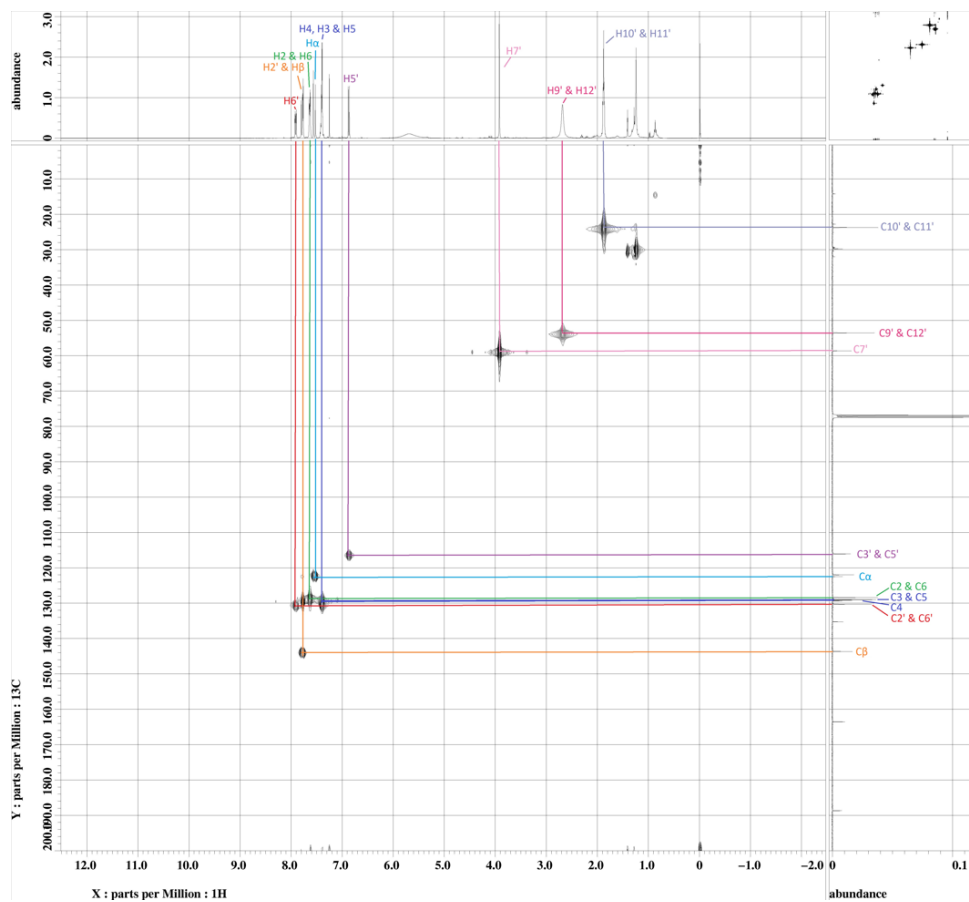
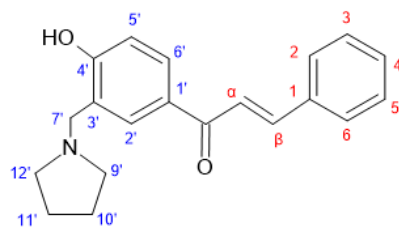


Figure E4: HMBC NMR spectrum of 4'-hydroxy-3'-pyrrolidinomethylchalcone (**PY2**).

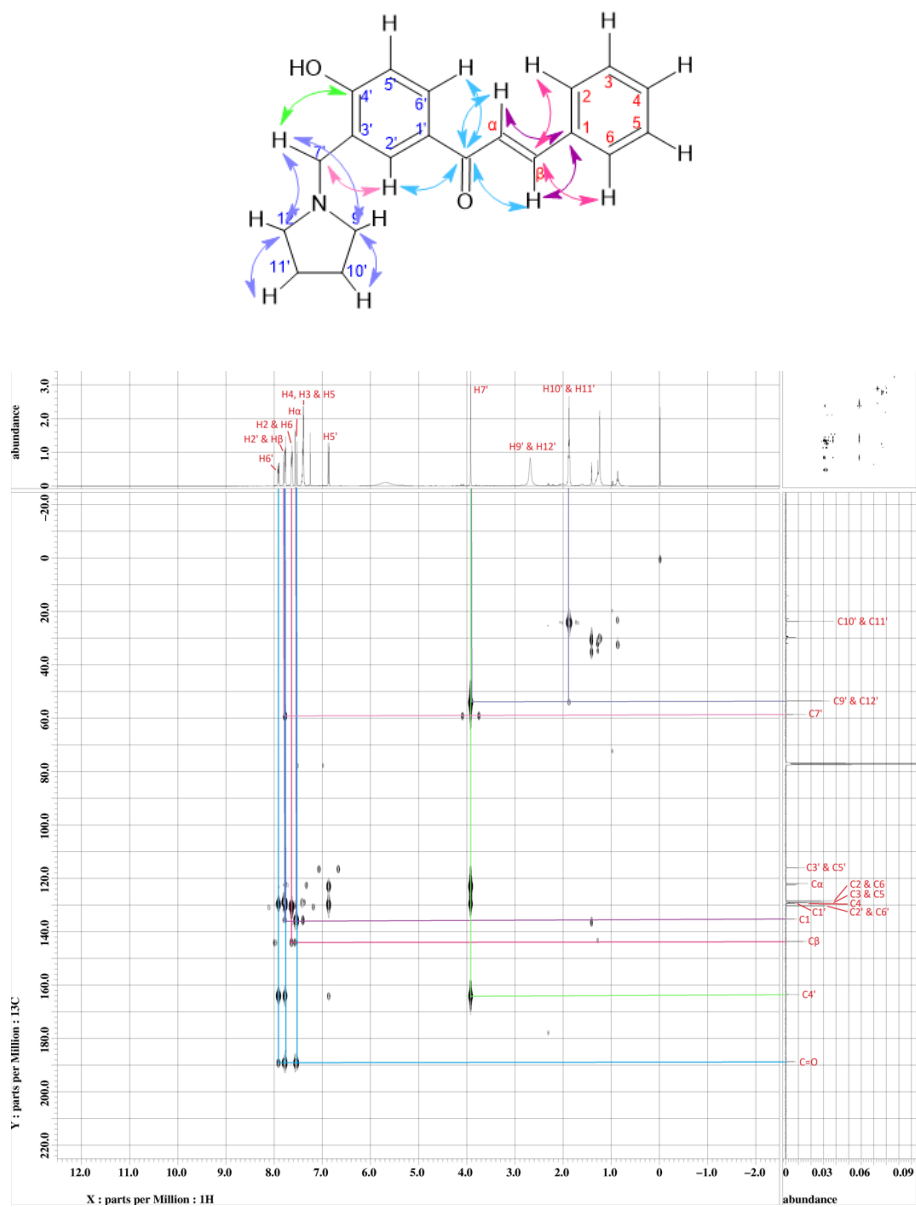


Figure E5: HMBC NMR spectrum of 4'-hydroxy-3'-pyrrolidinomethylchalcone (**PY2**).

APPENDIX F

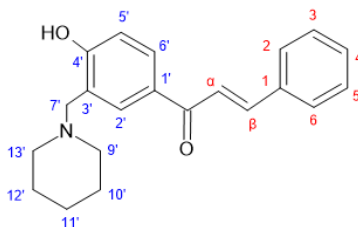


Table F1: ^1H , ^{13}C and DEPT NMR spectral data of **PI2**.

Atom Number	^1H (δ_{H} , ppm)	^{13}C (δ_{C} , ppm)
C=O	-	188.7
α	7.54 (d, $J = 15.24$ Hz)	122.0
β	7.78 (d, $J = 15.88$ Hz)	143.7
1	-	135.3
2 & 6	7.64 (m)	128.4
3 & 5	7.40 (t, $J = 4.88$ Hz)	129.0
4	7.40 (t, $J = 4.88$ Hz)	129.4
1'	-	129.8
2'	7.78 (d, $J = 15.88$ Hz)	130.3
3'	-	116.2
4'	-	163.6
5'	6.86 (d, $J = 8.52$ Hz)	116.2
6'	7.90 (dd, $J = 1.84$ Hz, 8.56 Hz)	130.3
7'	3.75 (s)	61.9
9' & 13'	1.98 (t)	23.8
10' & 12'	1.64 (t, $J = 4.88$ Hz)	25.7
11'	1.24 (m)	29.8

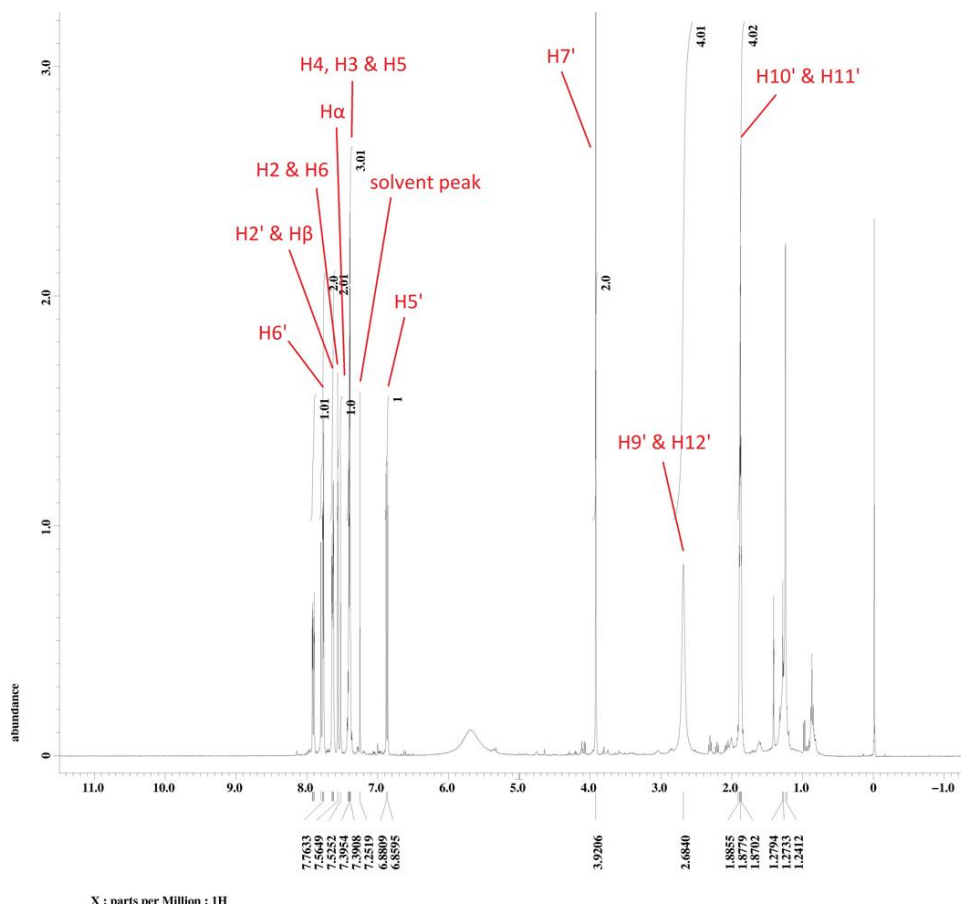
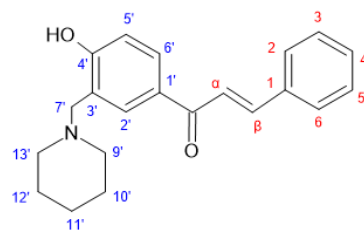


Figure F1: ^1H NMR spectrum of 4'-hydroxy-3'-piperidinomethylchalcone (**PI2**) (400 MHz, CDCl_3).

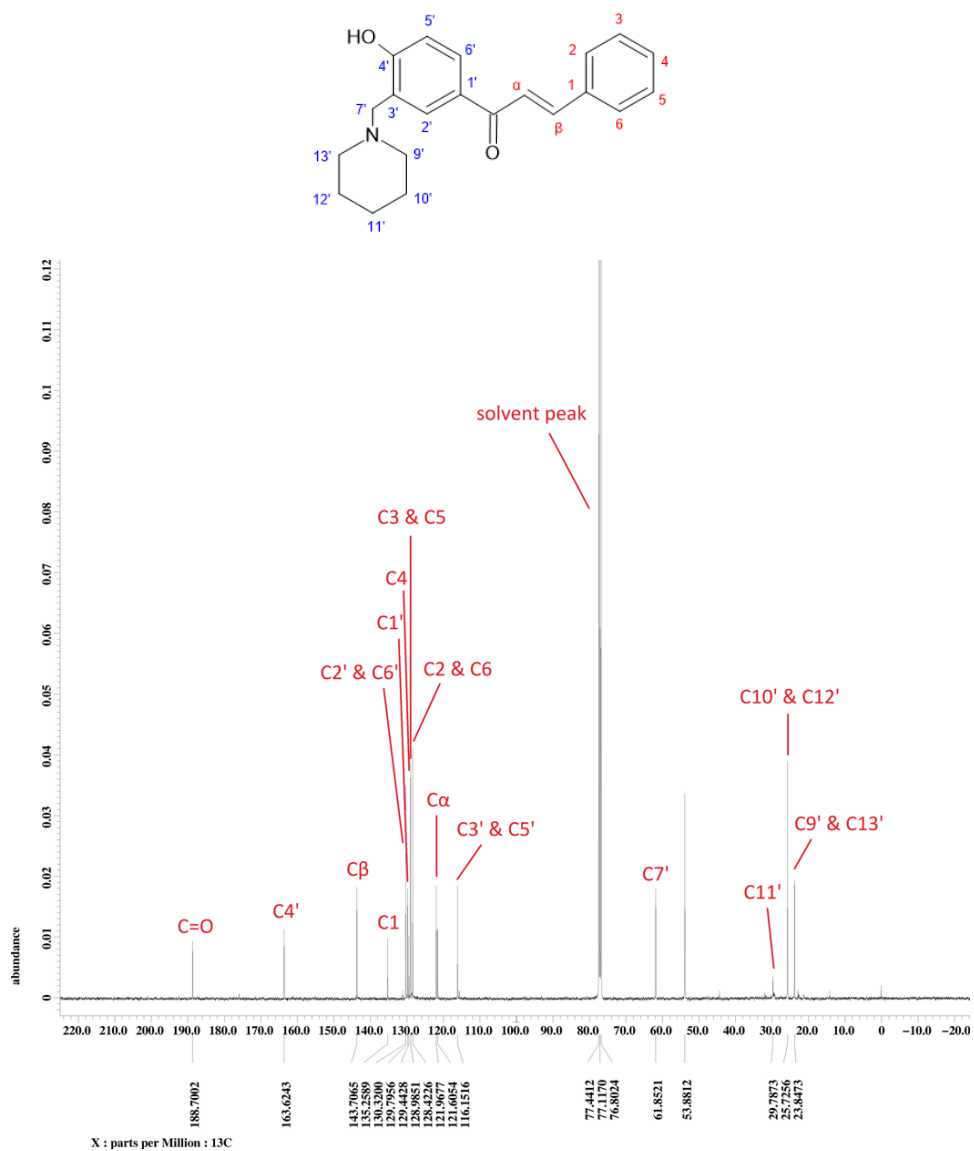


Figure F2: ^{13}C NMR spectrum of 4'-hydroxy-3'-piperidinomethylchalcone (**PI2**) (100 MHz, CDCl_3).